# 博士学位請求論文

論文題目　Effect of lignocellulosic components on the anaerobic digestibility of aquatic weeds and development of a predictive model of methane production

専 攻 名　環境共生工学専攻

学籍番号　18D5702

氏　　　名　藤原正明

指導教員　戸田　龍樹

創 価 大 学 大 学 院
工 学 研 究 科

DISSERTATION


**Effect of lignocellulosic components on the anaerobic digestibility**

**of aquatic weeds and development of a predictive model of**

**methane production**


2022


SOKA UNIVERSITY

GRADUATE SCHOOL OF ENGINEERING


MASAAKI FUJIWARA

Effect of lignocellulosic components on the anaerobic

digestibility of aquatic weeds and development of a predictive

model of methane production

March 2022

Masaaki  FUJIWARA

SOKA UNIVERSITY

Author:        Masaaki Fujiwara

Title:         Effect of lignocellulosic components on the anaerobic

               digestibility of aquatic weeds and development of a predictive

               model of methane production

Department:    Environmental Engineering for Symbiosis

Faculty:       Engineering

Degree:        Ph. D.

Convocation:   March 2022

We certify that we have read this dissertation and that, in our opinion, it is satisfactory in scope and quality as a dissertation for the degree of Doctor of Philosophy in Engineering.

March 2022

DISSERTATION COMMITTEE

Prof. Dr. Tatsuki Toda

Prof. Dr. Tatshushi Matsuyama

Prof. Dr. Shinjiro Sato

Prof. Dr. Shyuhei Ban

# Effect of lignocellulosic components on the anaerobic digestibility of aquatic weeds and development of a predictive model for methane production

March 2022

Masaaki Fujiwara

# Contents

# ACKNOWLEDGEMENTS

# ABSTRACT

Although the anaerobic digestion of aquatic weeds has been attempted all over the world, few studies focus on the relationship between anaerobic digestibility and chemical compositions. The biomass harvested from waterbody has variety of aquatic weeds species, and species composition and chemical composition in each species might vary with the change of season. In this doctoral thesis, development of the estimation method of annual methane productivity from seasonality of the chemical composition and species composition of harvested aquatic weeds was performed as follows: seasonal changes of the chemical compositions and estimation of monthly methane potential of harvested aquatic weeds from lake Biwa (Study 1), correlation analysis between chemical composition and anaerobic digestibility calculated by fitting to modified Gompertz model (Study 2). In study 1, among three species harvested in monthly from Spring to Fall, chemical composition was changed seasonally in two species, but another species did not change, indicating that life cycle of aquatic weeds affects the seasonality of the chemical composition. On the other hand, although methane yield were significantly varied, the difference was larger in each species: thus, methane potential of harvested aquatic weeds can be mainly determined depending on the species compositions. Estimation of monthly methane potential of aquatic weeds harvested from Lake Biwa was low in autumn to spring seasons ($171–186$ mL g-VS$^{-1}$) due to the predominance of *P. maackianus*. In study 2, significant correlations were obtained between cellulose/lignin and ultimate methane yield, cellulose/hemicellulose and maximum methane production rate, and hemicellulose content and T80, respectively. From the equations explaining each kinetic parameters and annual estimated chemical

compositions of harvested aquatic weeds, anaerobic digestibility was estimated. In Study 3, ADM1 was developed and simulated for the aquatic weeds biomass, incorporating these relationships. As a result, the ADM1 was able to estimate the methane production of water plant biomass with high accuracy. In the general discussion, the operational stability of the continuous treatment was estimated by the model and discussed for the social implementation of this treatment.

# Chapter 1

# General Introduction

## 1.1. Environmental and social issues associated with overgrowth of aquatic weeds

Aquatic weed is a vascular plant that grows in or near water and is either emergent, submergent or floating. Generally, aquatic weeds play essential roles in providing a habitat and spawning ground of fishes, preventing algal bloom, including harmful algae by absorbing nutrients in the aquatic biotope, and providing oxygen into water (Gallegos et al. 2018). However, in the last decades, excessive growth of aquatic weeds has occurred worldwide (Figure 1-1). The triggers causing overgrowth of aquatic weeds are considered as follows; introduction of high-growth (invasive) alien species, eutrophication by increasing nutrient loading from industrial effluent, domestic wastewater, and agriculture (Pugliese et al. 2015), and no more comprehensive collection of aquatic weeds for utilization (Ban et al. 2018).

Excessive propagation of aquatic weeds is causing severe environmental issues and economic losses. For example, in India, approximately 1.32 to 2.06 Mha (9 – 14% of wetland) was infested by aquatic weeds (Space Applications Centre, 2011). Especially, the overgrowth of *Salvinia molesta*, *Hydrilla verticillate*, and *Eichhornia crassipes* in lakes and marshes have caused a decrease in the availability of irrigation water due to transpiration as well as economic damage due as it hinders hydraulic power generation (Kaur et al., 2017). In Lake Victoria, severe economic losses in transportation and fisheries, accounting for 350 million US Doller per annual was caused by the propagation of water hyacinth *E. crassipes* (Mkumbo and Marshall, 2014). In Lake Biwa, one of

western Japan's reservoirs and the largest lake in Japan, the overgrowing aquatic weed has caused

severe social, economic and environmental issues such as sailing disturbances, a decrease in fishery

catches, and landscape issues (Haga et al., 2006; Maruno et al. 2016). Furthermore, excessive growth

of aquatic weeds has deteriorated the water quality in Lake Biwa; therefore, managing the excessive

growth of aquatic weed biomass has been considered a national-scale problem. In order to promote

the harvesting and treatment of aquatic weeds, the Ministry of the Environment and Shiga Prefecture

implemented the policy "Plan for Conservation of Lake Water Quality" and "Mother Lake 21 Plan",

respectively (Ministry of the Environment, 2010; Scientific Committee for Comprehensive

Conservation of Lake Biwa, 2010). Currently, around 5,000 tons of macrophytes in Lake Biwa were

harvested with 0.3 billion yen per year (Shiga Prefecture, 2018). It directly affects people who depend

on aquatic ecosystem services for their livelihood, health and recreational opportunities. The

propagation of alien aquatic weeds affects to biodiversity. They can be mediated by competitively

excluding or out-competing the less robust native species, preying on native species, or altering the

natural aquatic or riparian habitat in which they reside. They can also adversely impact the

recreational and amenity use of infested watercourses by restricting angling, boating, swimming and

other water-based leisure pursuits (Stokes et al. 2004; Minchin 2007).

To solve these problems and protecting ecosystem, biomass in waterbody should be reduced.

The primary option to reducing aquatic weeds is physical removal (harvest). However, several

management options such as applying herbicides, modifying the bottom by covering concrete, and

biological removal are also attempted. Because a sustainable amount of aquatic weed biomass should

be remained to maintain the beneficial function of aquatic weeds, physical removal is considered the most suitable method for managing biomass. The introduction of physical removal of aquatic weeds requires post-treatment for harvested biomass at the same time. In most cases, harvested biomass was piled in land and just left without any treatment or was incinerated after sun drying. Thus, the establishment of an effective utilization process of harvested aquatic weeds can contribute to the promotion of a recycling-based society.

## 1.2. Treatment of harvested aquatic weeds

As a treatment of harvested aquatic weeds, sustainable methods of converting harvested aquatic weeds into useful products have been examined including e.g., anaerobic digestion (Koyama et al., 2014), bioethanol (Rabemanolontsoa and Saka, 2012), feed for livestock (Tewabe et al., 2016) and composting (Jain and Kalamdhad, 2018). Typically, harvested biomass is piled up for several days, and transferred and has been either incinerated or composted. Incineration is considered to be unfeasible due to the high moisture content (80-95%wet-weight) of aquatic weed. Currently, composting has been the main treatment method of aquatic weeds in Lake Biwa. Composting is advantageous in nutrient recycling in low treatment cost, but it is still not competitive against chemical fertilizer mainly due to the long treatment time and the difference between the fertilizer application time and the growth period of the aquatic weeds (Shiga Prefecture, 2012). In addition, harvested macrophytes often contains harmful contaminants such as fish hook, which can be a risk for farmers to get injury or contamination to the crops by using macrophyte compost. With the same

reason, utilization of aquatic weeds to animal feed is limited. On the other hand, bioethanol fermentation has recently been attempted for renewable biofuel production from aquatic weeds. Bioethanol is advantageous in transportation by its liquid form. However, it is widely known that bioethanol fermentation of lignocellulosic biomass has a significant drawback: high cost for the addition of enzymes.

Recently, anaerobic digestion has been receiving attention for the effective treatment method of aquatic weeds. This method treats biomass with high moisture content, such as aquatic weeds. Anaerobic digestion involves a series of metabolic reactions in which complex components of the substrate are sequentially converted to methane which is used for energy. Numerous studies performed the anaerobic digestion of various species of aquatic weeds and extensive methane yield range of 66–418 mL g-VS$^{-1}$ (Abbasi et al., 1990; Kobayashi et al., 2014; Koyama et al., 2014; Fujiwara et al., 2019) has been recorded. Koyama et al. (2014) revealed that the methane yield of aquatic weeds differs between species due to differences in the lignin contents. Lignin is a key component that affects digestibility since it has a low degradability and coats cellulose and hemicellulose, thereby limiting the attachment of enzymes and microbes to the others cell wall components (Mussatto et al. 2008). This is because, although some aquatic weed species have the same methane potential as food waste, the methane potentials of other species are lower. Thus, lignocellulosic components affect to the anaerobic digestibility of harvested aquatic weeds (Figure 1-2).

## 1.3. Establishment of model predicting methane productivity and its application

To assume the treatment process of anaerobic digestion, the variation of methane potential should be evaluated. BMP from a mixture of food waste drastically varied due to the seasonal variation of components ratio (Karai et al., 2018). In the case of harvested aquatic weeds, BMP of harvested aquatic weeds may vary due to seasonal variations in both of species composition depending on biomass abundant of each species and chemical composition depending on the species maturity and lifecycle may lead to the variation through a year. Numerous studies performed correlation analysis between chemical composition and BMP of plant biomass such as straw, cannary grass, and weed biomass, and found out the significant correlation. However, there were few studies investigating not only the cumulative methane yield but also the production rate. Numerous studies have applied kinetic models in the study of the anaerobic digestibility of substrate (Buitrón et al., 2019; Kafle and Kim, 2013; Koyama et al., 2016). Modified Gompertz model was often applied, which can identify the anaerobic digestibility as ultimate methane yield, maximum methane production rate, lag phase, and T80 (the required period to finish 80% of the ultimate methane yield). By linking these kinetic parameters and chemical composition, the degradability of each components could be clarified.

## 1.4. Objectives

Overall research objective of this Ph.D. thesis is to clarify the key parameters determining the anaerobic digestibility of aquatic weed and establish the predictive model of anaerobic digestibility

from chemical composition. The specific objectives were: to investigate the seasonality of the lignocellulosic components and methane yield of harvested aquatic weeds (ChapterII); to clarify the relationships between lignocellulosic components and their anaerobic digestibility and develop to a mathematical model for estimating annual methane recovery (ChapterIII). Finally, validation of the obtained model and based on the validated in General Discussion part.

(a) Role of suitable biomass aquatic weeds

Wave extinguish

N    P

Water purification

O₂    Provide O₂

Provide habitats

(b) Influence of aquatic weeds with biomass

Eutrophication

P

N

Decrease of O₂

Disappearance of habitats
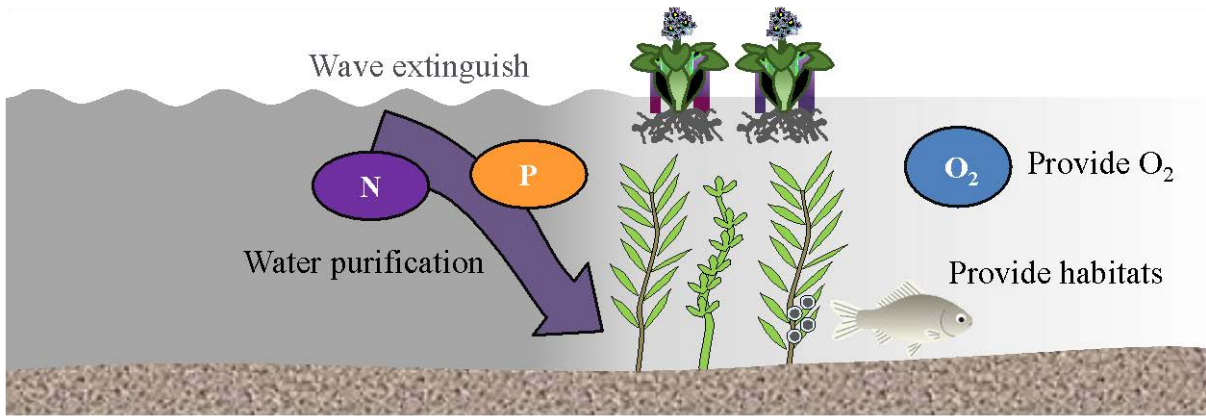
Figure1-1. Tolerance and problems of aquatic weeds in aquatic ecosystem. (a) Role of suitable biomass aquatic weeds, (b) Influence of aquatic weeds with biomass.
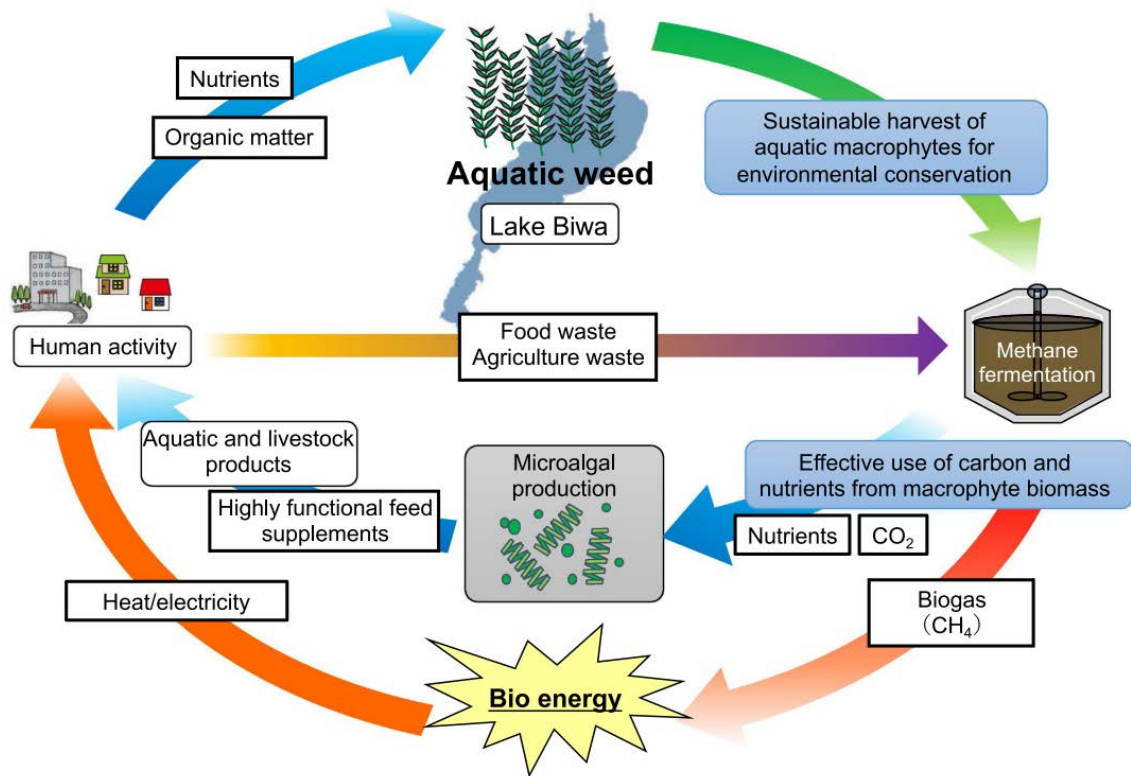
Figure1-2. Schematic diagram of the concept of a 'recycling-oriented social system through sustainable utilization of macrophytes' proposed by Ban et al. (2018).

# Chapter Ⅱ

# Seasonal variation in the chemical composition and methane potential of harvested aquatic weeds

## 2.1.  Introduction

Generally, seasons are the main factor affecting biomass yield, growth speed, and maturity for plant biomass. (Santamaría and Hootsmans, 1998; Hoffmann and Rooney, 2014; Dragoni et al., 2015). Previous studies have revealed that the chemical composition of plant biomass such as maize, faba bean residue, rye, Cocksfoot, giant reed, Timothy, and some others changes seasonally and depends on the maturity level of the biomass (Schittenhelm, 2008; Hübner et al. 2011; McEniry et al. 2013). Therefore, seasonal changes in the chemical composition, especially the amount of lignocellulosic components, may affect methane yields of plant biomass (Godin et al., 2015). Kandel et al. (2013) reported that seasonal changes in the chemical components, such as lignin content and cellulose content, significantly affected the methane yield of canary grass. Although the seasonality of the total biomass, total carbon, total nitrogen, starch contents, and biogas yield of aquatic weeds has already been reported, the seasonality of the methane yield and its relationship with the lignocellulose contents have not. The lifecycle and growth stages of aquatic weeds differ depending on the species, indicating that the chemical composition may change and thereby affect the methane yield. Kandel et al. (2013) reported the relationships between the seasonal changes in the chemical composition and methane yield of reed canary grass. In addition, Lake Biwa, located in temperate

area, experience four distinct seasons. The optimal temperature and light intensity allow the highest aquatic weed growth rates to differ between species (Imamoto et al. 2008), leading that the species composition can vary seasonally. Therefore, the seasonal variation of both of chemical composition and species composition might affect the methane potential of harvested aquatic weeds. To assess the possibility for implementation of anaerobic digestion, approximate methane potential and its seasonality should be evaluated.

## 2.2. Materials and methods

### 2.2.1. Substrate and inoculum

*Potamogeton maackianus, Elodea nuttallii*, and *Egeria densa*, which are the dominant aquatic weeds in Lake Biwa (Figure 2-1), were harvested from the lake monthly from June to October in 2015 and used as substrates. The harvested macrophytes were dried at 80 °C for 12 hours and milled into particles smaller than 3 mm to prevent bias from variations in the chemical composition between different parts of the plants (i.e., leaf, stem, and root). The milled macrophytes were used for the biological methane potential (BMP) test and chemical composition analysis. Mesophilic anaerobic sludge was collected from the Hokubu Sludge Treatment Center, Kanagawa Prefecture, Japan, treating sewage sludge and wastewater. The collected sludge was stored for two days at 37±1 ºC in a walk-in, temperature-controlled laboratory to allow the removal of the residual substrate.

### 2.2.1. Batch anaerobic digestion

A biomethane potential (BMP) test was conducted to evaluate the anaerobic digestibility of the harvested macrophytes. Deionized water was added to the dried macrophytes to increase the moisture content to that of the initial samples. An automatic methane potential test system (AMPTS II) supplied by Bioprocess Control was used for the BMP tests. The substrate and 300 mL of seed sludge were added to a 500-mL medium bottle, resulting in a volatile solids (VS) ratio of 1:2, and topped up to 350 mL with distilled water. The headspace of the batch reactors was initially purged with $N_2$ gas to ensure anaerobic conditions, and the reactors were placed in a water bath controlled to $37\pm1$ °C. The BMP tests then commenced and continued until day 14 after confirming that biogas production had ceased. The mixture in each bottle was stirred using a rod and an electric motor. The non-methane gases, such as carbon dioxide and hydrogen sulfide, in the generated biogas, were removed in 80-mL vials containing a 3 M solution of sodium hydroxide (NaOH). The amount of biomethane released from each reactor was then measured by the device according to the liquid displacement and buoyancy principles. Three blanks were tested, and activity tests with cellulose powder as a substrate were conducted to determine the gas yield from the inoculum itself and confirm the methane productivity ($314\pm5.3$ mL g-VS$^{-1}$). All tests and blanks were conducted in triplicate, and the net methane production values were calculated.

### 2.2.2. Analytical parameters

The total solids (TS) contents were determined from the weights of samples dried oven at 105 °C until a constant weight was reached. The VS contents were then determined after drying at 550 °C for four hours in a muffle furnace. The lignocellulose, total carbon, total nitrogen contents, and methane yields were also measured. Standard methods from APHA (2005) were followed in the analysis of TS and VS. The lignocellulose (cellulose, hemicellulose, and lignin) contents were measured with a fiber analyzer (Model: A-200, Ankom, USA) by according to a detergent method (Van Soest et al. 1991). The total carbon and nitrogen were measured by elemental analysis using a CHN analyzer (Model: EA 1110, CE Instruments, Italy). Protein contents were calculated by multiplying the total nitrogen content by 6.25 (Triolo et al., 2011).

### 2.3. Results and discussion

### 2.3.1. Seasonal variation of chemical composition

The chemical composition of the aquatic weeds harvested from Lake Biwa was shown in Table 2-1. The average TS and VS content of *E. densa* and *E. nuttallii* were similar, while lower than those of *P. maackianus*. These results agreed with previous reports for fresh aquatic weeds (Kobayashi et al. 2014; Koyama et al. 2014). A previous study revealed that the C/N ratio of aquatic weeds, such as *E. densa*, P. malaianus, and *H. verticillate* ranged from 8.5 to 12.9 (Rabemanolontsoa and Saka, 2012; Kobayashi et al. 2013). In this study, similar ratios of 10.09 to 12.45, 11.18 to 13.79, and 10.02 to 13.48 for *E. densa*, *E. nuttallii*, and *P. maackianus* were obtained, respectively.

The seasonal changes in the chemical composition of each aquatic weed species are shown in Figure 2-2. While the chemical compositions of *E. densa* and *E. nuttallii* varied seasonally, *P. maackianus* did not. The lignocellulose contents of *E. densa* and *E. nuttallii*, consisting of lignin, hemicellulose, and cellulose, decreased in August and increased in October. In August, the levels of substances not measured in this study increased. Previous studies have revealed that aquatic weeds contain approximately 20% starch and 15% lipid (Kobayashi et al., 2014; Rabemanolontsoa and Saka, 2012). Therefore, most of the substances not lignocellulosic components may be starch and lipid. During summer, these two species develop lateral branches that are poor in lignocellulose to efficiently photosynthesize (Yarrow et al., 2009; Zehnsdorf et al., 2015). *E. densa* and *E. nuttallii* are native species of South America and are commonly found in tropical climates (Carrillo et al. 2006). These species have yearly life cycles in tropical areas. However, in temperate zones, such as Lake Biwa, these species follow annual life cycles (Haramoto and kushima, 1988) (Figure 2-3 and 2-4). It is known that *E. densa* and *E. nuttallii* remove their leaves, roots, and apical buds (Van Wijk, 1988), which contained a lower concentration of lignin than the stems (Zhang et al., 2014; Rueda et al., 2016). Therefore, these aquatic weed species become stem-main from summer to autumn. The content of some of the lignocellulose components, particularly the lignin content of *E. densa* and *E. nuttallii*, became higher during the autumn. However, *P. maackianus* is a perennial plant and does not defoliate in winter (Imamoto et al. 2008). Therefore, the chemical composition of *P. maackianus* did not vary compared to the other two species. According to the above results, the aquatic weed species having an annual lifecycle would change the chemical composition with the season.

### 2.3.2.  Seasonal variation of methane yields

Figures 2-5 represent the methane productions of each aquatic weed species. In all conditions, methane production almost finished ultimately within four days. Tonon et al. (2017) reported that methane production from duckweed almost finished within ten days. Koyama et al. (2014) reported that methane yield from aquatic weeds was almost completed within 7–14 days. These results are related to the high accessibility of the substrate to enzymes and microorganisms. The moisture content of fresh aquatic weed biomass is high (>90%) and may lead to rapid decompositions than terrestrial plants with a rigid structure and low moisture content. In addition, the higher amount of soluble exocellular polymers in the aquatic weeds may also contribute to the fast methane production.

The seasonal changes in the methane productivity of each aquatic weed species were Figure 2-6. The seasonal variations in the methane yields differed between each macrophyte species. The methane yield of *E. nuttallii* varied significantly, ranging from 211.6-251.5 mL g-VS$^{-1}$ and 189.2-284.1 mL g-VS$^{-1}$. This fluctuation is related to the seasonal changes in the chemical composition. However, the methane yield of *P. maackianus* varied slightly from 139.8-164.7 mL g-VS$^{-1}$ as the chemical composition of *P. maackianus* did not change seasonally. The methane potentials of *E. densa* and *E. nuttallii* are similar to those of the manures of calves, cattle, piglets, sows, pig fatteners (197-417 mL g-VS$^{-1}$; Triolo et al., 2011), which are already implemented to treat in anaerobic digestion. This indicates that these two species are easily degradable and could be implemented as substrates for anaerobic digestion. The methane yield of *E. densa* varied little, despite the seasonal changes in

the lignin content, while the methane yield of *E. nuttallii* varied seasonally with the change of lignin content. However, the methane yield of *P. maackianus* was remarkably lower than that of the other two species, indicating that the differences in the methane yields between different species were more extensive than those between different months for the same species. According to these results, the methane yields of the seasonally harvested aquatic weeds varied depending on the species composition. Therefore, the actual methane yield of the seasonally harvested aquatic weeds can be estimated according to the seasonal variations in the species composition.

### 2.3.3. Estimation of annual methane potential

Figure 2-7 shows the species composition and theoretical monthly methane yield (TMMY) of the harvested aquatic weeds. The dominant species remarkably varied seasonally. In April, the most abundant harvested aquatic weed was *P. maackianus*, and its ratio was gradually decreased over the summer. In contrast, the ratios of *E. nuttallii* and *H. verticillata* increased from June to August. In the fall, the ratio of *P. maackianus* increased again and constituted over 50% of the harvested aquatic weeds. The seasonality of species composition might be regulated by the different responses of each aquatic weed growth rate to water temperature. Imamoto et al. (2008) reported that *P. maackianus* and *E. nuttallii* relative had high growth rates at low temperatures, and *H. verticillata* was higher at a high temperature (Imamoto et al., 2008). These results corresponded to the seasonal predominance of *E. nuttallii* in May, *H. verticillate* from June to August, and *P. maackianus* in the fall. Along with the seasonal changes in the species composition, the TMMY varied from 171–231 $m^3$ ton-VS$^{-1}$. Notably,

the TMMY decreased to 75% from August to September with an increase in the abundance of *P. maackianus*, which had a low BMP. With the continuous anaerobic digestion of a less biodegradable substrate, undegraded solid components likely remain in the reactor, leading to the washing-out of microorganisms. To avoid a failure in the anaerobic digestion process, pre-treatment or co-digestion would be required for increasing the methane yield when *P. maackianus* becomes the dominant species in Lake Biwa.
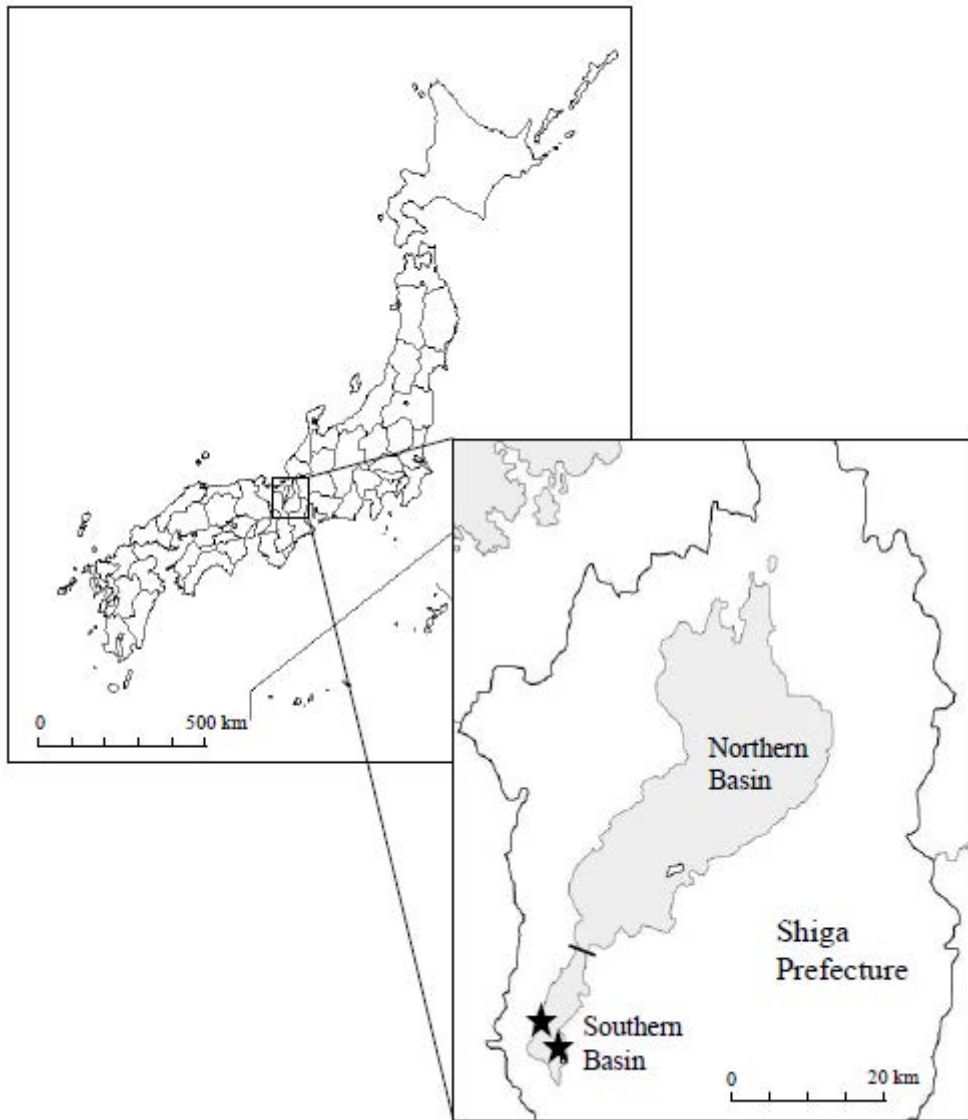
Figure 2-1. Sampling point of aquatic weeds.

Table 2-1. Proximate and ultimate analysis of harvested aquatic weeds.

(a) *Egeria densa*

|  | June | July | August | September | October | Average | SD |
|---|---|---|---|---|---|---|---|
| TS (%-FM) | - | 8.8 | 9.7 | 7.8 | 8.0 | 8.6 | 0.9 |
| VS (%-FM) | - | 7.9 | 8.2 | 6.4 | 6.2 | 7.2 | 1.0 |
| Moisture (%-FM) | - | 91.2 | 90.4 | 92.2 | 92.1 | 91.4 | 0.9 |
| Total carbon (mg g-VS$^{-1}$) | - | 342.0 | 314.5 | 310.4 | 301.3 | 317.1 | 17.5 |
| Total nitrogen (mg g-VS$^{-1}$) | - | 29.0 | 25.3 | 30.8 | 24.3 | 27.3 | 3.1 |
| C/N (%) | – | 11.8 | 12.5 | 10.1 | 12.4 | 11.7 | 1.1 |

(b) *Elodea nuttallii*

|  | June | July | August | September | October | Average | SD |
|---|---|---|---|---|---|---|---|
| TS (%-FM) | 7.9 | 8.2 | 10.5 | 11.0 | 9.4 | 9.4 | 1.3 |
| VS (%-FM) | 6.4 | 6.9 | 9.1 | 9.2 | 8.3 | 8.0 | 1.3 |
| Moisture (%-FM) | 92.1 | 91.8 | 89.5 | 89.0 | 90.6 | 90.6 | 1.3 |
| Total carbon (mg g-VS$^{-1}$) | 307.9 | 313.8 | 305.2 | 328.5 | 357.0 | 322.5 | 21.3 |
| Total nitrogen (mg g-VS$^{-1}$) | 24.8 | 26.4 | 23.1 | 29.4 | 25.9 | 25.9 | 2.3 |
| C/N (%) | 12.4 | 11.9 | 13.2 | 11.2 | 13.8 | 12.5 | 1.0 |

(c) *Potamogeton maackianus*

|  | June | July | August | September | October | Average | SD |
|---|---|---|---|---|---|---|---|
| TS (%-FM) | 12.9 | 15.1 | 13.3 | 15.8 | 11.6 | 13.7 | 1.7 |
| VS (%-FM) | 11.3 | 11.7 | 11.8 | 13.8 | 10.6 | 11.8 | 1.2 |
| Moisture (%-FM) | 87.2 | 84.9 | 86.7 | 84.2 | 88.4 | 86.3 | 1.7 |
| Total carbon (mg g-VS$^{-1}$) | 335.0 | 291.3 | 311.4 | 342.5 | 368.8 | 329.8 | 29.7 |
| Total nitrogen (mg g-VS$^{-1}$) | 24.9 | 21.7 | 25.9 | 34.2 | 31.7 | 27.7 | 5.2 |
| C/N | 13.5 | 13.4 | 12.0 | 10.0 | 11.6 | 12.1 | 1.4 |
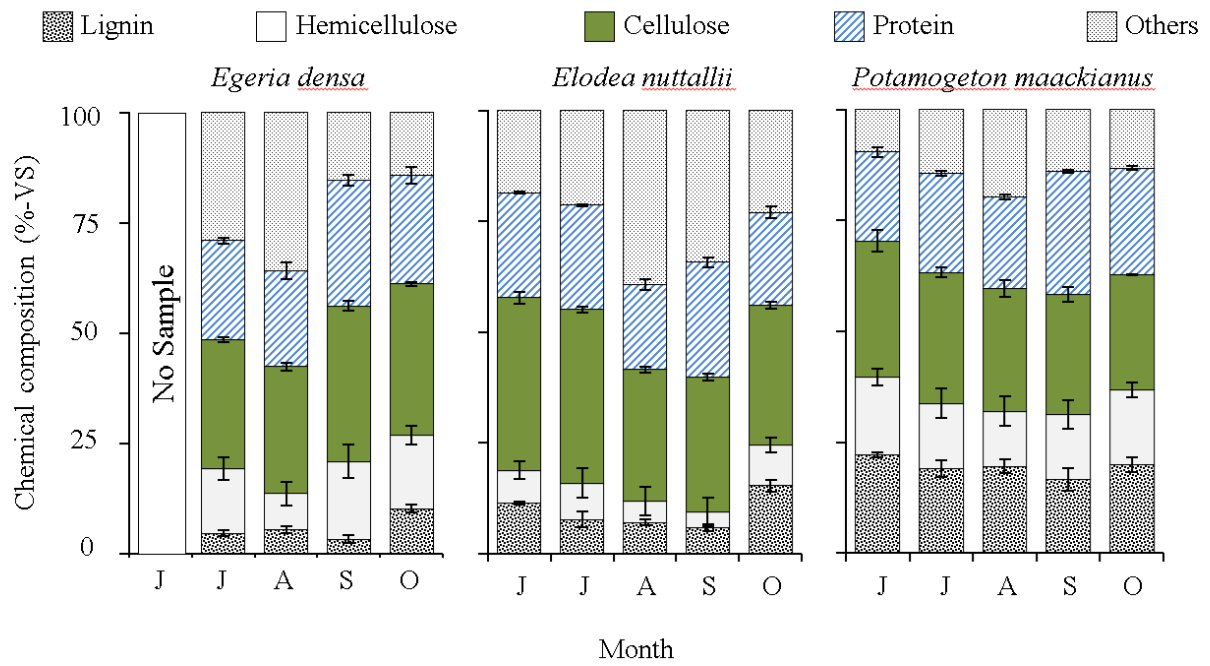
Figure 2-2. Seasonal changes of chemical composition of submerged macrophytes. Error bars mean standard deviation.

(a) *Egeria densa*

Surface water temp.(°C)

| 0 | 9 | 10 | 19 | 20 | 21 | 30 | 31 | 17 | 14 | 5 |

Ice covering

———— Flowering ————

Max. root biomass

Branching

·········——— Elongation ———

Max. shoot biomass

| Winter type | Summer type | Winter type |

Water surface

Distance from bottom (m)

1.5

1.0

0.5

0

Jan  Feb  Mar  Apr  May  Jun  Jul  Aug  Sep  Oct  Nov  Dec

(b) *Elodea nuttallii*

| Surface | 6 | 10 | 12 | 18 | 24 | 24 | 25 | 27 | 27 | 34 | 32 | 30 | 29 | 24 | 22 | 16 | 12 | 8 |
| Bottom | 6 | 9 | 11 | 15 | 19 | 21 | 23 | 23 | 23 | 22 | 23 | 24 | 23 | 19 | 17 | 15 | 11 | 8 |

Water temp. (°C)

———Flowering———         New root development

Max. root biomass                Min. root biomass

————— Defoliation —————

———Branching———

———Elongation———         Max. shoot biomass

Sinking

Distance from bottom (m)

2

1

leafy stem →

← leafless stem

← root

0

Jan  Feb  Mar  Apr  May  Jun  Jul  Aug  Sep  Oct  Nov  Dec

Figure 2-3. Lifecycle of (a) *Egeria densa* (Described by Haramoto and Ikushima 1987) and (b) *Elodea nuttallii* (Described by Kunii 1987) in Japan.
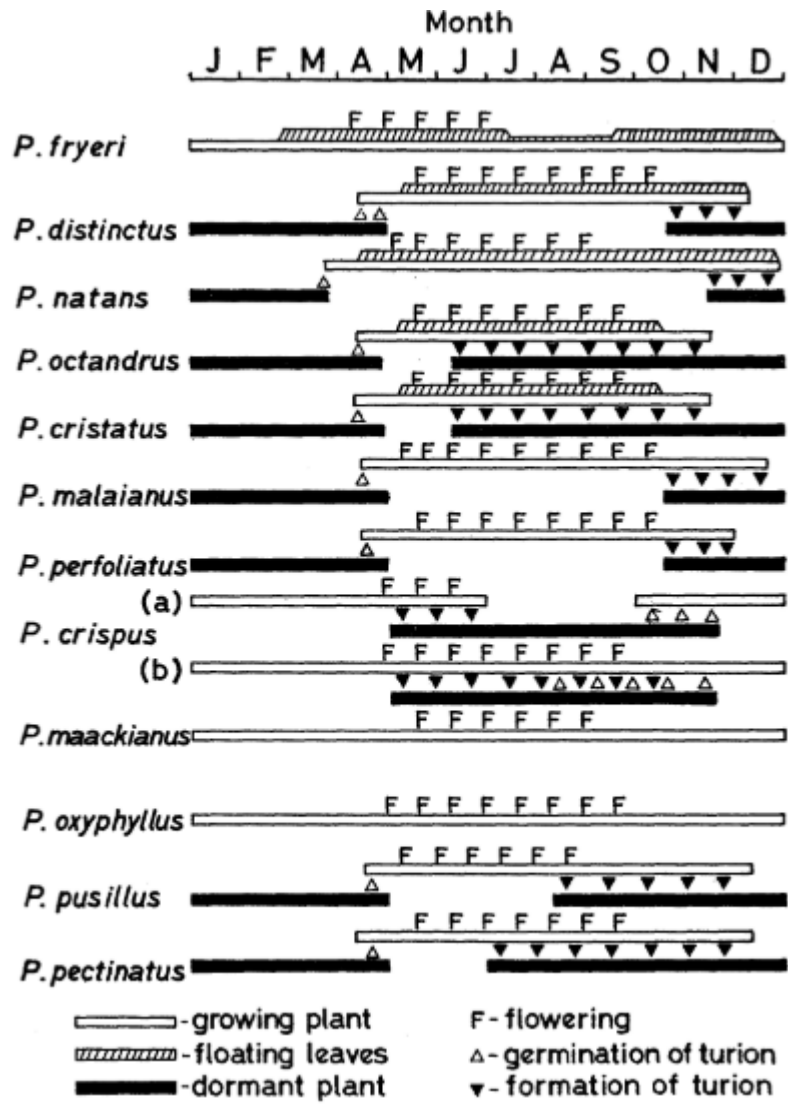
Figure 2-4. Lifecycle of 12 *potamogeton* species observed in the southwestern part of Japan. (Described by Kadono 1984)
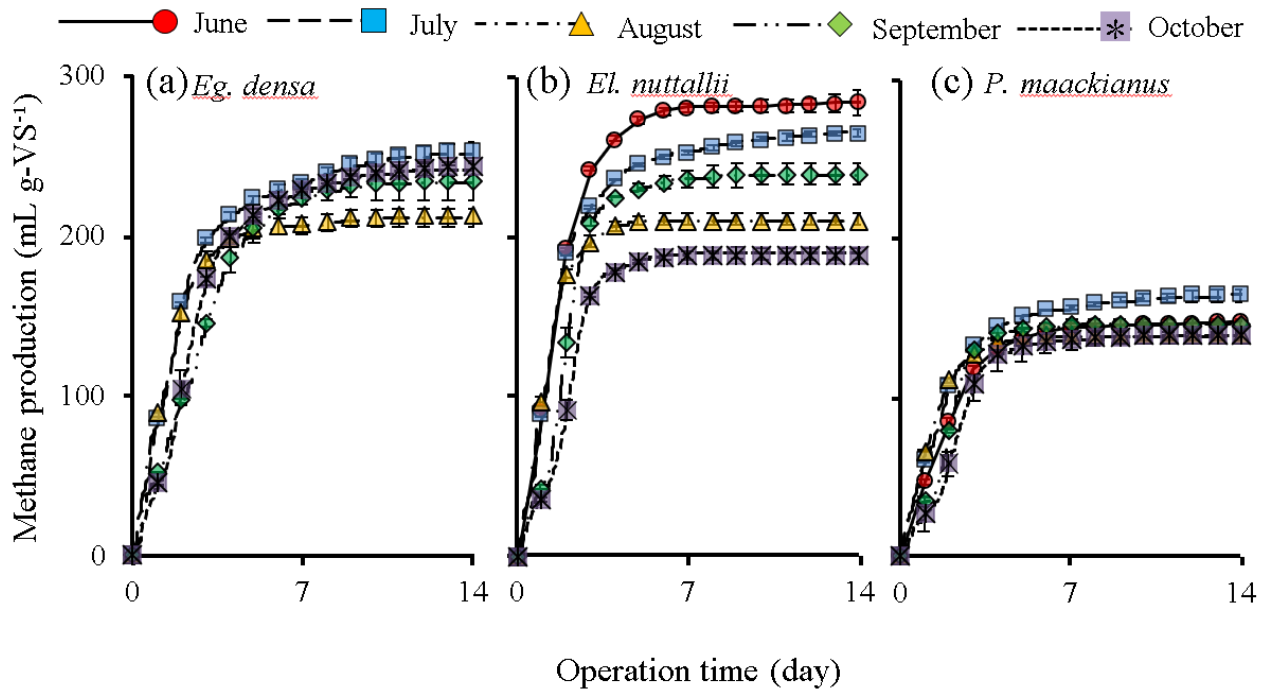
Fig. 2-5. Methane yield of three submerged macrophyte species harvested in different months. Error bars mean standard deviation.
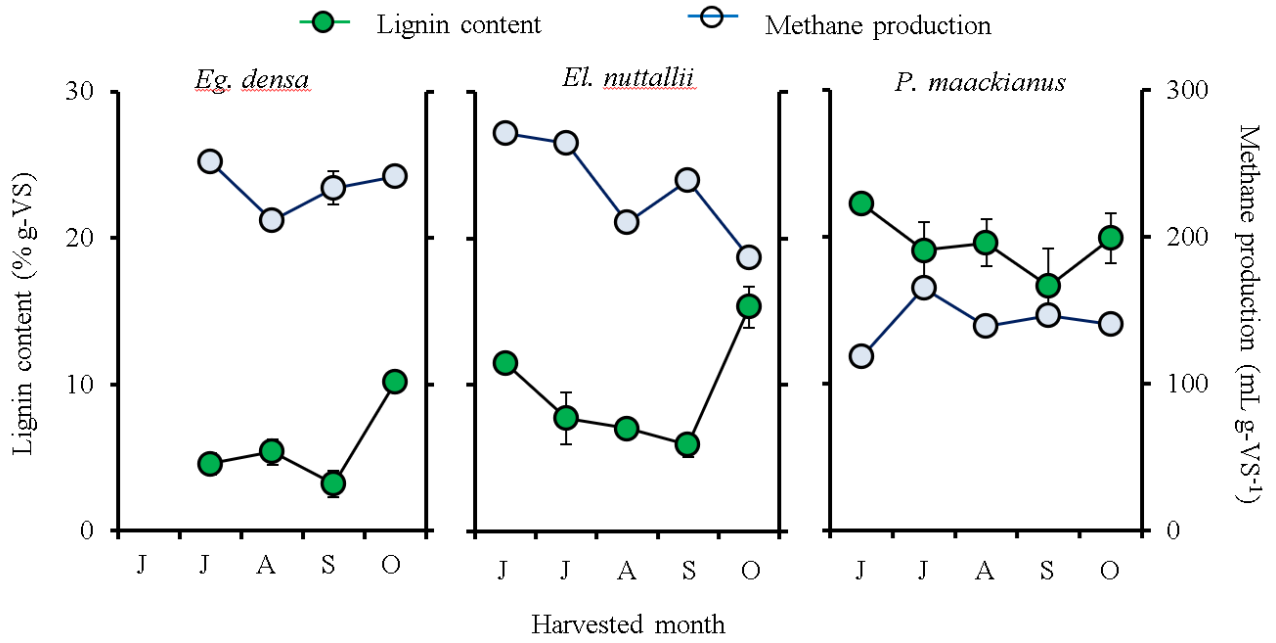
Fig. 2-6. Seasonal changes of lignin content and methane production of submerged macrophyte species. Error bars mean standard deviation.
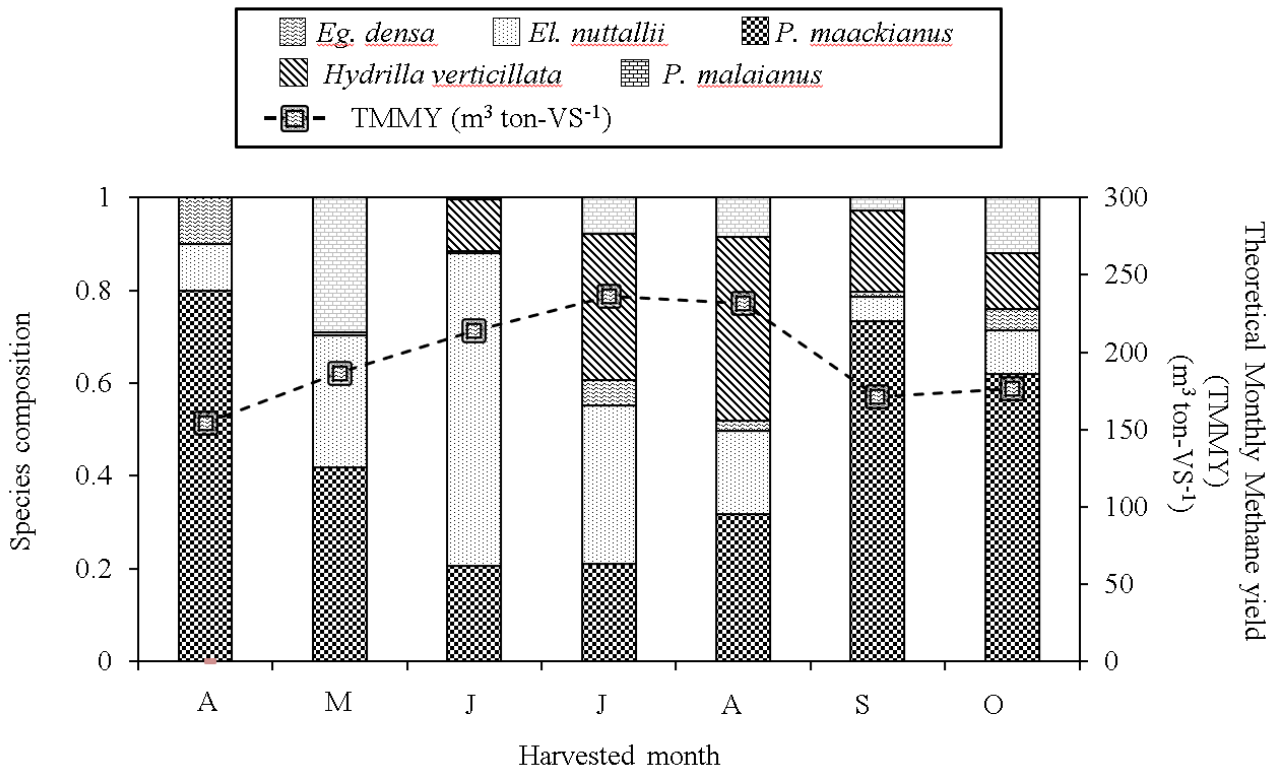
Fig. 2-7. Seasonal changes of species composition and TMMY of harvested aquatic weeds in lake Biwa.

# Chapter Ⅲ

# Relationships between the lignocellulosic components and anaerobic digestibility

## 3.1. Introduction

The ratio of each lignocellulosic component would influence the anaerobic digestibility since lignocellulosic components are covered/linked to each other. Previous studies on terrestrial plants reported that cellulose/lignin or (cellulose + hemicellulose)/lignin significantly affects methane yield (Liu et al., 2015; Wang et al., 1994) due to the coverage of lignin to cellulose and hemicellulose. Clarifying the relationships between lignocellulosic components and not only methane yield but also these kinetic parameters makes it possible to understand the characteristics of anaerobic digestibility by only analyzing its lignocellulosic composition. To understand the anaerobic digestibility of substrate, a kinetic model such as modified Gompertz was applied in numerous studies. Linking lignocellulosic components and kinetic parameters may help to assume significant pre-treatment options, appropriate operational conditions such as hydraulic retention time (HRT), and estimation of approximate methane recovery for implementation of anaerobic digestion of aquatic weeds.

## 3.2. Materials and methods

### 3.2.1. Substrate and inoculum

For the substrates, nineteen samples of freshwater aquatic weed used were harvested from Lake Biwa, Shiga prefecture, and Japan (35°20′N, 136°10′E). The data of lignocellulosic

compositions and BMP tests of *Egeria densa*, *Elodea nuttallii*, and *Potamogeton maackianus* were used from Study 1. *Spirodela polyrhiza* and *Trapa japonica* were harvested in August 2018, and *Hydrilla verticillata* was harvested in August, September and October 2015. All harvested aquatic weeds were dried at 80°C for 12 hours, milled, and passed through a 2 mm sieve as same as study 1. The milled aquatic weeds were then used for BMP tests and lignocellulose composition analysis. For the seed sludge, the mesophilic anaerobic sludge from Hokubu Sludge Treatment Center, Kanagawa Prefecture, Japan, was applied. The collected sludge was left for 2 – 4 days in the temperature-controlled room at 37 ± 1°C to allow for the removal of the residual substrate.

### 3.2.2. Batch anaerobic digestion

To evaluate the anaerobic digestibility of aquatic weeds, the BMP tests were conducted. An automatic methane potential test system (AMPTS II) supplied by Bioprocess Control (Sweden) was applied for the tests. Identical medium bottles with an effective volume of 300 mL were used as reactors. The substrate and seed sludge were added to the medium bottle in a volatile solids (VS) basis ratio of 1: 2. To make an anaerobic condition, reactors were purged with $N_2$. The BMP tests were performed at 37 ± 1°C for 14 days with a stirring setting of 10 seconds mixing and 10 seconds resting at the speed of 120 rpm. Generated biogas in digester flows into flowmeter via 80 mL vials containing 3 M solution of sodium hydroxide (NaOH) to remove the non-methane gases, such as carbon dioxide and hydrogen sulfide. The amount of biomethane was then measured by the device according to the liquid displacement and buoyancy principles. All tests and blanks were conducted in

triplicate, and the net methane production values were calculated. Furthermore, additional BMP tests were conducted to investigate the anaerobic digestibility of cellulose and sugars composing hemicellulose contained in aquatic weeds. According to the report of saccharified sugars composition in aquatic weeds (Rabemanolontsoa and Saka, 2012), crystalline cellulose and various hemicellulosic sugars such as arabinogalactan (AG), Xylo-oligo saccharide (XOS), glucomannan (GM), beta-glucan (BG) were selected as substrates.

### 3.2.3. Analytical parameters

Total solids (TS), volatile solids (VS) and methane yield were measured and analyzed using the standard procedure from APHA (2005). Lignocellulose (cellulose, hemicellulose and lignin) contents were measured by a detergent method as specified by Van Soest et al. (1991) using a fiber analyzer (Model: A-200, Ankom, USA). Methane yield was measured using AMPTS II.

### 3.3.    Results and discussion

### 3.3.1 Kinetics parameters obtained by modified Gompertz model

Lignocellulosic components and kinetic parameters calculated by fitting to the modified Gompertz model were shown in Table 3-1. Contents of cellulose, hemicellulose and lignin contents in previously recorded ranges of $217 - 518$ mg g-VS$^{-1}$, $7.1 - 226$ mg g-VS-1 and $38 - 206$ mg g-VS$^{-}$$^{1}$, respectively (Güngören Madenoğlu et al., 2019; Kaur et al., 2019; Kist et al., 2018; Kobayashi et al., 2014; Li et al., 2019; Rabemanolontsoa and Saka, 2012), which are similar to the result of this

research. All fitting results to the modified Gompertz model were high $R^2$ values of more than 0.96, indicating high reliability on obtained parameters. Ultimate methane yields in this study were 139 – 281 mL g-VS$^{-1}$. The maximum methane production rate showed 30 – 119 mL g-VS-1 day$^{-1}$, which is higher than fruits waste (4.2 – 42.8 mL g-VS$^{-1}$ day$^{-1}$; Sanjaya et al., 2016), livestock manures (5.5 – 25.2 mL g-VS$^{-1}$ day$^{-1}$; Kafle and Chen, 2016) and common reed (13.0 – 25.6 mL g-VS$^{-1}$ day$^{-1}$; Dragoni et al., 2017 ) and similar to or lower than food waste (40.6 – 148 mL g-VS$^{-1}$ day$^{-1}$, Alibardi and Cossu, 2015; Marañón et al., 2020). Especially, *E. densa*, *E. nuttallii* and *H. verticillata* showed a high maximum methane production rate, indicating these species were easily degradable. Because of the relatively short lag phase, 0.00 – 0.66 days, suggests all aquatic weed species were readily accessible for microbes. T80 of aquatic weeds were 1.9 – 4.2 days, which were shorter than that of corn stover (22 – 35 days, Wei et al. 2015), food waste (11.5 – 14.5 days, Marañón et al. 2020), and municipal solid waste (11.1 – 22.2 days, Dasgupta and Chandel, 2019) respectively, indicating that a most of easily degradable substances in aquatic weeds were rapidly decomposed in the short period, and thereafter, relatively uneasily degradable compounds were decomposed gradually. These variations in anaerobic digestibility parameters may affected by the variations of chemical compositions, especially lignocellulosic components.

### 3.3.2 Relationships between chemical compositions and kinetic parameters

Figure3-1 showed the relationships between lignocellulosic components and anaerobic digestibility parameters from the modified Gompertz model. Lignin content showed a significant

negative correlation with the methane yield (Figure3-1 (c), p < 0.05). A similar result was reported by Koyama et al. (2014), while Kobayashi et al. (2014) reported no significant relationship. The difference in the results in the result of this study and the findings of Kobayashi et al. (2014) may be due to variations in the operational periods. Therefore, the relationship between lignin and ultimate methane yield may change with the operational period in the BMP test. To discuss the potential and challenges for utilizing the aquatic weed as feedstock, BMP results in shorter operational periods (15 – 30 days) would be desirable. Cellulose showed a significant positive correlation with the ultimate methane yield (Figure 3-1 (a), $p < 0.05$) and maximum methane production rate (Figure 3-1 (d), $p < 0.05$). The amount of cellulose in the biomass would have contributed to the ultimate methane production since cellulose is composed of only glucose, which is a degradable substance for anaerobic digestion (Mussatto et al., 2008). Hemicellulose content was not correlated with ultimate methane yield. Hemicellulose is a chain of hetero-polysaccharides with a short-branch consisting of various sugar units such as mannose, arabinose, xylose, glucose and galactose with lower polymerization degree in the range of 80 – 200 (Rabemanolontsoa and Saka, 2013). Generally, hemicellulose has been considered a readily biodegradable component because hemicellulose is hydrolyzed with weak acid and heating (Peng et al., 2012). Unexpectedly, hemicellulose had a significant negative correlation with the maximum methane production rate (Figure 3-1 (e), $p < 0.01$) and positive correlation with T80 (Figure 3-1 (h), $p < 0.05$). These results imply that hemicellulose of aquatic weed is not much easily degradable. The detailed insight for the low hemicellulose degradability will be discussed in the following sections. Incidentally, no correlation was recorded between the lag phase

and lignocellulosic components, suggesting lignocellulosic components did not enhance or inhibit the microbial activity in early degradation steps during anaerobic digestion. Regarding to other non-lignocellulosic components, they did not have significant correlations with any kinetic parameters.

### 3.3.3. Relationships between lignocellulosic ratios and kinetic parameters

The complicated linkage existing between cellulose, hemicellulose, and lignin may affect others' degradability. The relationship between the ratio of the lignocellulosic components (cellulose/lignin, hemicellulose/lignin, cellulose/hemicellulose) and anaerobic digestibility (ultimate methane yield and maximum methane production rate) were analyzed to investigate the synergetic effect of the complicated linkage between three cell wall components (Figure3- 2). T80 and lag phase did not show significant correlations with any ratio of lignocellulosic components. The ultimate methane yield of aquatic weeds was adequately expressed by cellulose/lignin ($R^2 = 0.657$) and the maximum methane production rate by cellulose/hemicellulose ($R^2 = 0.829$), respectively, as shown in Figure 3-2. This apparent relationship between cellulose/lignin and ultimate methane yield may have resulted from the resistance of cellulose to degradation due to the masking effect of lignin and adsorption of the enzyme cellulase by lignin (Koyama et al., 2016). According to Liu et al. (2015), a significant linear correlation between cellulose/lignin and BMP in agricultural residues such as corn stover, wheat straw, and sugarcane bagasse was reported, indicating that methane yield from lignocellulosic biomass (i.e., both terrestrial plants and aquatic weeds) can be predicted by cellulose/lignin. The strong correlation of cellulose/hemicellulose and maximum methane production

rate could be related to the coverage of cellulose by hemicellulose, which accounts for the recalcitrance of cell walls (Kumagai and Endo, 2018).

### 3.3.4. Investigation of factors determining the degradability of hemicellulose

To investigate how hemicellulose affects anaerobic digestibility of lignocellulosic biomass, BMP tests of sugars composing hemicellulose such as arabinogalactan (AG), xylo-oligo saccharide (XOS), glucomannan (GM), beta-glucan (BG) were performed. Figure 3-3 shows the result of BMP tests of sugars composing hemicellulose. Crystallized cellulose was also tested its BMP for comparison. Ultimate methane yield of crystalized cellulose recorded a methane yield value of 354 ml g-VS$^{-1}$ (Table 3-2), suggesting easily degradable. Maximum methane production rate and T80 of crystalized cellulose were 111.1 mL g-VS$^{-1}$ day$^{-1}$ and 4.9 days, respectively. Comparing crystalized cellulose with AG, GM and BG, a higher maximum methane production rate (75.2 – 143.8 mL g-VS$^{-1}$ day$^{-1}$) and shorter T80 (2.4 – 5.1 days) and almost the same ultimate methane yield (361 – 382 mL g-VS$^{-1}$) were recorded. On the other hand, XOS showed a lower methane yield of 286 mL g-VS$^{-1}$. Furthermore, XOS showed 2.5 – 4.8 times lower maximum methane production rate (29.8 mL g-VS$^{-1}$ day$^{-1}$) and 1.5 – 3.3 times longer T80 (7.9 days) than other hemicellulosic sugars. XOS is the polymer of xylose which accounted 22 to 70% of hemicellulosic sugars in *E. densa*, *E. nuttallii*, *P. maackianus*, *H. verticillata* and water hyacinth (Rabemanolontsoa and Saka, 2013). Similar to this study, BMP tests of xylose performed by Li et al. (2018) recorded methane yield of 203 mL g-VS$^{-1}$, and lower maximum methane production rate than other hemicellulosic sugars. Therefore, the amount of xylose

might relate to the low degradability of hemicellulose in aquatic weeds.

To evaluate the effect of xylose on anaerobic digestibility of aquatic weeds, xylose amount was estimated by multiplying hemicellulose contents in this study and proportion of hemicellulosic sugars in each biomass obtained by Rabemanolontsoa and Saka (2013). Notably, the maximum methane production rate showed stronger significant positive correlation with estimated xylose amount (Figure 3-4) than that with hemicellulose (Figure 3-2 (i)). This result accorded to BMP tests of hemicellulosic sugars which suggested that xylose has a low degradability. These results imply that the low degradability of hemicellulose is related to xylose in aquatic weeds; thus, xylose amount or its ratio on lignocellulosic components possibly affect kinetic parameters of the methane production. The maximum methane production was also adequately expressed with cellulose/estimated xylose ($p < 0.005$) (Figure3-5). The results of fitting between cellulose/estimated xylose and maximum methane production rate suggest that the low degradability of xylose limits the degradation of cellulose. Furthermore, the structural features of the xylose in hemicellulose also might contribute to the strong correlation recorded. Xylose is the main component of the linear polysaccharide such as xyloglucan and arabinoxylan, and other hemicellulosic sugars such as rhamnose, arabinose and galactose form a branch of the primary linear polymer (Rennie and Scheller, 2014). Thus, a high xylose ratio in hemicellulosic sugars probably indicates a high linear polymerization of hemicellulose that will be high resistant to degradation. The work of Terrett and Dupree (2018) shows that xylose composes the hemicellulose-lignin module via to ferulate which is a phenol composing lignin. Grabber et al. (1998) reported that during the enzymatic degradation of maize, decreasing the cross-

linking of xylan (a group of hemicellulose) to lignin with ferulate improved degradation efficiency. Following the gradient degradation of xylose during the anaerobic digestion, the masking effect of lignin on lignocellulose was possibly moderated. These results show that presence of the steady amount of xylose linked with cellulose and lignin can regulate the degradability of lignocellulosic biomass.

### 3.3.5 Comparison of the effect of lignocellulosic components on anaerobic digestibility between aquatic weed and terrestrial plants

The relationships between the ratio of lignocellulosic components and anaerobic digestibility of terrestrial herbaceous plants and aquatic weeds were performed (Figure 3-6). The relationship between cellulose/lignin and ultimate methane yield including the aquatic weeds and terrestrial herbaceous plants was fitted to an equation, $y = 61.7 \ln(x) + 170.4$, n= 94, $R^2$= 0.60 (Figure 3-6, (A)). This result indicated that the adsorption of cellulase by the lignin and limitation of cellulose degradation were almost to the same degree in the terrestrial herbaceous plants and aquatic weeds. Cellulose/hemicellulose and maximum methane production rate was not fitted in the same model; $y = 29.6\ ln(x) + 34.7$, $n= 33$, $R^2$= 0.47 in aquatic weeds and $y = 12.1\ ln(x) + 16.2$, $n= 61$, $R^2$= 0.44 in terrestrial herbaceous plants (Figure3-6). The model including aquatic weeds and terrestrial plants was fitted to $y = 32.7\ ln(x) + 18.1$, $n= 94$, $R^2$= 0.57. Aquatic weeds had a higher maximum methane production rate compared to the terrestrial herbaceous plants. The differences recorded in the biomass may be due to the ratio and structural differences, such as xylose ratio in the aquatic weeds and

terrestrial herbaceous plants. By multiplying the proportion of hemicellulosic sugars from Rabemanolontsoa and Saka (2013) and hemicellulose contents in aquatic weeds in the present study, the amount of xylose in the biomass was estimated. The maximum methane production rate was adequately expressed with cellulose/estimated xylose (p < 0.005) on an equation including both aquatic weeds and terrestrial plants (Figure3-8), with a higher $R^2$ compared to the cellulose/hemicellulose ratio. Cellulose/estimated xylose ratio in terrestrial herbaceous plants was recorded in a small variation between 0.80 – 3.26, while in aquatic weed, a wide variation of 3.21 – 35.92 was recorded. Maximum methane production rate also showed a narrow range of 9.8 – 36.0 mL g-VS$^{-1}$ day$^{-1}$ in terrestrial herbaceous plants and a wide range of 45.5 – 119.4 mL g-VS$^{-1}$ day$^{-1}$ in aquatic weeds. These results might be led to the difference in the ratio of xylose in hemicellulosic sugars, which in aquatic weeds showed a smaller value of 22 – 50% while terrestrial plants showed a high and narrow range of 60-80%, reported by Rabemanolontsoa and Saka (2013). Consequently, the higher variation of xylose in aquatic weeds may lead to the difference in maximum methane production rate, although terrestrial herbaceous plants showed small variations of the xylose amount and maximum methane production rate. To our knowledge, this is the first result that revealed clear correlations between cellulose/lignin and ultimate methane yield in aquatic weeds, and between cellulose/hemicellulose, cellulose/xylose and maximum methane production rate in lignocellulosic biomass, including aquatic weeds, making it possible to clarify the effect of lignocellulosic components and the ratio on the methane productivity.

Table 3-1. Lignocellulosic composition and anaerobic digestibility of the aquatic weeds estimated by fitting to modified Gompertz model. $B_0$: ultimate methane yield, $\mu_m$: maximum methane production rate, $\lambda$: lag phase.

| | Harvested month | Cellulose (mg g-VS⁻¹) | Hemicellulose (mg g-VS⁻¹) | Lignin (mg g-VS⁻¹) | $B_0$ (mL g-VS⁻¹) | $\mu_m$ (mL g-VS⁻¹ day⁻¹) | $\lambda$ (d) | T80 (d) | $R^2$ |
|---|---|---|---|---|---|---|---|---|---|
| *Egeria densa* | Jul. 2015 | 292.1 | 146.7 | 45.6 | 248.9 | 75.9 | 0.000 | 3.28 | 0.984 |
| | Aug. 2015 | 288.0 | 82.2 | 53.6 | 209.5 | 86.1 | 0.058 | 2.43 | 0.995 |
| | Sep. 2015 | 352.7 | 176.7 | 31.9 | 233.8 | 54.8 | 0.208 | 4.23 | 0.998 |
| | Oct. 2015 | 342.3 | 167.2 | 101.3 | 237.1 | 68.8 | 0.361 | 3.69 | 0.995 |
| *Elodea nuttallii* | Jun. 2015 | 389.5 | 73.0 | 114.8 | 280.8 | 109.4 | 0.192 | 2.55 | 0.998 |
| | Jul. 2015 | 392.0 | 81.5 | 77.1 | 257.6 | 103.9 | 0.156 | 2.52 | 0.990 |
| | Aug. 2015 | 297.4 | 48.3 | 70.0 | 210.4 | 119.4 | 0.205 | 1.89 | 0.998 |
| | Sep. 2015 | 304.5 | 35.3 | 58.8 | 237.4 | 103.9 | 0.640 | 2.76 | 0.995 |
| | Oct. 2015 | 316.1 | 91.5 | 153.0 | 188.7 | 76.7 | 0.664 | 2.90 | 0.993 |
| *Potamogeton maackianus* | Jun. 2015 | 306.9 | 174.6 | 222.3 | 146.7 | 45.5 | 0.076 | 3.04 | 0.996 |
| | Jul. 2015 | 295.2 | 147.2 | 190.4 | 161.2 | 54.5 | 0.004 | 2.85 | 0.994 |
| | Aug. 2015 | 276.7 | 124.4 | 195.6 | 138.9 | 70.3 | 0.110 | 2.04 | 0.997 |
| | Sep. 2015 | 271.9 | 145.9 | 165.9 | 146.8 | 59.4 | 0.501 | 2.81 | 0.986 |
| | Oct. 2015 | 258.5 | 169.9 | 198.8 | 139.4 | 47.5 | 0.600 | 3.51 | 0.994 |
| *Hydrilla verticillata* | Aug. 2015 | 356.1 | 94.4 | 110.9 | 216.6 | 84.1 | 0.471 | 2.84 | 0.998 |
| | Sep. 2015 | 386.3 | 121.0 | 139.6 | 199.5 | 86.1 | 0.369 | 2.53 | 0.991 |
| | Oct. 2015 | 394.5 | 202.9 | 177.0 | 199.1 | 81.0 | 0.439 | 2.70 | 0.997 |
| *Trapa japonica* | Aug. 2018 | 229.4 | 101.3 | 91.9 | 138.5 | 53.0 | 0.000 | 2.69 | 0.978 |
| *Spirodela polyrhiza* | Aug. 2018 | 202.1 | 178.5 | 132.8 | 144.7 | 30.3 | 0.000 | 3.94 | 0.976 |
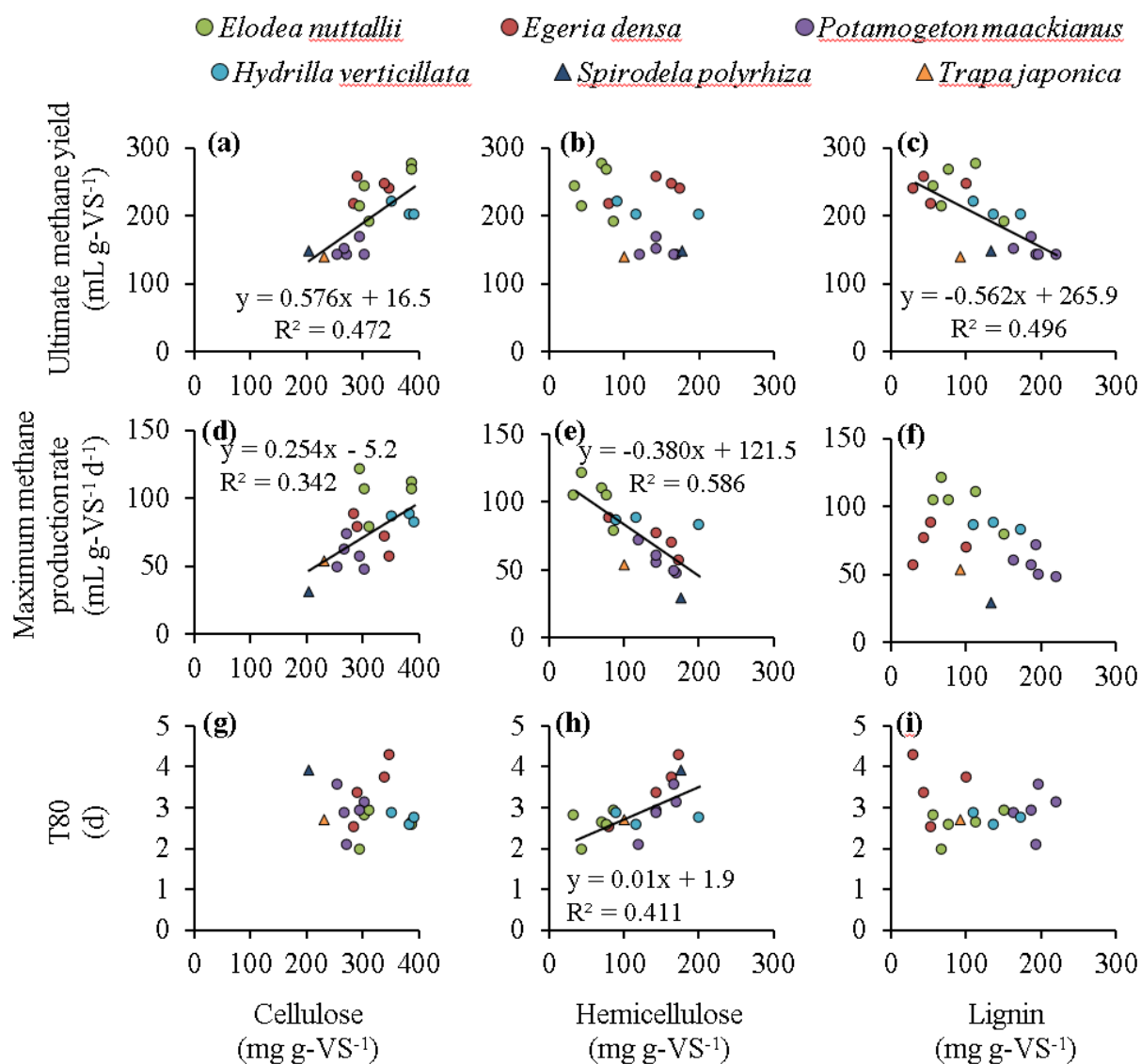
Figure 3-1. Relationship between lignocellulosic compositions (cellulose, hemicellulose and lignin) and anaerobic digestibility (ultimate methane yields, maximum methane production rate and T80). Solid lines represent $p < 0.05$.

Figure 3-2. Relationship between the ratio of lignocellulosic components (cellulose/ lignin, cellulose/hemicellulose, and hemicellulose/lignin) and anaerobic digestibility (ultimate methane yield and maximum methane production rate). Solid lines represent $p < 0.05$.

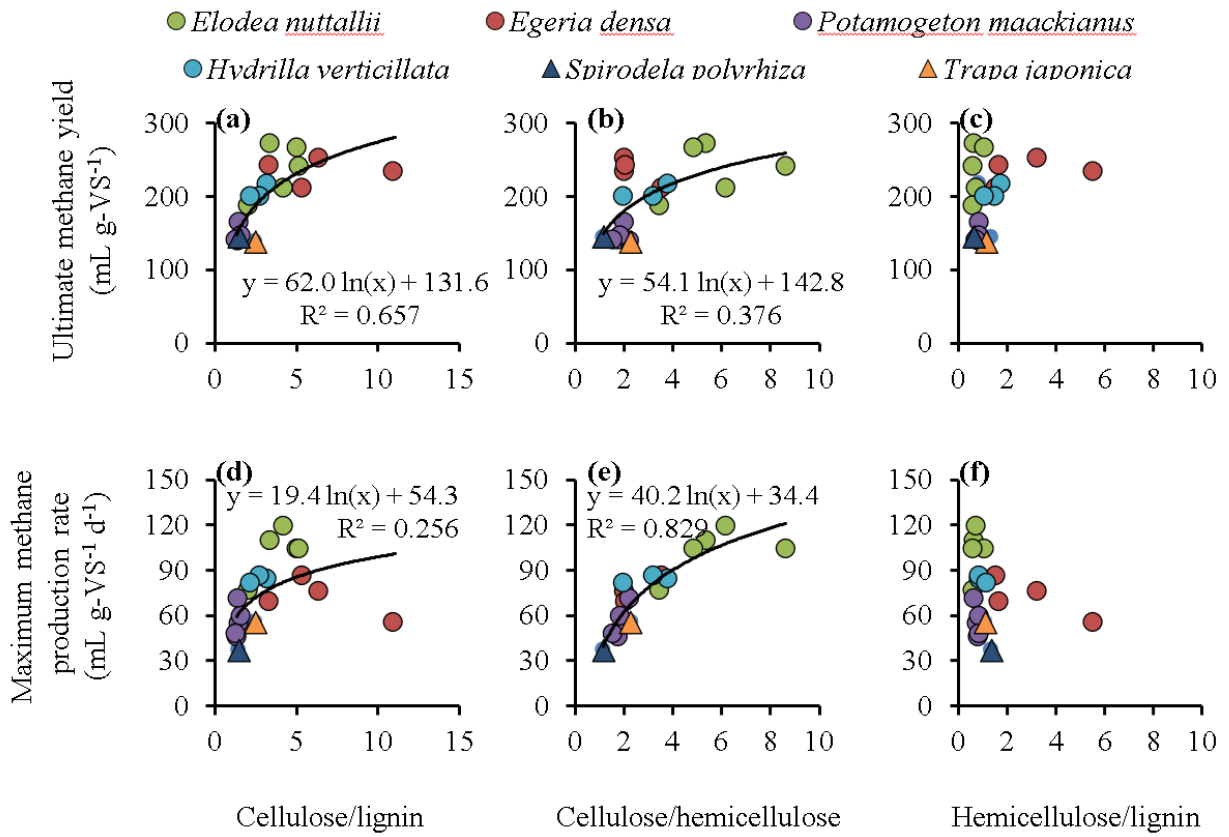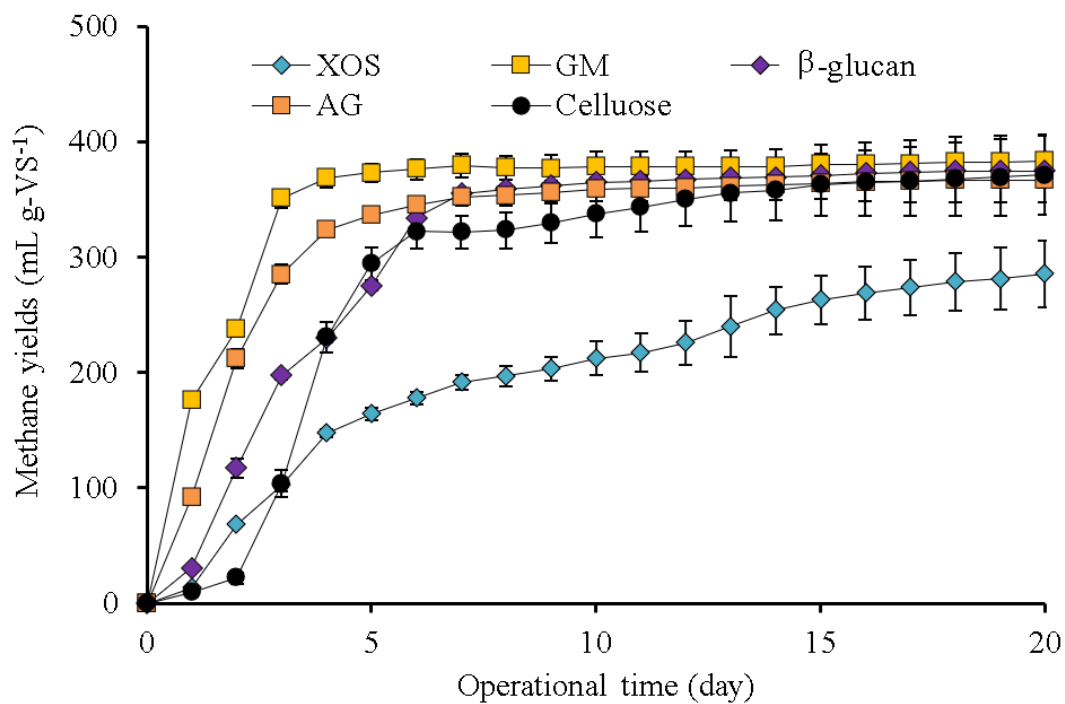Figure 3-3. Methane yields of sugars composing cellulose and hemicellulose. XOS: xylo-oligo saccharide, GM: glucomannan, β-glucan: beta-glucan, AG: arabinogalactan. Vertical bars represent standard deviation.

Table 3-2. Obtained parameters by fitting to modified Gompertz model

| Substrate | $B_0$ (mL g-VS$^{-1}$) | $\mu_m$ (mL g-VS$^{-1}$ day$^{-1}$) | $\lambda$ (d) | $R^2$ | T80 (day) |
|---|---|---|---|---|---|
| Cellulose | 354.1 | 111.09 | 1.98 | 0.990 | 4.93 |
| β-glucan | 372.5 | 75.24 | 0.59 | 0.995 | 5.14 |
| Glucomannan | 382.3 | 143.77 | 0.00 | 0.985 | 2.44 |
| Arabinogalactan | 360.9 | 117.93 | 0.23 | 0.996 | 3.06 |
| Xylo-oligo saccharide | 259.1 | 27.90 | 0.00 | 0.965 | 8.28 |
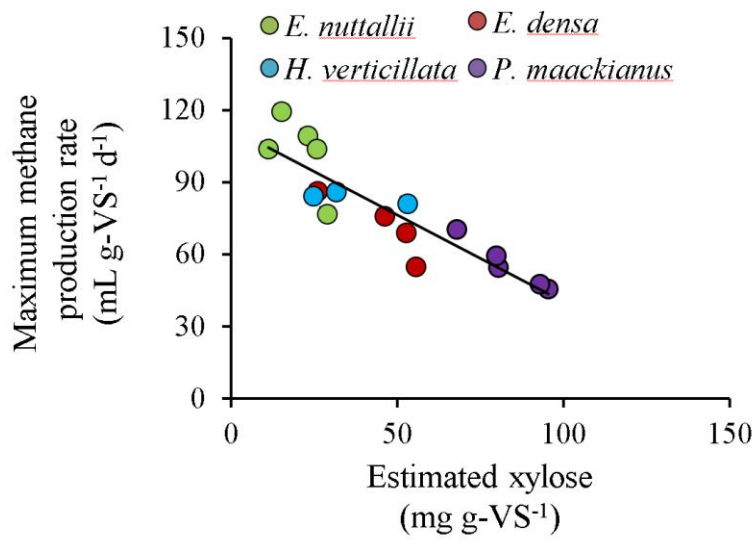
Figure 3-4. Relationship between maximum methane production rate and estimated xylose. Obtained equation was $y = -0.72x + 112.5$, $R^2 = 0.809$ ( $p < 0.005$).
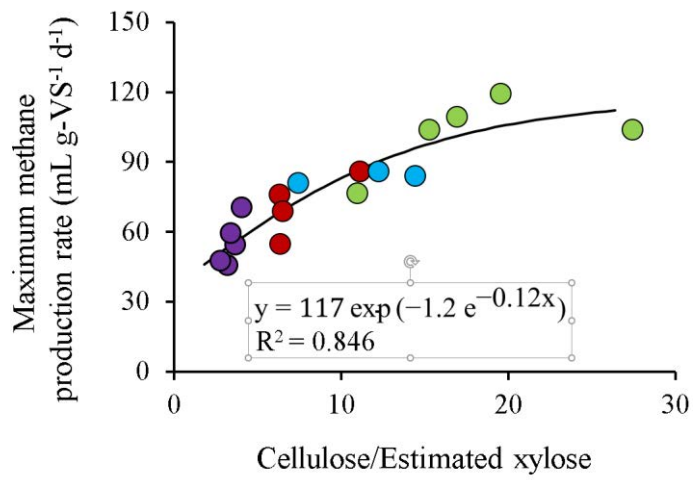
Figure 3-5. Relationships between the estimated xylose concentration in the aquatic weeds and methane yield, Cellulose/ Estimated xylose and maximum methane production rate. Solid lines represent $p < 0.05$.
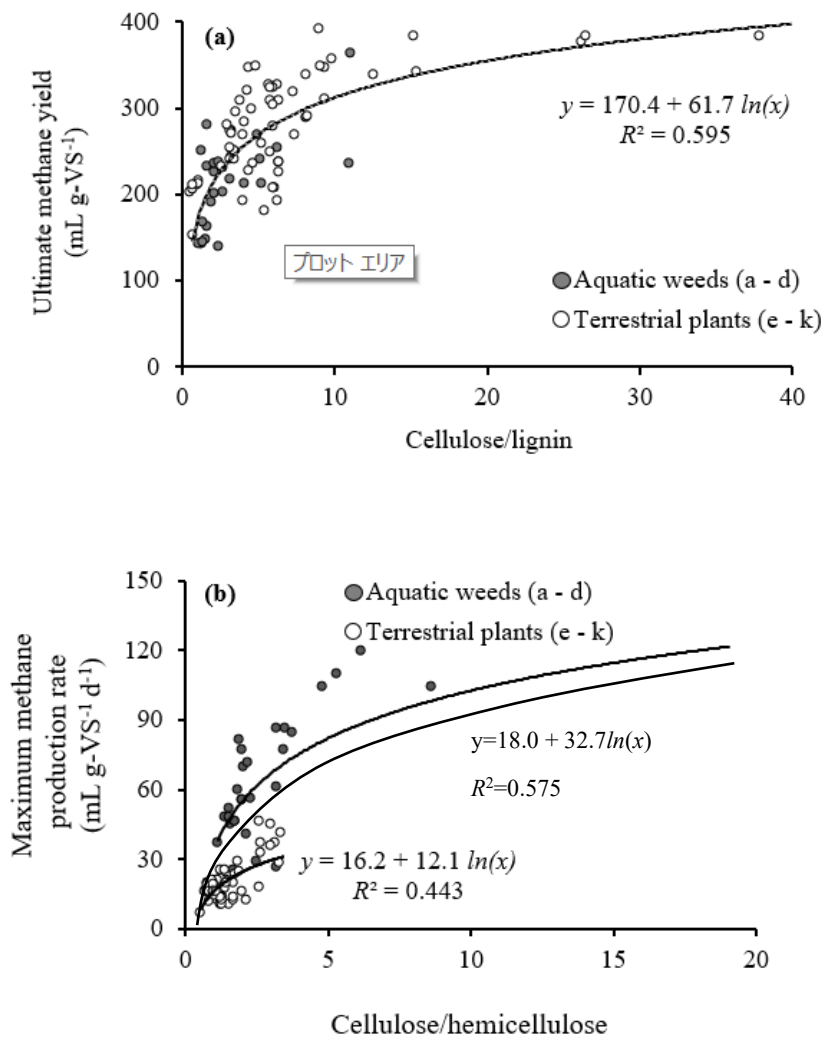
Figure 3-6. Relationships between cellulose/lignin and ultimate methane yield (a), between cellulose/hemicellulose and maximum methane production rate (b), and between maximum methane production rate. (a) This study, (b) Koyama et al. (2014), (c) Kist et al. (2018), (d) Li et al. (2019), (e) Triolo et al. (2011), (f) Melts et al. (2014), (g) Dahunsi et al. (2019), (h) Li et al. (2017), (i) Chen et al. (2019), (j) Kandel et al. (2013), (k) Dragoni et al. (2017). Solid lines represent $p < 0.05$, and plot line represents $p > 0.05$.
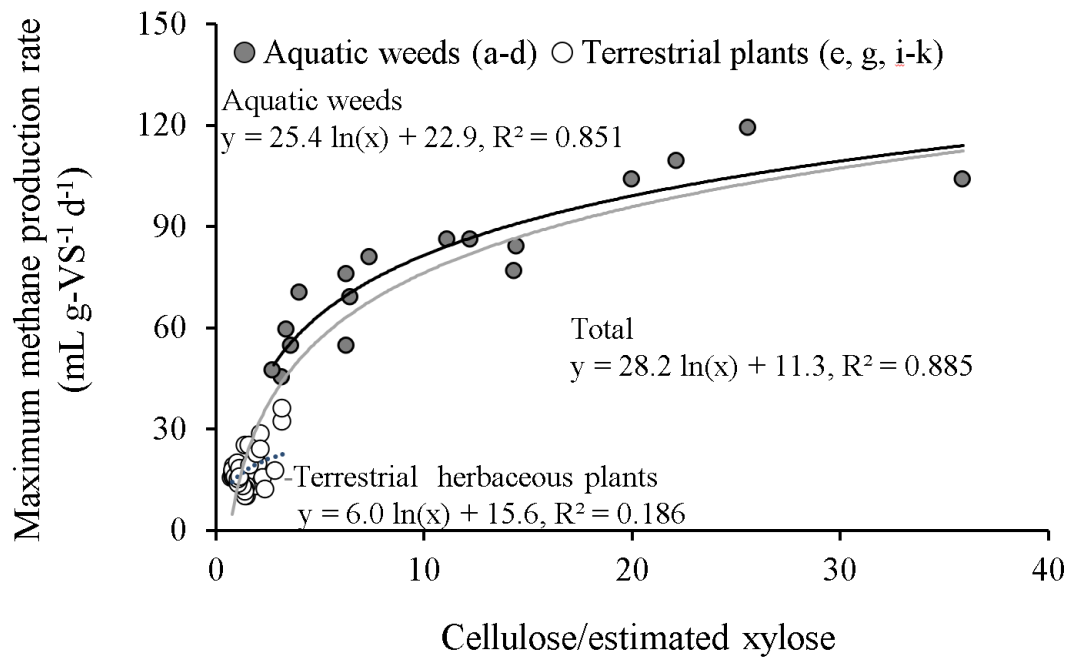
Figure 3-7. Relationship between maximum methane production rate and cellulose/estimated xylose in aquatic weeds and terrestrial plants. (a) This study, (b) Koyama et al. (2014), (c) Kist et al. (2018), (d) Li et al. (2020), (e) Triolo et al. (2011), (f) Melts et al. (2014), (g) Dahunsi et al. (2019), (h) Li et al. (2017), (i) Chen et al. (2019), (j) Kandel et al. (2013), (k) Dragoni et al. (2017). Solid lines represent $p < 0.05$, and plot line represents $p > 0.05$.

# Chapter Ⅳ

# Establishment of ADM1 inserting the effect of the lignocellulosic components and their ratios

## 4.1. Introduction

The relationship between the kinetic parameters of the anaerobic digestibility (methane production and maximum methane production rate) and lignocellulose components obtained by the modified Gompertz equation suggested that the coverage structure by each lignocellulose component determined the anaerobic digestibility of aquatic weeds. By fitting the modified Gompertz model, anaerobic digestibility could be quantified and evaluated. However, in order to estimate the optimum operating condition and the treatment performance for the implementation, more experiments were needed to accumulate more knowledge regarding the relationship between each anaerobic digestion parameter and the actual treatment performance. This is because the regression equation obtained in this analysis is limited to the conditions in which the substrate and sludge are fed in the VS ratio of 1:2. Therefore, the coefficient in the regression equation is expected to change continuously from the actual continuous methane fermentation process in which the bacteria concentration increases or decreases during the treatment period. Therefore, in order to use the relationship between cellulose/hemicellulose ratio obtained by the Gompertz equation, it is necessary to further analyze how the coefficients change under the conditions of different substrates and sludge VS ratios. This is quite a challenging approach because treatment efficiency in semicontinuous operation, considered

to be used as a treatment operation of the aquatic weeds in implementation, is influenced by lots of parameters such as organic loading rate, hydric retention time, feeding rate and so on.

As well as the modified Gompertz model, the anaerobic digestion model (ADM1) has been developed as a model for anaerobic digestion (Batstone et al., 2002) and has attracted much attention in recent years. In anaerobic digestion, the components in the feedstock are degraded to low molecular compounds by continuous microbial metabolism, as shown in Figure 4-1, and the gaseous components, which are part of the final product, are transferred from the liquid phase to the gas phase. ADM1 mathematically simulates these biochemical steps (decomposition, hydrolysis, acid production, acetic acid production, methane production) and physicochemical processes (ion association/dissociation, vapor-liquid equilibrium) to approximate the component concentrations and gas production. The mathematical reaction equations of the components in ADM1 are summarized in Table 4-1 and 4-2. The concentration variation of the components can be explained by the concentration of the component, the concentration of microbes, the absorption efficiency of microbes, the degradation rate constant, the maximum reaction rate coefficient, and the inhibition functions. Furthermore, different from the modified Gompertz model, ADM1 can estimate not only the methane fermentation characteristics but also the actual bacteria concentration and the concentration of each component in the reactor. This allows not only to compare treatment performance but also to predict optimal operating conditions and process failure through simulation.

Although ADM1 is considered a valuable method to simulate methane fermentation, the application to aquatic weeds needs to incorporate the effect of lignocellulose coating structure as

described in chapter Ⅲ. Anaerobic Digestion Modelling Task Group belonged to International Water Association (IWA) firstly developed ADM1 for sewage sludge (Batstone et al., 2002). In this original ADM1, cellulose and hemicellulose are treated as carbohydrates and lignin as an inactive component not involved in the degradation. Therefore, there would be a possibility of overestimating the methane production due to ignoring the degradation limitation of cellulose and hemicellulose by the lignin. In the previous study using an aquatic weed, *H. verticillate*, lignin and cellulose were treated as inactive components (Chen et al., 2016). However, Chapter Ⅲ clarified that cellulose was a component that contributed to methane production. While the model developed by Chen et al. (2016) may fit well for biomass with high lignin content, it may not fit well for aquatic weed biomass with low lignin content. Furthermore, both previous studies considered starch and hemicellulose as the same component and did not take into account the differences in their degradability. The degradability of cellulose and hemicellulose might be affected by the lignin coating structure.

In ChapterⅢ, I found that the lignocellulose component affected the anaerobic digestibility of aquatic weeds. By including these effects in ADM1, it may be possible to estimate the anaerobic digestibility in the semicontinuous operation. Hence, the objective of this study was to develop a model that can simulate methane production from the chemical composition of aquatic weeds, and ADM1 was developed, and its accuracy was evaluated.

**4.2.Materials and methods**

**4.2.1.  Overview of each reaction process in ADM1**

**4.2.1.1.The distribution rate of components in miniaturization**

As shown in Figure 4-1, the miniaturization process separates the organic mixture into carbohydrates, proteins, lipids, and inert components. In the hydrolysis process, carbohydrates, proteins, and lipids are hydrolyzed to produce monosaccharides, amino acids, and high fatty acids. In the acid generation and acetic acid generation processes, monosaccharides, amino acids, and higher fatty acids are used to generate volatile fatty acids, namely, valeric acid, butyric acid, propionic acid, and finally acetic acid and hydrogen are generated. The methanogenic process produces methane from acetic acid and hydrogen. In each of the processes of acid production, acetic acid production, and methane production, part of the components to be decomposed is used for the growth of the fungus itself ($Y_{i, j}$). In the hydrolysis process, all carbohydrates and proteins were considered to be converted to monosaccharides and amino acids, respectively, while 95% of lipids were considered to be converted to higher fatty acids (palmitic acid in the equation) and 5% to monosaccharides (glycerol), based on the calculation of the degradation reaction of palmitic acid triglyceride. For the distribution rates of the acid/acetic acid formation and methane formation processes, the values recommended by the ADM1 report were adopted.

**4.2.1.2.Rection rate equations**

For the miniaturization process and the hydrolysis process, the degradation rate of

component $\rho_i$ is expressed by a linear equation that depends on the concentration of component $i$ ($X_i$) [kg-COD/m$^3$].

$$\rho_i = k_{m,i} \cdot X_i$$

where, $k_{m,i}$ [day$^{-1}$] represents reaction rate constant. The degradation rate of component $i$ in the acidogenesis and methanogenesis process is expressed by following the Monod equation.

$$\rho_i = k_{m,i} \frac{S_i}{K_{m,i} + S_i} X_i I_i$$

where, $k_{m,i}$ [day$^{-1}$] and $K_{m,i}$ [kg-COD/m$^3$] represent maximum specific reaction rate and rate constant, respectively. $I_i$ is an inhibition function that indicates the effect of pH and hydrogen/ammonia concentration on reducing the reaction rate (inhibiting the reaction). As an example, the pH inhibition function $I_{pH,i}$ is shown.

If pH $\geq$ pH$_{UL,i}$

$$I_{pH,i} = 1$$

pH $<$ pH$_{UL,I}$

$$I_{pH,i} = exp\left\{-3 \left(\frac{pH - pH_{UL,i}}{pH_{UL,i} - pH_{LL,i}}\right)^2\right\}$$

where $pH_{UL,i}$ and $pH_{LL,i}$ are the pH inhibition function thresholds for component i. For the reaction rate constant $k_m$, the ADM1 report value was adopted.

### 4.2.1.3. Inorganic carbon, nitrogen balance, and liquid-gas equilibrium

In the acidogenesis process, along with the degradation of monosaccharides ($S_{su}$), amino acid

($S_{aa}$), propionic acid ($S_{pro}$), and acetic acid ($S_{ac}$), carbon dioxide is produced. In the methanogenesis process, $CO_2$ is consumed to produce methane from hydrogen ($S_{h2}$). The reaction rate of carbon dioxide $\rho CO_2$ [kmol/m³ /day] can be explained following equation (coefficient represents the conversion factor from kgCOD to kmol).

$$\rho_{CO_2} = 0.0068\rho_{su} + 0.0032\rho_{aa} + 0.0084\rho_{pro} + 0.0184\rho_{ac} - 0.0166\rho_{h_2}$$

Since ammonia ($NH_3$), an inorganic nitrogen component, is produced by the decomposition of amino acids and consumed by the growth of the microbes, the reaction rate $\rho_{NH3}$ [kmol/m³/day] can be expressed by the following equation.

$$\rho_{NH_3} = 0.007\frac{dS_{aa}}{dt} - \frac{1}{160}\sum_i \frac{dX_i}{dt}$$

where, $S_{aa}$ is amino acid concentration, and $X_i$ is seven kinds of microbe concentrations.

For hydrogen, methane, and carbon dioxide (CO2), the gaseous component is treated in addition to the liquid component. The mass transfer rate between liquid and gas, $\rho$T,i[kmol/day], is calculated by the following equation, assuming that the mass transfer between liquid and gas follows the Henry's law.

$$\rho_{T,i} = K_{la}\left(S_{liq,i}/r_{COD/MOL}\right) - K_{h,i}\rho_{gas,i}$$

where $S_{liq,i}$ is the concentration of component $i$ in the sludge [kmol/m3 ]. $K_{h,i}$ is Henry's constant for component i, and COD conversion factor $r_{COD/MOL}$[kg/kmol] is g-COD per mol for each component. Also, $p_{gas,i}$[bar] is the partial pressure of the gas of component $i$ and is obtained by the following equation.

$$\rho_{gas.i} = S_{gas,i}RT$$

where $S_{gas,i}$ [kg-COD/m3 ] represents the concentration of component $i$ in the gas phase.

### 4.2.2. Estimation procedure

Data for the chemical composition of the aquatic weeds as well as their methane productions

were based on aquatic weeds analyzed in the previous chapter. The ratios of the chemical

compositions of the aquatic weeds were used for the distribution rate of the fed substrate to the other

components. Table 4-3 and 4-4 shows the value of fundamental parameters of ADM1 and seed sludges

used in this study. Table 4-5 represented the distribution rate of the aquatic weed samples used in this

study. ADM1 by the International Water Association (IWA) was used for the decomposition rate

constant and bacterial compositions of the sludge. The 36 components are composed of organic

components (15), bacteria (7), inorganic components (2), gas components (3), and ionic components

(9). In addition to the fermentation reaction of organic matter, the balance of inorganic carbon and

nitrogen, ionic equilibrium, and gas equilibrium were calculated.

### 4.2.3. Alterations in ADM1 developed in this study

In the model developed in this study, cellulose and hemicellulose contained in carbohydrates

were established as separate parameters. Furthermore, lignin content has been treated as an inert

component in the previous study, but in this study, it was independently set as a component in order

to model the effect of lignin coating. The distribution coefficients of cellulose and hemicellulose in

the miniaturization process were determined as follows to model the amount of undegraded cellulose

and hemicellulose due to the lignin coating.

$$f_{cell,xc} = m_{cell,xc} \times (m_{cell,xc} / (m_{cell,xc} + f_{lig,xc} \times 3.383))$$

$$f_{hemi,xc} = m_{hemi,xc} \times (m_{hemi,xc} / (m_{hemi,xc} + f_{lig,xc} \times 1.123))$$

$$f_{xI,xc} = m_{xI,xc} + (m_{cell,xc} - f_{cell,xc}) + (m_{hemi,xc} - f_{hemi,xc})$$

where $f_{cell,xc}$, $f_{hemi,xc}$, $f_{lig,xc}$, and $f_{xI,xc}$ denote the distribution ratio from fed substrate to each component, and $m_{cell,xc}$, $m_{hemi,xc}$, and $m_{xI,xc}$ represent the percentage of each component in the chemical composition of aquatic weeds. The parentheses on the right side indicate the coverage of lignin to cellulose and hemicellulose, and the higher percentage of lignin led to the larger the percentage of undecomposed cellulose and hemicellulose ($f_{xI,xc}$). In addition to the correction factors of 3.383 and 1.123 shown in above equations, the reaction rates of cellulose, hemicellulose and lignin ($k_{hyd, sta}= 10$, $k_{hyd, cel}=3$, $k_{hyd, hemi}=1$) were calculated by the least-squares method and applied to the model developed in this study.

### 4.3.Results and discussion

### 4.3.1.  Estimation results

Figure 4-2 shows the estimated results of methane production in original ADM1. The methane productions of the aquatic weeds obtained in the batch tests were 150-250 mL g-VS$^{-1}$, while that of the original ADM1 was estimated to 500-700 mL g-VS$^{-1}$. In the original ADM1, cellulose and hemicellulose are treated as easily degradable carbohydrates. The previous studies (Kandel et al. (2011), Koyama et al. (2014)) and this study revealed that lignin limits the degradation of cellulose.

Since the model did not take into account the effect of the coating structure of lignin and hemicellulose on the degradation rate, the estimated values may have greatly overestimated the measured values. Therefore, this model is not suitable for simulating methane fermentation in aquatic weeds.

The ADM1 fitting to *H. verticillate* in previous study (Chen et al. 2016) was used to compare with the measured values in batch experiment (Figure 4-5 to 7). Although the values were relatively close to those of the original ADM1, the cumulative methane yields were lower than the measured ones in all condition. The model in the previous study treated cellulose and lignin as undegraded components. The difference between the estimated and measured values was caused by ignoring the methane production by the cellulose. The simulated values obtained in *P. maackianus*, which has a high lignin content, were relatively close to the measured value than those of other species. This indicates that when the lignin content is high, cellulose was not decomposed and as aresult methane production is decreasing. Therefore, although the models reported in the previous studies can be the better estimation results for the aquatic weed biomass with high lignin content, the accuracy of the estimation results will be greatly reduced when the lignin content was low.

The estimation results by developed ADM1 in this study are shown in Figure 4-8 to 4-10. The ADM1 obtained in this study, which takes into account the effect of lignocellulose composition, showed almost the same values as the measured values under all conditions. This result indicates that the lignocellulose coating structure of aquatic weeds determines their anaerobic digestibility. Furthermore, the model indicates that the lignin coverage limits the degradation of cellulose and hemicellulose. The accuracy analysis of the model shows that the model can estimate the methane

production with an accuracy of $R^2 = 0.984$. Therefore, it can be concluded that the lignocellulosic components and the coverage structure have a great influence on the anaerobic digestibility and the production rate in aquatic weeds. Furthermore, the chemical composition of aquatic weeeds is characterized by the fact that they contain about 20% protein and less than 10% starch and lipid, even though the species is different (Rabemanolontsoa and Saka, 2013). Therefore, changes in the anaerobic digestibility of aquatic weeds are considered to be mainly influenced by the content of lignocellulose components. In this study, we developed a model to estimate the degradation rate and amount of cellulose and hemicellulose based on the lignocellulose component ratio. Therefore, the estimationby developed ADM1 was consistent with the actual results even for aquatic weeds with different lignocellulose components ratios. This model may also be used to estimate the performance of the methane fermentation process in semicontinuous treatment.

### 4.3.2. Simulation with different lignocellulosic components

To evaluate the effect of lignin coating structure on the methane production, simulations were performed (Figure 4-11). In this simulation, chemical compositions of substrate was assumed to 300 mg g-VS$^{-1}$ of cellulose, different amount of the lignin to make different cellulose/lignin ratio, and inert as a remain. The simulation suggested that 300 mg g-VS$^{-1}$ of cellulose potentially have a methane potentials of 150 mL g-VS$^{-1}$ (= 500 mL g-cellulose$^{-1}$). However, when the cellulose/lignin decreased to 0.4, methane yield showed 42 mL g-VS$^{-1}$. Due to the coating of cellulose by lignin, 73.3% of the methane yield possibly be decreased in the simulated conditions. Figure 4-12 represented the relationships between cellulose/lignin ratio and simulated methane yield. There was

a clear significant correlation, suggesting that the lignin coverage on the cellulose was successfully
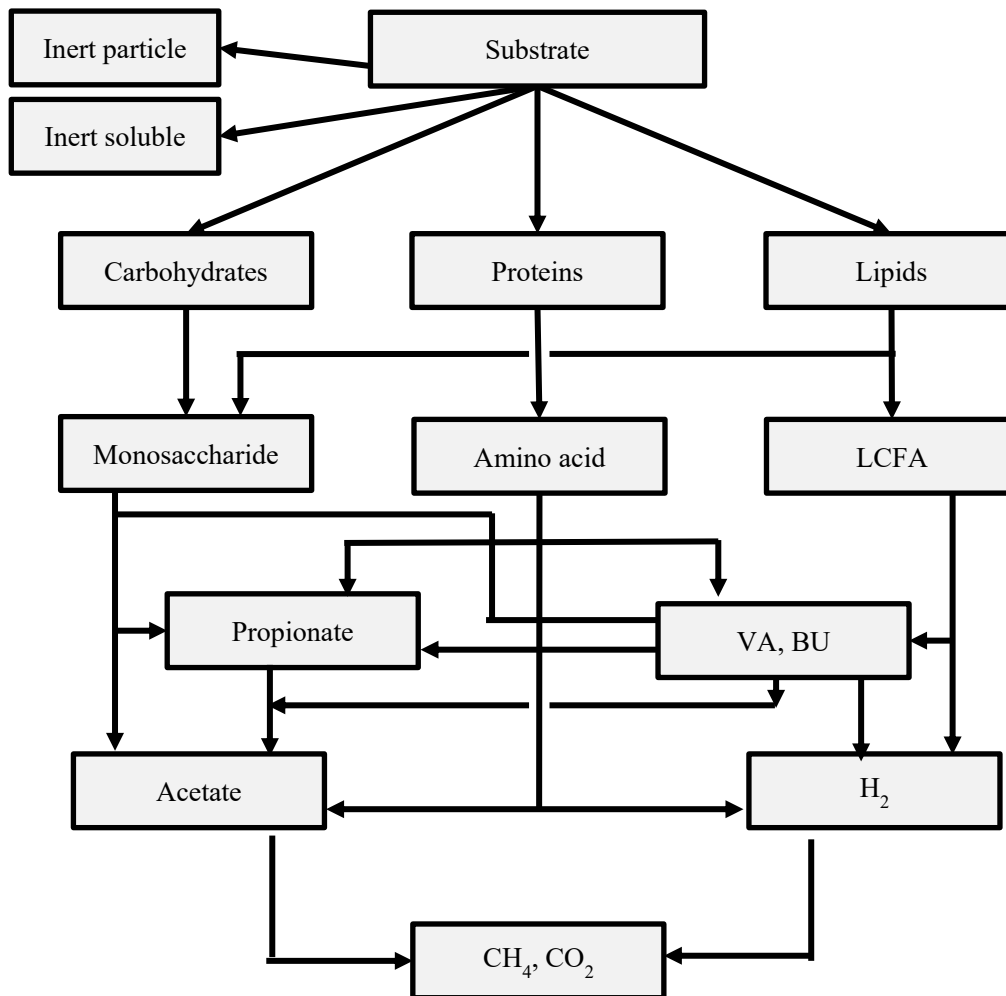
simulated in this model.

Figure 4-1. Reactions flow chart for anaerobic digestion modified from Oskar et al., 2014.

LCFA: Long chain fatty acid, Va: Valerate acid, Bu: Butyrate acid.

Table.4-1: Biochemical rate coefficient and kinetic rate equations for particulate components. The matrix comes from the task report with complementing equations.

| j | Process | 13 Composites $X_c$ | 14 Carbohydrates $X_{ch}$ | 15 Proteins $X_{pr}$ | 16 Lipids $X_{li}$ | 17 Sugar degraders $X_{su}$ | 18 Amino acid degraders $X_{aa}$ | 19 LCFA degraders $X_{fa}$ | 20 Valerate and butyrate degraders $X_{c4}$ | 21 Propionate degraders $X_{pro}$ | 22 Acetate degraders $X_{ac}$ | 23 Hydrogen degraders $X_{h2}$ | 24 Particulate inerts $X_I$ | 36 Total lactate $S_{lac}$ | 37 Lactate $X_{lac.f}$ | 38 Lactate $X_{lac.o}$ | 39 Total calcium $S_{ca}$ | Rate |
|---|---|---|---|---|---|---|---|---|---|---|---|---|---|---|---|---|---|---|
| 1 | Disintegration | -1 | $f_{ch,xc}$ | $f_{pr,xc}$ | $f_{li,xc}$ | | | | | | | | $f_{I,xc}$ | | | | | $k_{dis} \cdot X_c$ |
| 2 | Hydrolysis of Carbohydrates | | -1 | | | | | | | | | | | | | | | $k_{hyd,ch} \cdot X_{ch}$ |
| 3 | Hydrolysis of proteins | | | -1 | | | | | | | | | | | | | | $k_{hyd,pr} \cdot X_{pr}$ |
| 4 | Hydrolysis of lipids | | | | -1 | | | | | | | | | | | | | $k_{hyd,li} \cdot X_{li}$ |
| 5 | Uptake of sugars | | | | | $Y_{su}$ | | | | | | | | | | | | $k_{m,su}\frac{S_{su}}{K_s+S_{su}}X_{su}I_1$ |
| 6 | Uptake of amino acids | | | | | | $Y_{aa}$ | | | | | | | | | | | $k_{m,aa}\frac{S_{aa}}{K_s+S_{aa}}X_{aa}I_1$ |
| 7 | Uptake of LCFA | | | | | | | $Y_{fa}$ | | | | | | | | | | $k_{m,fa}\frac{S_{fa}}{K_s+S_{fa}}X_{fa}I_1$ |
| 8 | Uptake of Valerate | | | | | | | | $Y_{c4}$ | | | | | | | | | $k_{m,c4}\frac{S_{va}}{K_s+S_{va}}X_{c4}\frac{1}{1+S_{bu}/S_{va}}I_1$ |
| 9 | Uptake of Butyrate | | | | | | | | $Y_{c4}$ | | | | | | | | | $k_{m,c4}\frac{S_{bu}}{K_s+S_{bu}}X_{c4}\frac{1}{1+S_{va}/S_{bu}}I_1$ |
| 10 | Uptake of Propionate | | | | | | | | | $Y_{pro}$ | | | | | | | | $k_{m,pr}\frac{S_{pro}}{K_s+S_{pro}}X_{pro}I_2$ |
| 11 | Uptake of Acetate | | | | | | | | | | $Y_{ac}$ | | | | | | | $k_{m,ac}\frac{S_{ac}}{K_s+S_{ac}}X_{ac}I_3$ |
| 12 | Uptake of Hydrogen | | | | | | | | | | | $Y_{h2}$ | | | | | | $k_{m,h2}\frac{S_{h2}}{K_s+S_{h2}}X_{h2}I_1$ |
| 13 | Decay of $X_{su}$ | 1 | | | | -1 | | | | | | | | | | | | $k_{dec,Xsu}X_{su}$ |
| 14 | Decay of $X_{aa}$ | 1 | | | | | -1 | | | | | | | | | | | $k_{dec,Xaa}X_{aa}$ |
| 15 | Decay of $X_{fa}$ | 1 | | | | | | -1 | | | | | | | | | | $k_{dec,Xfa}X_{fa}$ |
| 16 | Decay of $X_{c4}$ | 1 | | | | | | | -1 | | | | | | | | | $k_{dec,Xc4}X_{c4}$ |
| 17 | Decay of $X_{pro}$ | 1 | | | | | | | | -1 | | | | | | | | $k_{dec,Xpro}X_{pro}$ |
| 18 | Decay of $X_{ac}$ | 1 | | | | | | | | | -1 | | | | | | | $k_{dec,Xac}X_{ac}$ |
| 19 | Decay of $X_{h2}$ | 1 | | | | | | | | | | -1 | | | | | | $k_{dec,Xh2}X_{h2}$ |
| 20 | Uptake of lactate (fer.) | | | | | | | | | | | | | -1 | $Y_{lacf}$ | | | $k_{m,lacf}\frac{S_{lac}}{K_s+S_{lac}}X_{lacf}I_1$ |
| 21 | Uptake of lactate (ox.) | | | | | | | | | | | | | -1 | | $Y_{laco}$ | | $k_{m,laco}\frac{S_{lac}}{K_s+S_{lac}}X_{laco}I_2$ |
| 22 | Decay of $X_{lac.f}$ | 1 | | | | | | | | | | | | | -1 | | | $k_{dec,Xlacf}X_{lacf}$ |
| 23 | Decay of $X_{lac.o}$ | 1 | | | | | | | | | | | | | | -1 | | $k_{dec,Xlaco}X_{laco}$ |
| 24 | *Precipitation of Calcium* | | | | | | | | | | | | | | | | -1 | $k_{r,CaCO3}\left(\sqrt{S_{Ca}S_{hCO3}}-\sqrt{K_{sp}CaCO_3}\right)^2$ |

63

Table.4-2: Biochemical rate coefficient and kinetic rate equations for soluble components. The matrix comes from the task report with complementing equations.

| j | Component / iProcess | 1 Sugars $S_{su}$ | 2 Amino acid $S_{aa}$ | 3 LCFA $S_{fa}$ | 4 Valerate $S_{va}$ | 5 butyrate $S_{bu}$ | 6 Propionate $S_{pro}$ | 7 Acetate $S_{ac}$ | 8 Hydrogen $S_{h2}$ | 9 Methane $S_{ch4}$ | 10 Inorganic carbon $S_{IC}$ | 11 Inorganic nitrogen $S_{IN}$ | 12 Soluble inerts $S_I$ | Rate |
|---|---|---|---|---|---|---|---|---|---|---|---|---|---|---|
| 1 | Disintegration | | | | | | | | | | | | $f_{sI,xc}$ | $k_{dis}\cdot X_c$ |
| 2 | Carbohydrate Hydrolysis | 1 | | | | | | | | | | | | $k_{hyd,ch}\cdot X_{ch}$ |
| 3 | Protein hydrolysis | | 1 | | | | | | | | | | | $k_{hyd,pr}\cdot X_{pr}$ |
| 4 | Lipid hydrolysis | $1-f_{fa,li}$ | | $f_{fa,li}$ | | | | | | | | | | $k_{hyd,li}\cdot X_{li}$ |
| 5 | Sugar uptake | -1 | | | | $(1-Y_{su})f_{bu,su}$ | $(1-Y_{su})f_{pro,su}$ | $(1-Y_{su})f_{ac,su}$ | $(1-Y_{su})f_{h2,su}$ | | $-\sum\limits_{\substack{i=1-9,\\11-29}} C_i v_{i,5}$ | $-(Y_{su})N_{bac}$ | | $k_{m,su}\dfrac{S_{su}}{K_s+S_{su}}X_{su}I_1$ |
| 6 | Uptake of amino acids | | -1 | | $(1-Y_{aa})f_{va,aa}$ | $(1-Y_{aa})f_{bu,aa}$ | $(1-Y_{aa})f_{pro,aa}$ | $(1-Y_{aa})f_{ac,aa}$ | $(1-Y_{aa})f_{h2,aa}$ | | $-\sum\limits_{\substack{i=1-9,\\11-29}} C_i v_{i,6}$ | $N_{aa}-(Y_{aa})N_{bac}$ | | $k_{m,aa}\dfrac{S_{aa}}{K_s+S_{aa}}X_{aa}I_1$ |
| 7 | Uptake of LCFA | | | -1 | | | | $(1-Y_{fa})0.7$ | $(1-Y_{fa})0.3$ | | | $-(Y_{fa})N_{bac}$ | | $k_{m,fa}\dfrac{S_{fa}}{K_s+S_{fa}}X_{fa}I_1$ |
| 8 | Uptake of Valerate | | | | -1 | | $(1-Y_{c4})0.54$ | $(1-Y_{c4})0.31$ | $(1-Y_{c4})0.15$ | | | $-(Y_{c4})N_{bac}$ | | $k_{m,c4}\dfrac{S_{va}}{K_s+S_{va}}X_{c4}\dfrac{1}{1+S_{bu}/S_{va}}I$ |
| 9 | Uptake of Butyrate | | | | | -1 | | $(1-Y_{c4})0.8$ | $(1-Y_{c4})0.2$ | | | $-(Y_{c4})N_{bac}$ | | $k_{m,c4}\dfrac{S_{bu}}{K_s+S_{bu}}X_{c4}\dfrac{1}{1+S_{va}/S_{bu}}I$ |
| 10 | Uptake of Propionate | | | | | | -1 | $(1-Y_{c4})0.57$ | $(1-Y_{c4})0.43$ | | $-\sum\limits_{\substack{i=1-9,\\11-29}} C_i v_{i,10}$ | $-(Y_{pro})N_{bac}$ | | $k_{m,pr}\dfrac{S_{pro}}{K_s+S_{pro}}X_{pro}I_2$ |
| 11 | Uptake of Acetate | | | | | | | -1 | | $(1-Y_{ac})$ | $-\sum\limits_{\substack{i=1-9,\\11-29}} C_i v_{i,11}$ | $-(Y_{pr})N_{bac}$ | | $k_{m,ac}\dfrac{S_{ac}}{K_s+S_{ac}}X_{ac}I_3$ |
| 12 | Uptake of Hydrogen | | | | | | | | -1 | $(1-Y_{h2})$ | $-\sum\limits_{i=1-9,11-29} C_i v_{i,12}$ | $-(Y_{h2})N_{bac}$ | | $k_{m,h2}\dfrac{h2}{K_s+S_{h2}}X_{h2}I_1$ |
| 13 | Decay of $X_{su}$ | | | | | | | | | | | | | $k_{dec,X_{su}}X_{su}$ |
| 14 | Decay of $X_{aa}$ | | | | | | | | | | | | | $k_{dec,X_{aa}}X_{aa}$ |
| 15 | Decay of $X_{fa}$ | | | | | | | | | | | | | $k_{dec,X_{fa}}X_{fa}$ |
| 16 | Decay of $X_{c4}$ | | | | | | | | | | | | | $k_{dec,X_{c4}}X_{c4}$ |
| 17 | Decay of $X_{pro}$ | | | | | | | | | | | | | $k_{dec,X_{pro}}X_{pro}$ |
| 18 | Decay of $X_{ac}$ | | | | | | | | | | | | | $k_{dec,X_{ac}}X_{ac}$ |
| 19 | Decay of $X_{h2}$ | | | | | | | | | | | | | $k_{dec,X_{h2}}X_{h2}$ |
| 20 | Uptake of lactate (fer.) | | | | | | $(1-Y_{lac,f})0.785$ | $(1-Y_{lac,f})0.215$ | | | $-\sum\limits_{\substack{i=1-9,\\11-29}} C_i v_{i,20}$ | $-(Y_{lac,f})N_{bac}$ | | $k_{m,lacf}\dfrac{S_{lac}}{K_s+S_{lac}}X_{lacf}\,I$ |
| 21 | Uptake of lactate (ox.) | | | | | | | $(1-Y_{lac,o})\tfrac{2}{3}$ | $(1-Y_{lac,o})\tfrac{1}{3}$ | | $-\sum\limits_{\substack{i=1-9,\\11-29}} C_i v_{i,21}$ | $-(Y_{lac,o})N_{bac}$ | | $k_{m,laco}\dfrac{S_{lac}}{K_s+S_{lac}}X_{laco}\,I_2$ |
| 22 | Decay of $X_{lac,f}$ | 1 | | | | | | | | | | | | $k_{dec,X_{lacf}}X_{lacf}$ |
| 23 | Decay of $X_{lac,o}$ | 1 | | | | | | | | | | | | $k_{dec,X_{laco}}X_{laco}$ |
| 24 | Precipitation of Calcium | | | | | | | | | | | | | $k_{r,CaCO3}\left(\sqrt{S_{Ca}\,S_{hCO3}}-\sqrt{K_{sp}\,CaCO_3}\right)^2$ |

64

Table.4-3: Applied parameters for the fundamental parameters.

| Parameter | Value | Unit |
|---|---|---|
| $N_{xc}$ | 0.0376/14 | kmole kgN-COD$^{-1}$ |
| $N_I$ | 0.06/14 | kmole kgN-COD$^{-1}$ |
| $N_{aa}$ | 0.007 | kmole kgN-COD$^{-1}$ |
| $C_{xc}$ | 0.02786 | kmole kgC-COD$^{-1}$ |
| $C_{sI}$ | 0.03 | kmole kgC-COD$^{-1}$ |
| $C_{ch}$ | 0.0313 | kmole kgC-COD$^{-1}$ |
| $C_{pr}$ | 0.03 | kmole kgC-COD$^{-1}$ |
| $C_{li}$ | 0.022 | kmole kgC-COD$^{-1}$ |
| $C_{xI}$ | 0.03 | kmole kgC-COD$^{-1}$ |
| $C_{su}$ | 0.0313 | kmole kgC-COD$^{-1}$ |
| $C_{aa}$ | 0.03 | kmole kgC-COD$^{-1}$ |
| $f_{fa,li}$ | 0.95 | - |
| $C_{fa}$ | 0.0217 | kmole kgC-COD$^{-1}$ |
| $f_{h2,su}$ | 0.19 | - |
| $f_{bu,su}$ | 0.13 | - |
| $f_{pro,su}$ | 0.27 | - |
| $f_{ac,su}$ | 0.41 | - |
| $N_{bac}$ | 0.08/14 | kmole kgN-COD$^{-1}$ |
| $C_{bu}$ | 0.025 | kmole kgC-COD$^{-1}$ |
| $C_{pro}$ | 0.0268 | kmole kgC-COD$^{-1}$ |
| $C_{ac}$ | 0.0313 | kmole kgC-COD$^{-1}$ |
| $C_{bac}$ | 0.0313 | kmole kgC-COD$^{-1}$ |
| $Y_{su}$ | 0.1 | - |
| $f_{h2;aa}$ | 0.06 | - |
| $f_{va,aa}$ | 0.23 | - |
| $f_{bu,aa}$ | 0.26 | - |
| $f_{pro,aa}$ | 0.05 | - |
| $f_{ac,aa}$ | 0.4 | - |
| $C_{va}$ | 0.024 | kmole kgC-COD$^{-1}$ |
| $Y_{aa}$ | 0.08 | - |
| $Y_{fa}$ | 0.06 | - |
| $Y_{c4}$ | 0.06 | - |
| $Y_{pro}$ | 0.04 | - |
| $C_{ch4}$ | 0.0156 | kmole kgC-COD$^{-1}$ |
| $Y_{ac}$ | 0.05 | - |
| $Y_{h2}$ | 0.06 | - |

Table.4-3: Applied parameters for the chemical compositions of the seed sludge (Oskar et al. 2014)

| | Components | Concentration (g-COD L⁻¹) | | Components | Concentration (g-COD L⁻¹) |
|---|---|---|---|---|---|
| 1 | $S_{su}$ | 0.001 | 22 | $X_{ac}$ | 0.76056 |
| 2 | $S_{aa}$ | 0.001 | 23 | $X_{h2}$ | 0.31702 |
| 3 | $S_{fa}$ | 0.0001 | 24 | $X_I$ | 25.61739 |
| 4 | $S_{va}$ | 0.0001 | 25 | Scat | 0.04 |
| 5 | $S_{bu}$ | 0.0001 | 26 | $S_{an}$ | 0.02 |
| 6 | $S_{pro}$ | 0.0001 | 27 | $S_{vam}$ | 0.0116 |
| 7 | $S_{ac}$ | 0.0001 | 28 | $S_{bum}$ | 0.01322 |
| 8 | $S_{h2}$ | 2.36E-09 | 29 | $S_{prom}$ | 0.01574 |
| 9 | $S_{ch4}$ | 2.36E-06 | 30 | $S_{acm}$ | 0.19724 |
| 10 | $S_{ic}$ | 0.039 | 31 | $S_{CHO3-}$ | 0.14278 |
| 11 | $S_{in}$ | 0.013 | 32 | $S_{NH3}$ | 0.00409 |
| 12 | $S_I$ | 0.009 | 33 | H2 | 1.02E-05 |
| 13 | $X_c$ | 0.3087 | 34 | CH₄ | 0 |
| 14 | $X_{ch}$ | 0.02795 | 35 | CO₂ | 0.0141 |
| 15 | $X_{pr}$ | 0.1026 | 36 | $S_{lac}$ | 0 |
| 16 | $X_{li}$ | 0.02948 | 37 | $X_{lacf}$ | 0 |
| 17 | $X_{su}$ | 0.42016 | 38 | $X_{laco}$ | 0 |
| 18 | $X_{aa}$ | 1.17917 | 39 | $S_{ca}$ | 0.001 |
| 19 | $X_{fa}$ | 0.24303 | 40 | $X_{cell}$ | 0 |
| 20 | $X_{c4}$ | 0.43192 | 41 | $X_{hemi}$ | 0 |
| 21 | $X_{pro}$ | 0.1373 | 42 | $X_{lig}$ | 0 |

Table.4-5: Input parameters for ADM1 in this study

| | Unit | E. densa July | E. densa August | E. densa September | E. densa October | E. nuttallii June | E. nuttallii July | E. nuttallii August | E. nuttallii September | E. nuttallii October |
|---|---|---|---|---|---|---|---|---|---|---|
| Xc | g g-TS⁻¹ | 0.776 | 0.708 | 0.756 | 0.67 | 0.665 | 0.711 | 0.689 | 0.693 | 0.674 |
| XI | g g-TS⁻¹ | 0.224 | 0.292 | 0.244 | 0.33 | 0.335 | 0.289 | 0.311 | 0.307 | 0.326 |
| f ch | g g-VS⁻¹ | 0.550 | 0.514 | 0.588 | 0.564 | 0.518 | 0.539 | 0.466 | 0.445 | 0.478 |
| f_pr_xc | g g-VS⁻¹ | 0.225 | 0.198 | 0.285 | 0.247 | 0.240 | 0.235 | 0.192 | 0.259 | 0.210 |
| f_li_xc | g g-VS⁻¹ | 0.090 | 0.117 | 0.047 | 0.044 | 0.063 | 0.074 | 0.136 | 0.119 | 0.080 |
| f_xl_xc | g g-VS⁻¹ | 0.226 | 0.288 | 0.127 | 0.189 | 0.241 | 0.226 | 0.342 | 0.296 | 0.312 |

| | Unit | P. maackianus June | P. maackianus July | P. maackianus August | P. maackianus September | P. maackianus October | H.verticillata June | H.verticillata July | H.verticillata August | T. japonica September | S. polyrhiza October |
|---|---|---|---|---|---|---|---|---|---|---|---|
| Xc | g g-TS⁻¹ | 0.656 | 0.591 | 0.654 | 0.69 | 0.69 | 0.668 | 0.629 | 0.609 | 0.676 | 0.5923 |
| XI | g g-TS⁻¹ | 0.344 | 0.409 | 0.346 | 0.31 | 0.31 | 0.332 | 0.371 | 0.391 | 0.324 | 0.4077 |
| f ch | g g-VS⁻¹ | 0.513 | 0.490 | 0.467 | 0.464 | 0.472 | 0.495 | 0.529 | 0.598 | 0.435 | 0.460 |
| f_pr_xc | g g-VS⁻¹ | 0.201 | 0.224 | 0.206 | 0.277 | 0.241 | 0.231 | 0.252 | 0.220 | 0.264 | 0.250 |
| f_li_xc | g g-VS⁻¹ | 0.032 | 0.048 | 0.066 | 0.046 | 0.044 | 0.082 | 0.040 | 0.002 | 0.105 | 0.079 |
| f_xl_xc | g g-VS⁻¹ | 0.286 | 0.286 | 0.327 | 0.259 | 0.287 | 0.275 | 0.220 | 0.181 | 0.301 | 0.291 |

(a) July 2015
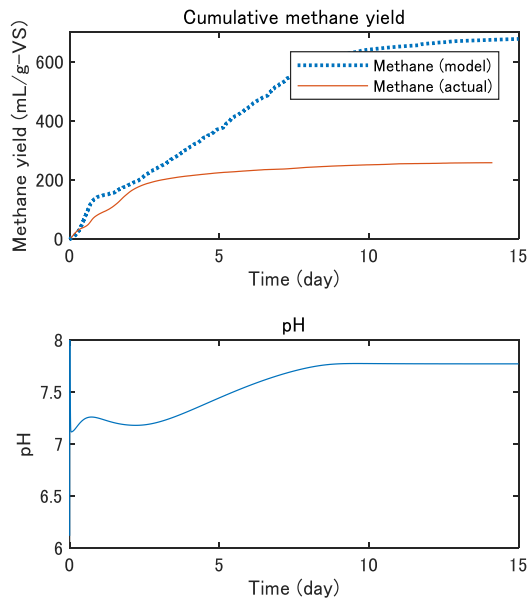
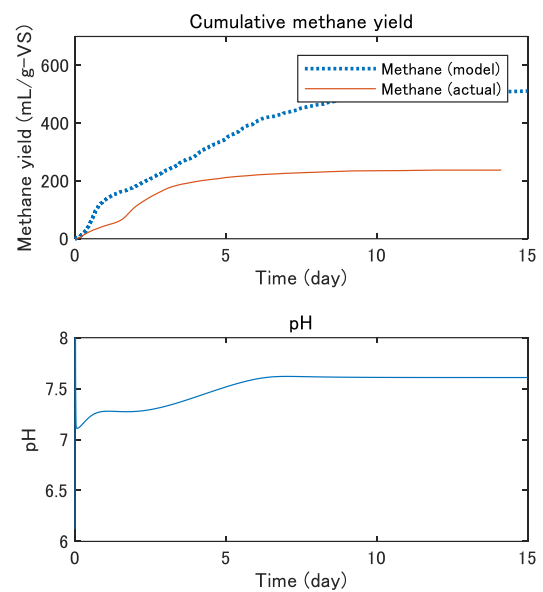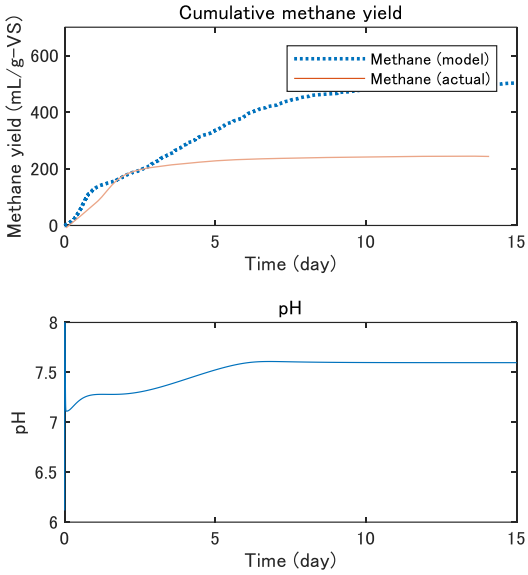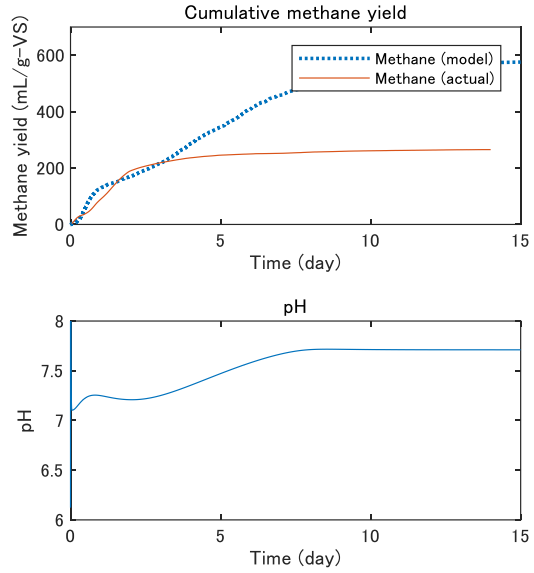(b) August 2015
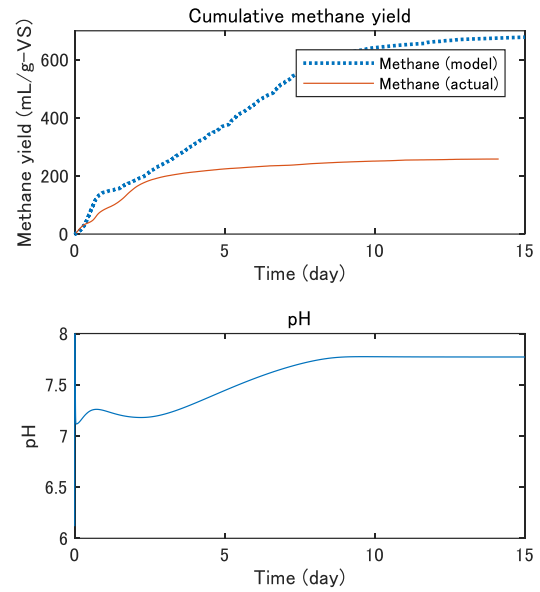
(c) September 2015
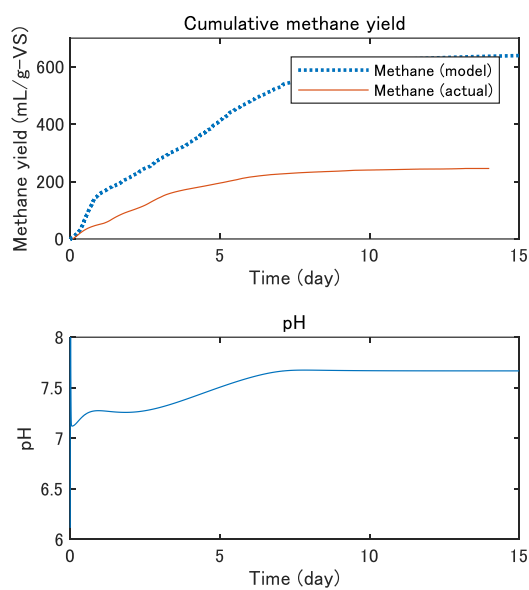
(d) October 2015

Figure 4-2. Simulation models and experimentally obtained actual data of batch anaerobic digestion by using chemical compositions of seed sludge and *Egeria densa*. Used ADM1 was cited from Batstone et al. 2002, which was fitted by the BMP results of sewage sludge. Solid line represents batch result and dot line means simulation result.
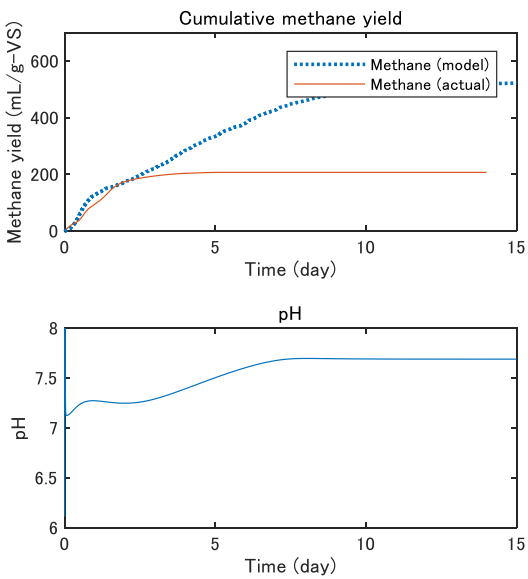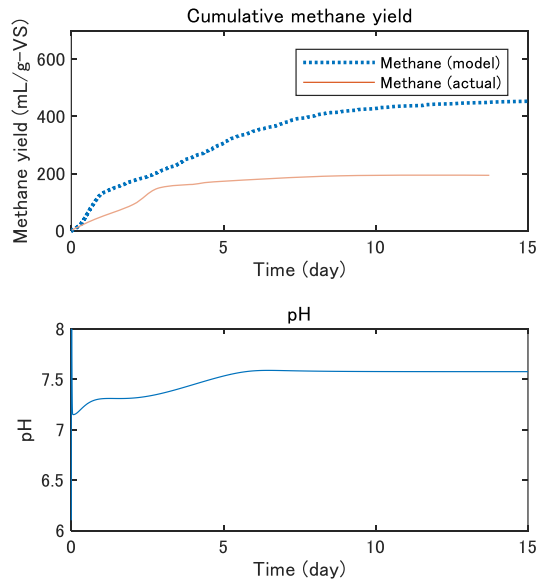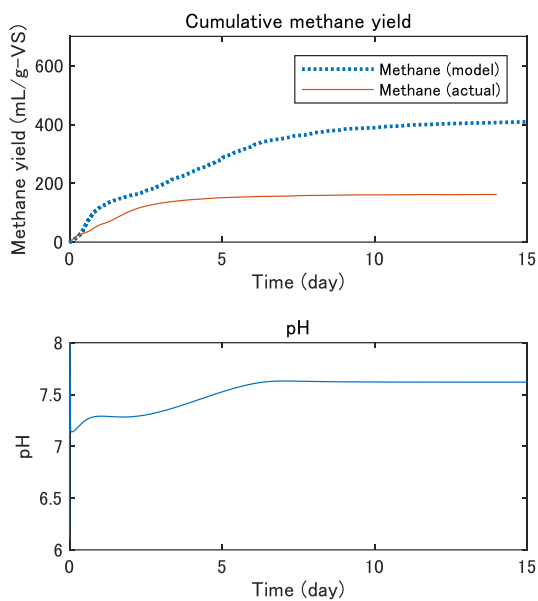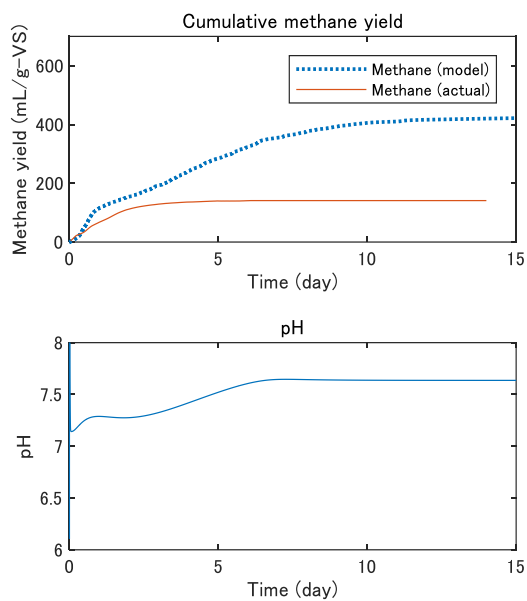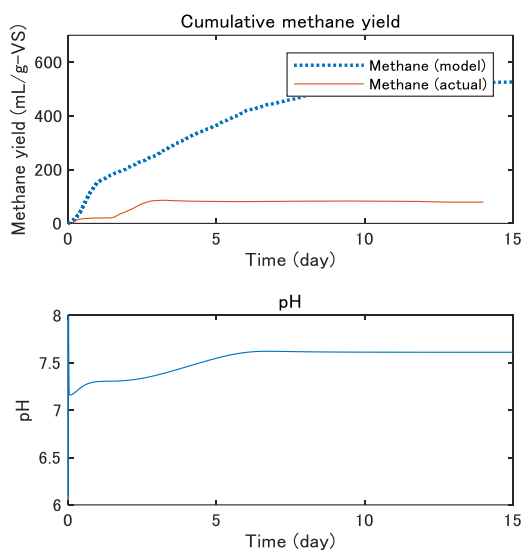
(a) July 2015



(b) August 2015
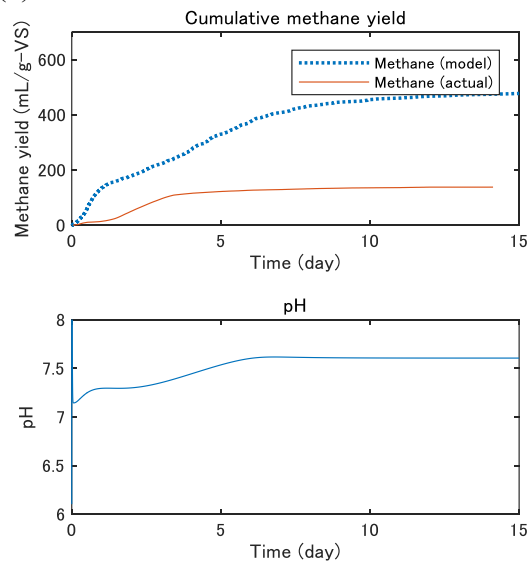
(c) September 2015

(d) October 2015

Figure 4-3. Simulation models and experimentally obtained actual data of batch anaerobic digestion by using chemical compositions of seed sludge and *Elodea nuttallii.* Used ADM1 was cited from Batstone et al. 2002, which was fitted by the BMP results of sewage sludge. Solid line represents batch result and dot line means simulation result.

(a) July 2015

(b) August 2015
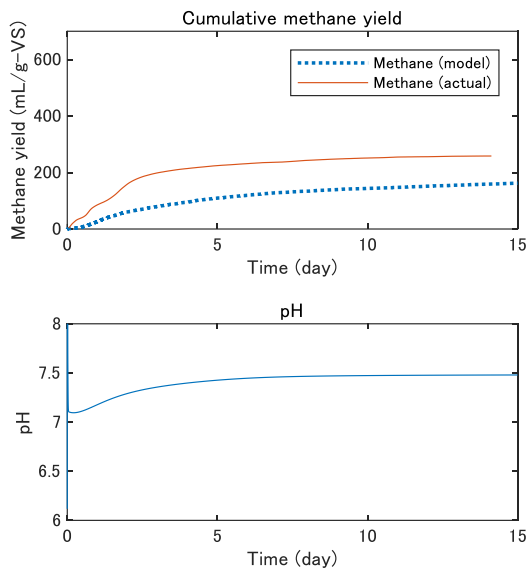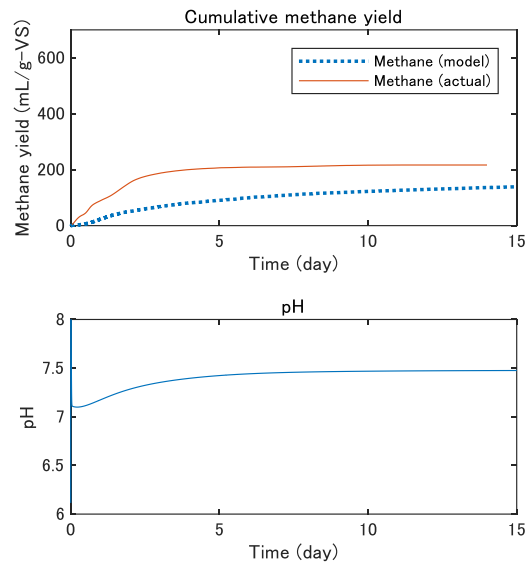
(c) September 2015

(d) October 2015



Figure 4-4. Simulation models and experimentally obtained actual data of batch anaerobic digestion by using chemical compositions of seed sludge and *Potamogeton maaciankus*. Used ADM1 was cited from Batstone et al. 2002, which was fitted by the BMP results of sewage sludge. Solid line represents batch result and dot line means simulation result.
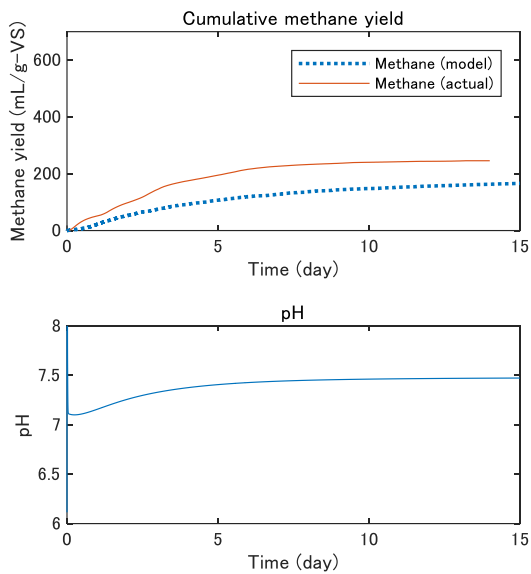
(a) July 2015

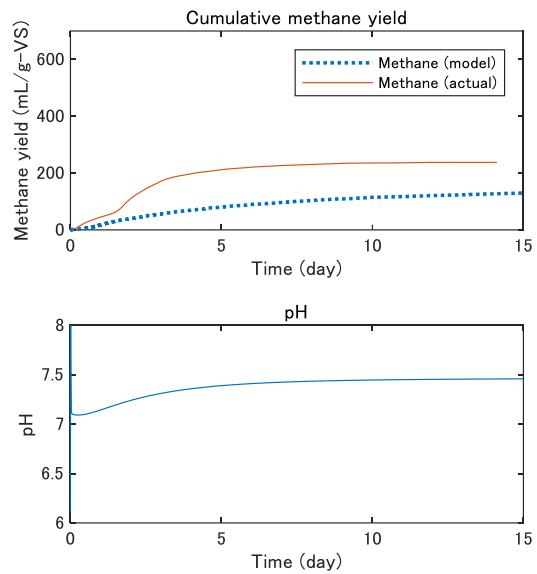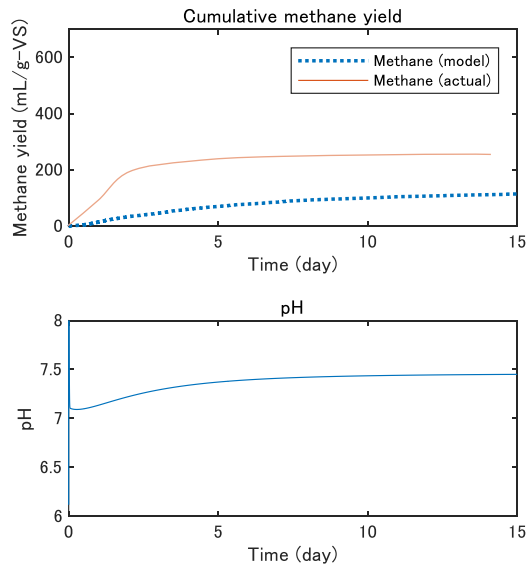(b) August 2015

(c) September 2015

(d) October 2015

Figure 4-5. Simulation models and experimentally obtained actual data of batch anaerobic digestion by using chemical compositions of seed sludge and *Egeria densa.* Used ADM1 was cited from Chen et al. 2016, which was fitted by the BMP results of *Hydrilla verticillate.* Solid line represents batch result and dot line means simulation result.

(a) July 2015

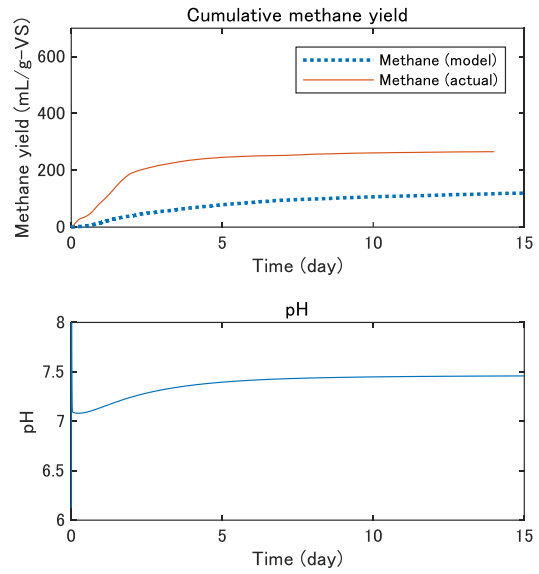(b) August 2015

(c) September 2015

(d) October 2015

Figure 4-6. Simulation models and experimentally obtained actual data of batch anaerobic digestion by using chemical compositions of seed sludge and *Elodea nuttallii.* Used ADM1 was cited from Chen et al. 2016, which was fitted by the BMP results of *Hydrilla verticillate.* Solid line represents batch result and dot line means simulation result.

(a) July 2015

(b) August 2015

(c) September 2015

(d) October 2015



Figure 4-7. Simulation models and experimentally obtained actual data of batch anaerobic digestion by using chemical compositions of seed sludge and *Potamogeton maackianus.* Used ADM1 was cited from Chen et al. 2016, which was fitted by the BMP results of *Hydrilla verticillate.* Solid line represents batch result and dot line means simulation result.
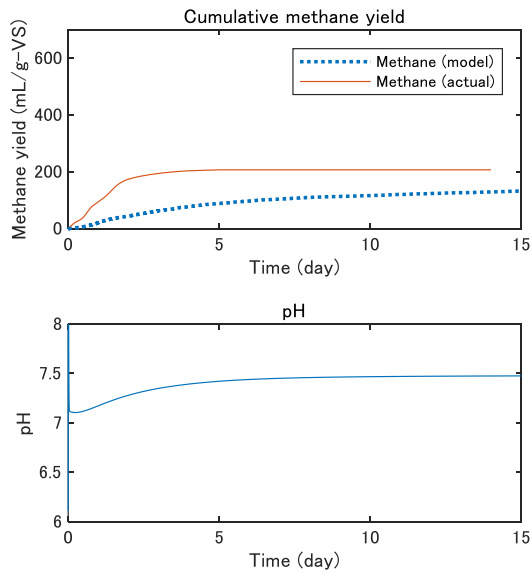
(a) July 2015
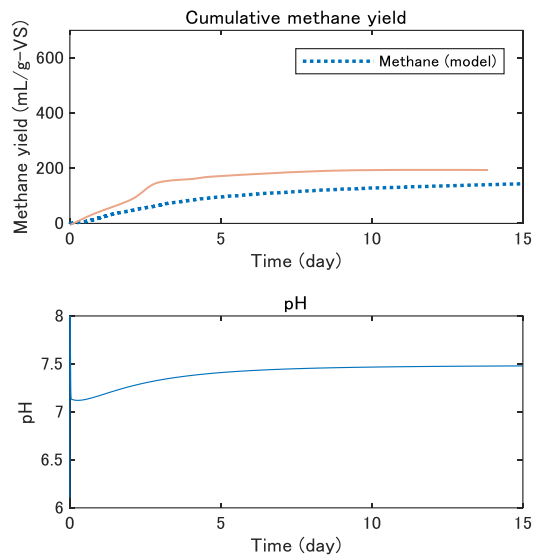
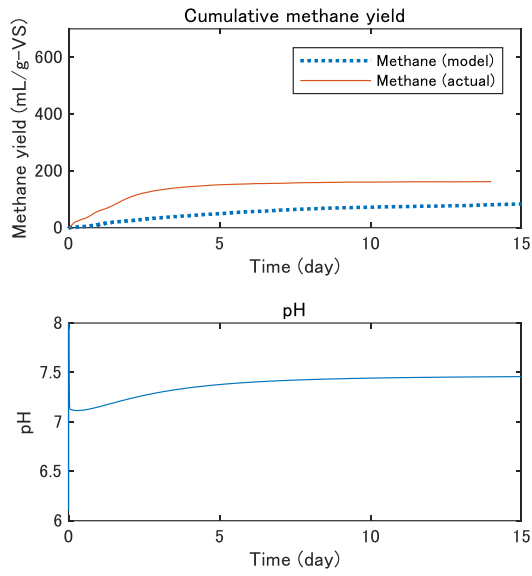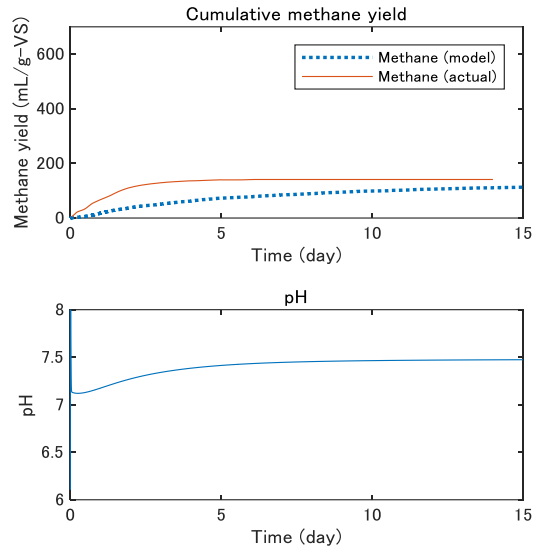(b) August 2015

(c) September 2015

(d) October 2015

Figure 4-8. Simulation models and experimentally obtained actual data of batch anaerobic digestion by using chemical compositions of seed sludge and *Egeria densa*. Used ADM1 was developed in this study, inserting the relationships of lignocellulosic components and their ratios. Solid line represents batch result and dot line means simulation result.

(a) July 2015

(b) August 2015

(c) September 2015

(d) October 2015

Figure 4-6. Simulation models and experimentally obtained actual data of batch anaerobic digestion by using chemical compositions of seed sludge and *Elodea nuttallii.* Used ADM1 was cited from Chen et al. 2016, which was fitted by the BMP results of *Hydrilla verticillate.* Solid line represents batch result and dot line means simulation result.
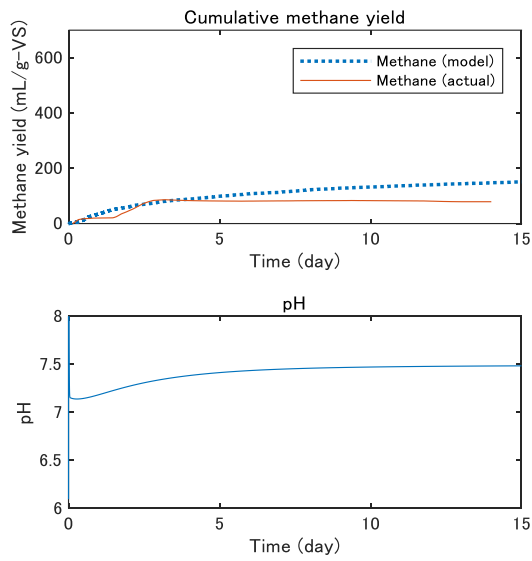
(a) July 2015

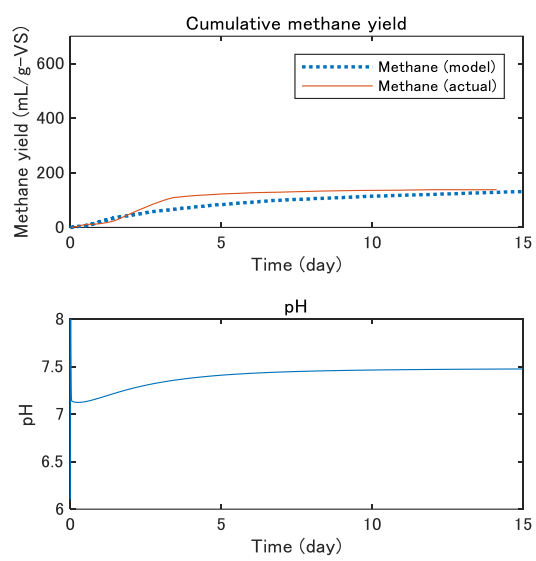(b) August 2015

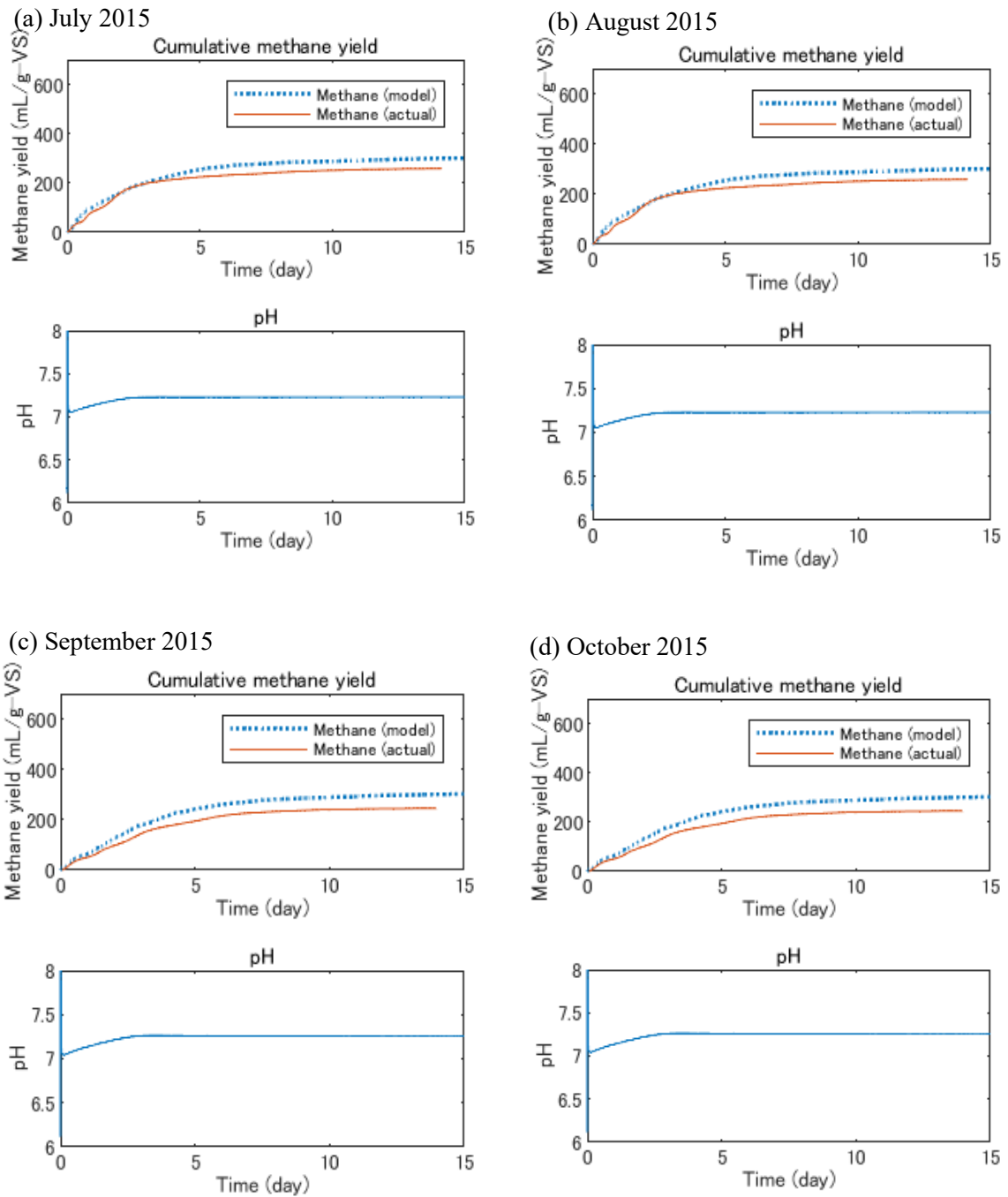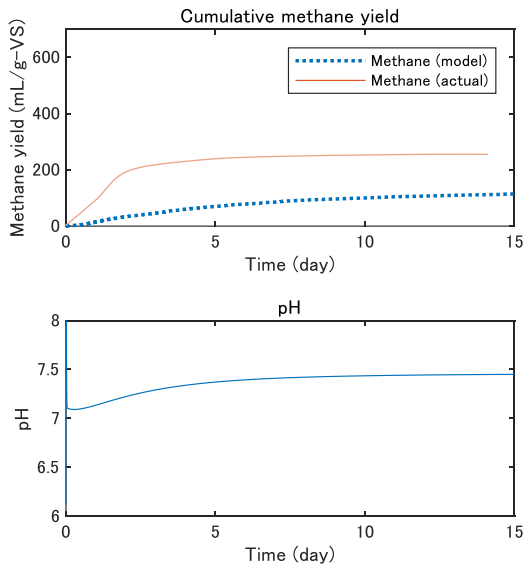(c) September 2015
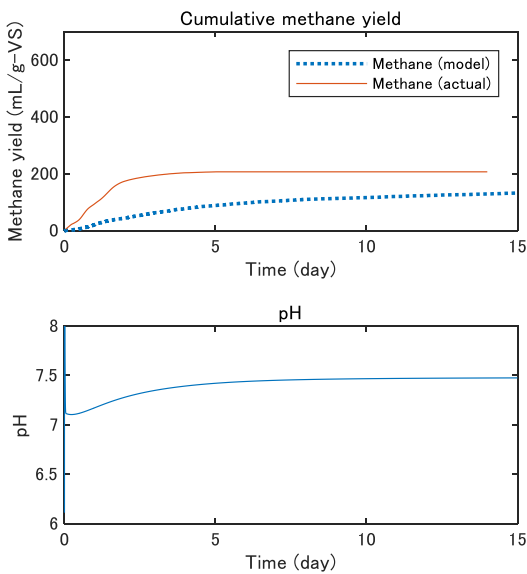
(d) October 2015
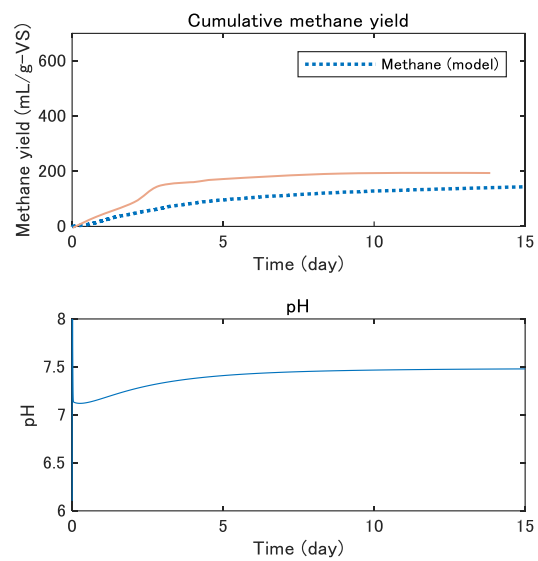
Figure 4-10. Simulation models and experimentally obtained actual data of batch anaerobic digestion by using chemical compositions of seed sludge and *Potamogeton maackianus*. Used ADM1 was developed in this study, inserting the relationships of lignocellulosic components and their ratios. Solid line represents batch result and dot line means simulation result.
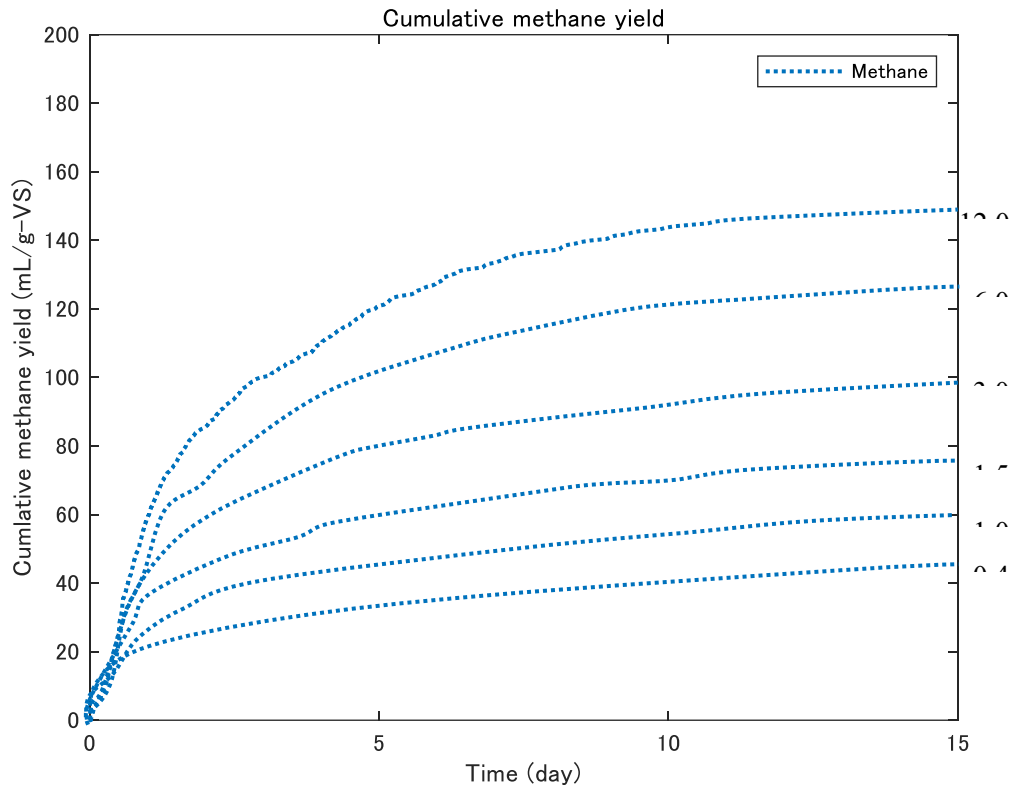
Figure 4-11. Simulation of batch anaerobic digestion of cellulose with different cellulose/lignin ratios. Used ADM1 was developed in this study, inserting the relationships of lignocellulosic components and their ratios. The value described in the right of each line represented cellulose/lignin .

The figure shows a scatter plot with fitted curve. The y-axis is labeled "Cumulative methane yield (mL g-VS$^{-1}$)" ranging from 0 to 160. The x-axis is labeled "Cellulose/lignin" ranging from 0 to 14.

$$y = 31.6 \ln(x) + 65.5$$
$$R^2 = 0.985$$

Figure 4-12. Relationships between the cellulose/lignin ratio and simulated cumulative methane yields from cellulose.

<center>**Chapter V**</center>

<center>**General discussion**</center>

**5.1. Estimation of the performance during semicontinuous anaerobic digestion of _P._**

**_maackianus_**

In Chapter 1, we discussed the problem regarding overgrowing aquatic weeds all over the world

as general discussion. Chapter 2 suggested that the seasonal changes of the species compositions

affected the stability of the annual methane recovery. Chapter 3 clarified that anaerobic digestibility

of the aquatic weeds had relationships with lignocellulosic components and their ratios. In Chapter 4,

The ADM1 was developed to inserting the effect of lignocellulosic components. In this General

Discussion, from the model developed in ChapterIV, the treatment performance was estimated based

on the literature values in semicontinuous anaerobic digestion experiments of untreated _P._

_maackianus_ (Koyama et al. 2017). The parameters such as the digester volume, hydraulic retention

time (HRT), and organic loading rate (OLR) were set to be the same with previous study (Effective

volume: 4.5 L, HRT: 40 days, OLR: 1.0 g-VS$^{-1}$ L$^{-1}$ day$^{-1}$). Figure 5-1 shows the comparison between

experimental result of Koyama et al., (2017) and the simulation result by the developed model. In

Koyama et al. (2017), the methane production rate became unstable in the early stage of operation
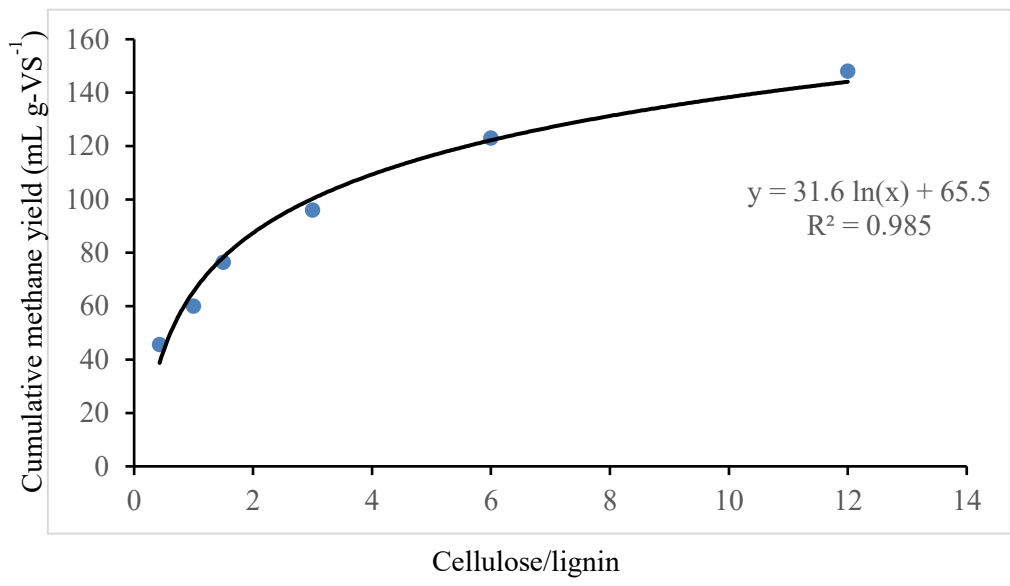
with the value of approximately 80 ml L$^{-1}$ day$^{-1}$. During this period, it was considered that the

microorganisms changed, resulting in temporary instability of the treatment performance. Thereafter,

methane production rate was stabilized at around 170 ml L$^{-1}$ day$^{-1}$. The simulation resulted the

methane production rate being 174 mL L$^{-1}$ day$^{-1}$ which was almost equivalent to those in the stabilized

period. This model does not take into account the inhibition to microorganisms and/or the change in

<center>79</center>

the microbial community due to the change in the substrate and other factors such as temperature, inhibitory compound productions and so on. Therefore, the difference in the methane production between model and measured values in the early stage of the operation would be caused. pH also had a difference in the early stage of operation, as same as methane production rate, but after stabilized, it showed almost the same value as in the previous study. Therefore, although it may not be well estimated due to the composition of the substrate and the condition of the sludge in the start-up of the experiment, the developed model can estimate the treatment performance under semicontinuous operation, as long as the sludge acclimation is completed.

This study and Koyama et al. (2017) used seed sludge collected from Hokubu Sludge Treatment Center, Yokohama, Japan, treating sewage sludge. To investigate the feasibility of the developed model, The simulation was also performed with the semicontinuous anaerobic digestion of *E. densa* using seed sludge obtained from a mesophilic digester treating food waste (Kobayashi et al., 2015). The simulated methane production rate showed a similar value ($300 - 370$ mL L$^{-1}$ day$^{-1}$) with the previous study ($374$-$386$ mL L$^{-1}$ day$^{-1}$). The simulation results with low VFAs concentrations and stable pH suggested that the anaerobic digestion of *E. densa* could be stably treated. Although the methane production in semicontinuous operation was successfully estimated by the simulation, more feasibility analysis will help to understand the effect of the difference in seed sludge.

## 5.2. Estimation of organic load tolerance in semicontinuous anaerobic digestion of aquatic weeds having different degradability

In order to estimate the highest HRT conditions that can be stably treated in the semicontinuous anaerobic digestion of aquatic weed biomass, the estimation was performed with increasing the inflow amount. Chemical compositions of an aquatic weeds *P. maackianus* were cited from Koyama et al., 2017, and applied to the developed model. The simulation was performed in HRT 40, 30, and 25 days by increasing the amount of substrate inflow step by step. The operation period in each HRT condition was set to three times the period of HRT (HRT40: Day 0-120, HRT30: Day 120-210, HRT25: Day 210-250). The simulation resulted that the treatment performance was stable in the conditions of HRT40, 35, and 30 days, respectively (Figure 5-2), but in the condition of HRT 25 days, the growth of acetic acid-degrading bacteria could not keep up with the circulation rate of sludge, resulting in the accumulation of organic acids in the reactor, and thus acidification occurred. In the previous study evaluated tolerance to HRT in semicontinuous anaerobic digestion of highly degradable aquatic weed, *E. densa*, the methane production rate was also decreased when the HRT became less than 25 days (Kobayashi et al. 2015). It was considered preferable to operate the semicontinuous anaerobic digestion of aquatic weeds with HRT of more than 30 days to maintain stable treatment performance. The applicability of this developed model for semicontinuous anaerobic digestion of aquatic weeds, including both easily and hardly degradable species, was validated.

## 5.3. Estimation of anaerobic digestibility of the aquatic weed biomass harvested from Lake Biwa

Three-year treatment performance was simulated in the semicontinuous methane fermentation experiment of harvested (five dominant species mixed) aquatic weeds from Lake Biwa. Data on the species composition of the harvested aquatic weeds were derived from the previous study in 2015 (Ohmi Environment Conservation Foundation, 2015). Five species occurred predominantly from April to December, but only *P. maackianus* was dominant during the winter season (January-March). The chemical compositions of the aquatic weeds were applied by the results in this study. Because approximately 4,000 tons-wwt of aquatic weeds have been harvested per year in Lake Biwa, substrate input was assumed to be 10 tons wet weight per day ($\fallingdotseq$4000 tons/ 365 days). The simulation was performed from 1$^{st}$ May (Day 0). The HRT was set to 30 days when hardily degradable aquatic weeds, *P. maackianus*, could be stably decomposed in Section 4.2.

Figure 5-3 shows the seasonality of the chemical composition of harvested aquatic weeds from Lake Biwa. Especially, cellulose, hemicellulose, and lignin contents were fluctuated throughout the year, although protein, lipid, and carbohydrate contents did not change. Based on the changes in these compositions, the variation of methane recovery in three-year operation was estimated. The estimated results are shown in Figure 5-4. The results showed that anaerobic digestion of harvested aquatic weeds could be treated without the failure caused by acidification and/or discharge of microbes. However, the range of methane production rate was 200-400 L m$^{-3}$ day$^{-1}$. The higher methane production was estimated in the winter season, although *P. maackianus* was low degradable aquatic

weeds. *P. maackianus* has 1.5-2.0 times high VS content than other aquatic weed species, thus, the methane production rate seems not to decrease in the winter season. It is assumed that the feeding amount will change daily for the actual operation. Therefore, the variation of feeding amount may lead to the failure of the reactor operation. To investigate the capacity of the fluctuations of substrate-fed amount, simulations were performed (Figure 5-5). The simulation results suggested that a 15% (11.5 ton/day) increment of the fed amount may lead to failure, although the 10% (11 ton/day) increment can maintain the treatment stability. Therefore, to maintain the treatment stability, the variation of the fed amount should be monitored not to the excess of 11 tons in the actual operation.

The amount of methane that could be collected was approximately 2565 - 3861 $m^3$ per month. From this value, the amount of electricity sold for each month was calculated. As assumptions for the calculation, the combustion heat of methane is considered to 55.54 MJ/kg, and generated biogas is converted to electricity with 30% electricity efficiency. In Japan, the tariff of generated electricity from biogas is currently 39 JPY (tax exclusive) per kWh (Ministry of Economy Trade and Industry (METI), 2020). Required electricity for the operation of anaerobic digester and the surrounding equipment was assumed to 10% of generated electricity, and the rest of generated electricity was sold. As a result, it was estimated that the annual income from electricity sales could be approximately 3 million yen. In the simulation of this study, the HRT was set at 30 days, which was adopted from the result of simulating the semicontinuous anaerobic digestion of *P. maackianu*s. In summer season, the percentage of *P. maackianu*s in the harvested biomass was low and the percentage of other easily degradable aquatic weeds also increases. Therefore, the biogas production efficiency may be further

improved by changing the HRT depending on the season. In addition, the winter period is dominated by the low degradable *P. maackianu*s. Koyama et al. (2016) reported that the rate of increase in methane production by alkaline treatment was greatly enhanced in *P. maackianu*s with high lignin content.

## 5.4. Future study

### 5.4.1. Applications for the other inland water area

This study focused on the treatment of overgrowing aquatic weeds in Lake Biwa. Similar to Lake Biwa, many areas worldwide have been suffering from the overgrowth of aquatic weeds. The model could be applied to these water bodies to facilitate the estimation of methane fermentation treatment performance. Several studies have revealed that over two aquatic weed species co-exist in the same aquatic ecosystem (Toron et al. 2017; Aloo et al., 2013; Chappuis et al.,2014). On the other hand, although the overgrowth of aquatic weeds is a major problem in many parts of the world, such as Lake Parentis Biscarrosse (Lake PAR.) in France (Rajagopal et al., 2013) and Chirata dam in Indonesia (Syaichurrozi, 2017), there are no reports on there are no reports on the seasonality of species composition. The model established in this study can be used to more accurately estimate methane production and treatment performance by investigating the seasonality of species composition of aquatic weed biomass in lakes, especially since the model can be estimated even when the main composition changes.

## 5.4.2. Application of pre-treatments to developed ADM1

From the results of this study, a high ratio of lignin and hemicellulose was considered the limiting factor to the anaerobic digestion of aquatic weeds. Low cellulose/lignin and low methane yield were recorded in *P. maackianus*. To increase the methane production from this species, removing lignin by alkaline and fungi pre-treatments might be significant. Koyama et al. (2015) reported that alkaline pretreatment can enhance the methane yield of *P. maackianu* by 51% while that of *E. nuttallii* was increased by 24%. *S. polyrhiza* and *P. maackianus* showed lower cellulose/hemicellulose ratio with lower maximum methane production rates, although most of the others aquatic weeds showed low cellulose/hemicellulose. Therefore, the application of acid and steam explosion pre-treatments might be effective to enhance methane production rate which can derive and consequently remove hemicellulose from the substrate (Gonzales et al., 2016; Theuretzbacher et al., 2015). The predictive equations developed in this study cannot be used to estimate the anaerobic digestibility of pretreated lignocellulosic biomass. This is because the estimation methods depend on the lignocellulosic structure, although most pre-treatment methods disrupt and dissolve the lignocellulose structure. However, in the future, by clarifying the relationship between the lignocellulose composition ratio and the increment in methane yield by pre-treatment, it may be possible to calculate the optimal balance between the costs of pre-treatment and the benefits incurred from the increase in methane recovery. In previous studies, ADM1 has been applied to pretreated lignocellulosic biomass. There is a possibility that it can be applied to aquatic weeds biomass as well, however, there has been no reported case. In addition, the model is based on the

structure of lignocellulose, but the relationship may change with pre-treatment. For example, it is known that alkali treatment removes the bonds of lignin, while acid treatment solubilizes most hemicellulose. Therefore, whether this model can be applied to the raw materials after pre-treatment needs to be studied in the future.

### 5.4.3. Modifications of the ADM1 developed in this study

The flexibility of this model needs to be further evaluated as future studies for social implementation. For example, differences in seed sludge, operating temperature, and the structure of the reactor may affect the activity of microorganisms. Ivan et al. (2009) demonstrated increasing levels of ammonia decreased microbial diversity and thus treatment performance was decreased. Peces et al. (2018) performed long term continuous anaerobic digestion experiment with four different seed sludges, resulted the different treatment efficiency depending on the seed sludge, although most previous study of ADM1 have been applied the chemical compositions of seed sludge from previous study, as well as this study. Therefore, by clarifying the effect of microbial structure on anaerobic digestibility and linking to the ADM1, a higher reliability predictive model may be established.

Figure 5-1. Simulation models and experimental data of semicontinuous anaerobic digestion by using chemical compositions of seed sludge and *Potamogeton maackianus*. Chemical compositions and experimental data were quoted from Koyama et al., 2017. Used ADM1 was developed in the present study, inserting the relationships of lignocellulosic components and their ratios. Solid line represents batch result and dot line means simulation result.

Figure 5-2. Simulation results of semicontinuous anaerobic digestion of *Potamogeton maackianus* under different HRT conditions (HRT40: Day 0-120, HRT30: Day 120-210, HRT25: Day 210-250). Chemical compositions was quoted from Koyama et al., 2017. Used ADM1 was developed in the present study, inserting the relationships of lignocellulosic components and their ratios.
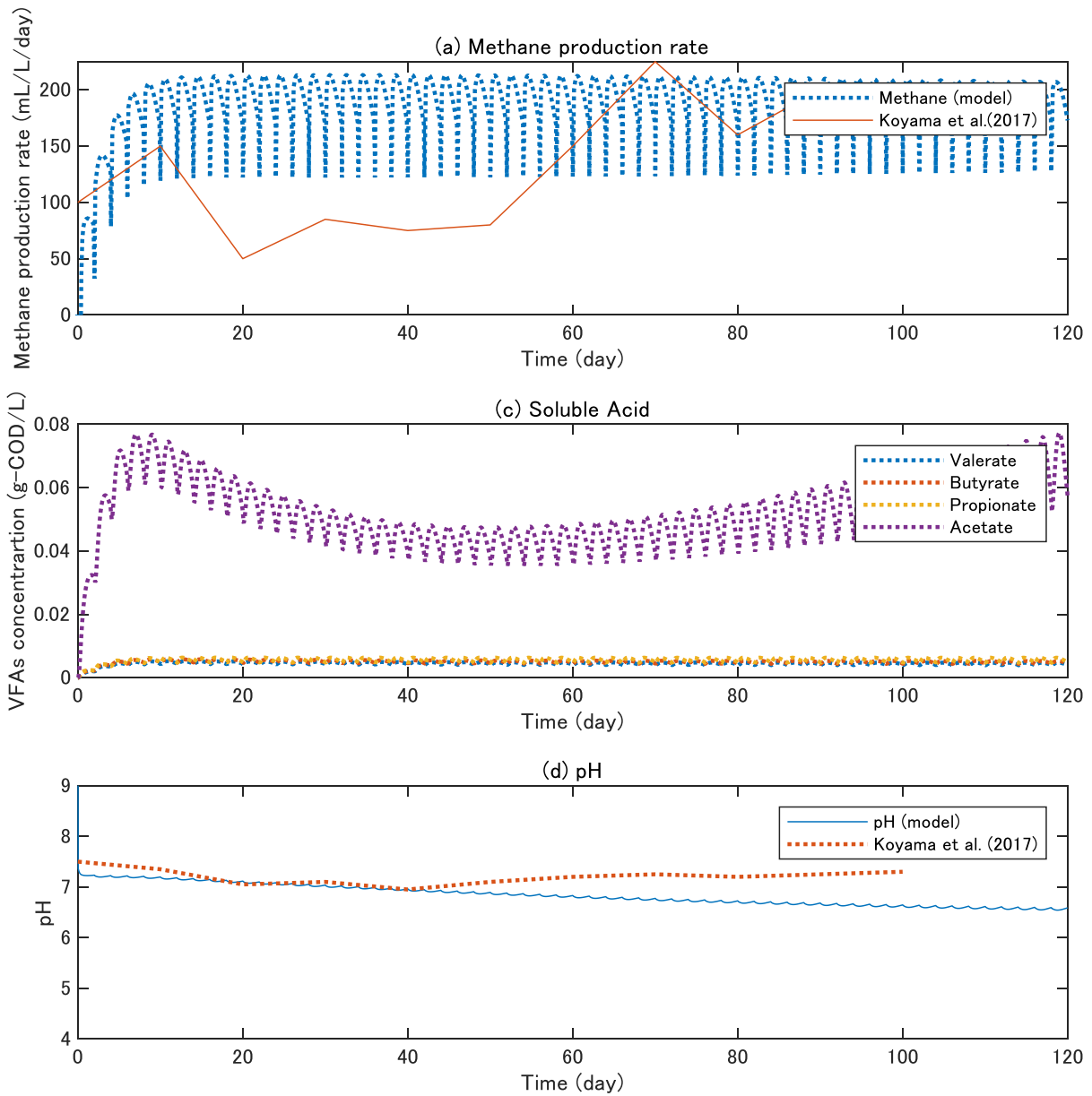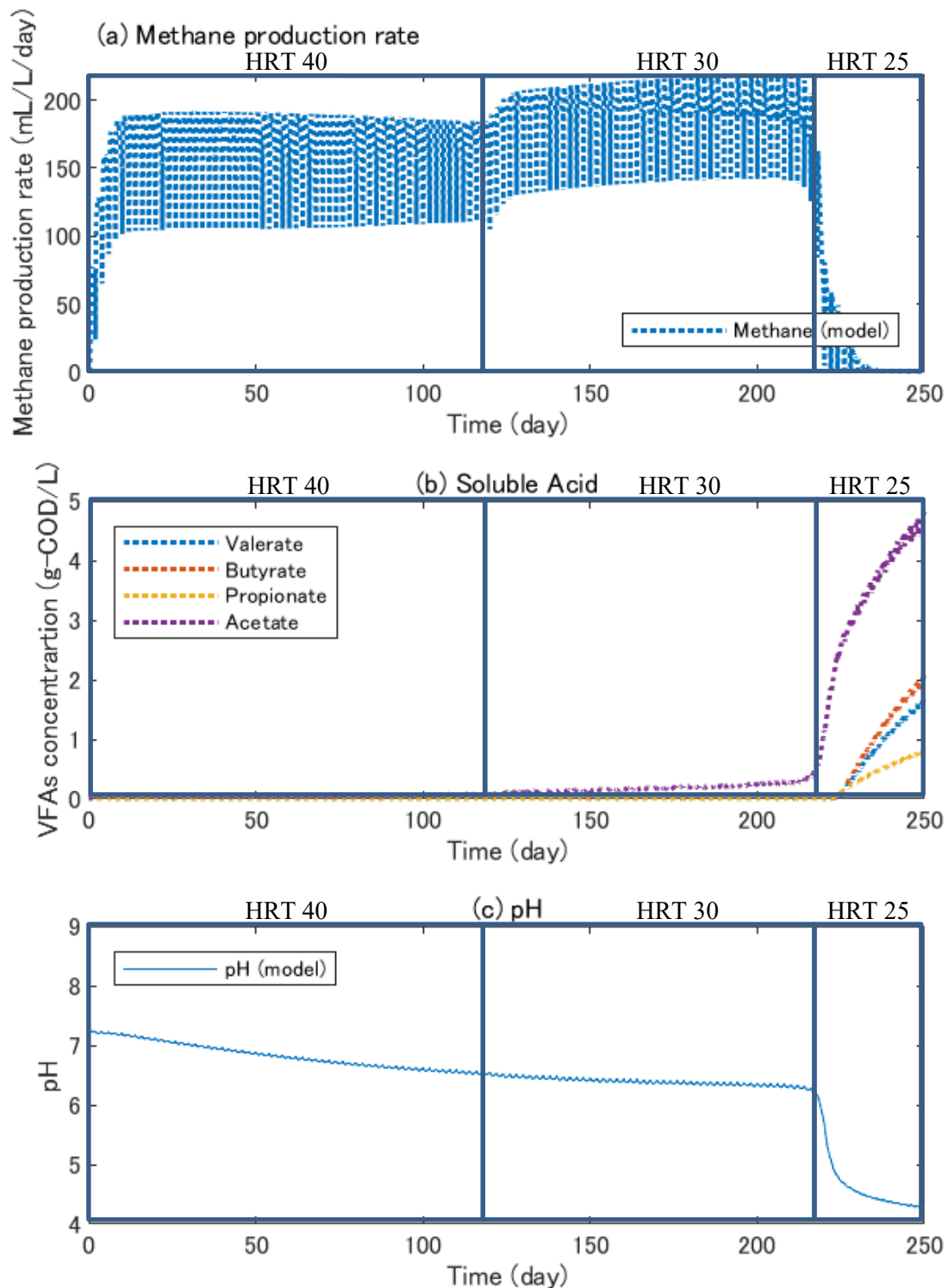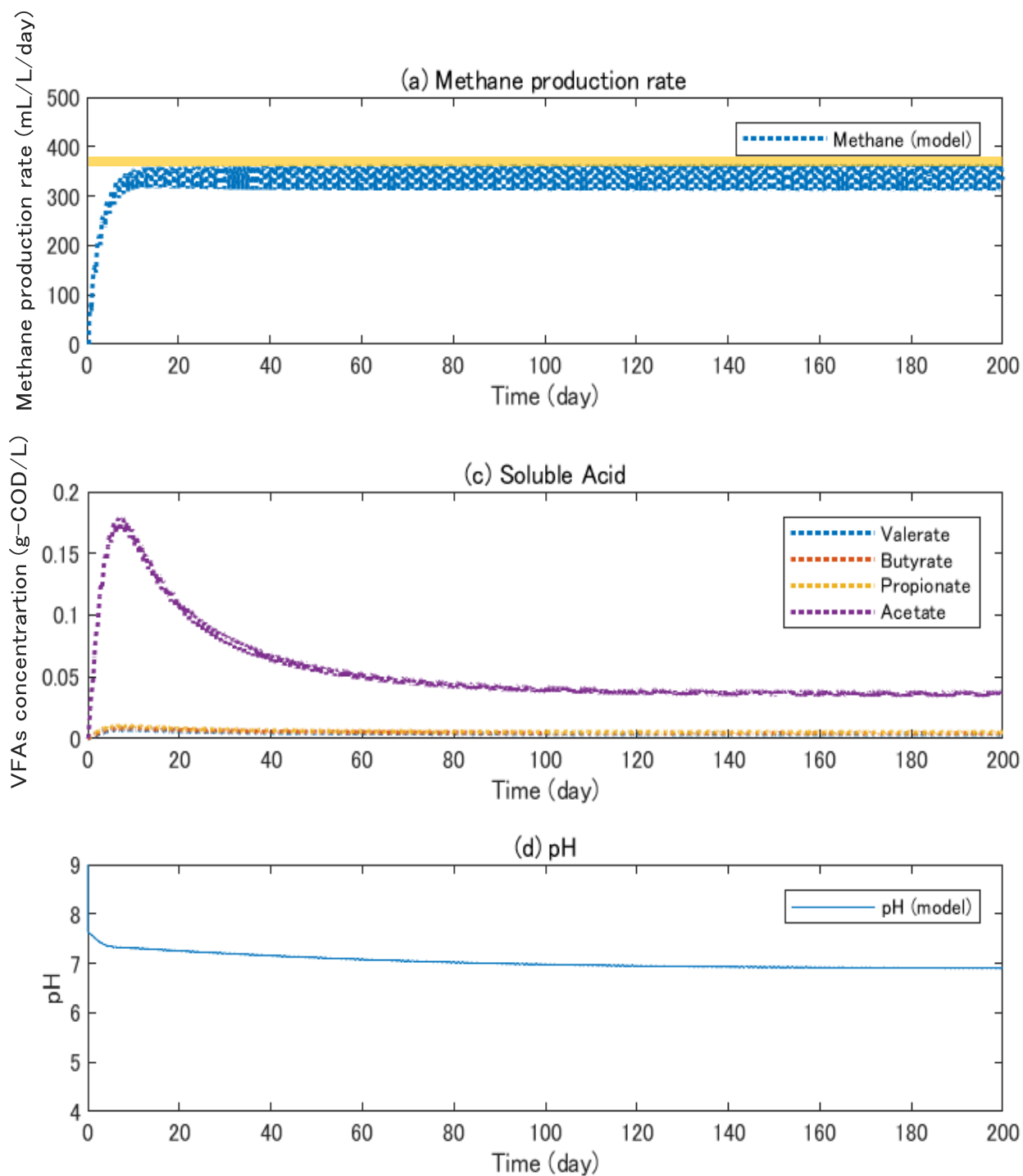
Figure 5-3. Simulation models and experimental data of semicontinuous anaerobic digestion by using chemical compositions of seed sludge and *Egeria densa*. Chemical compositions and experimental data were quoted from Kobayashi et al., 2015. Used ADM1 was developed in the present study, inserting the relationships of lignocellulosic components and their ratio. Yellow zone in (a) methane production rate represents the experimental value reported in the previous study.
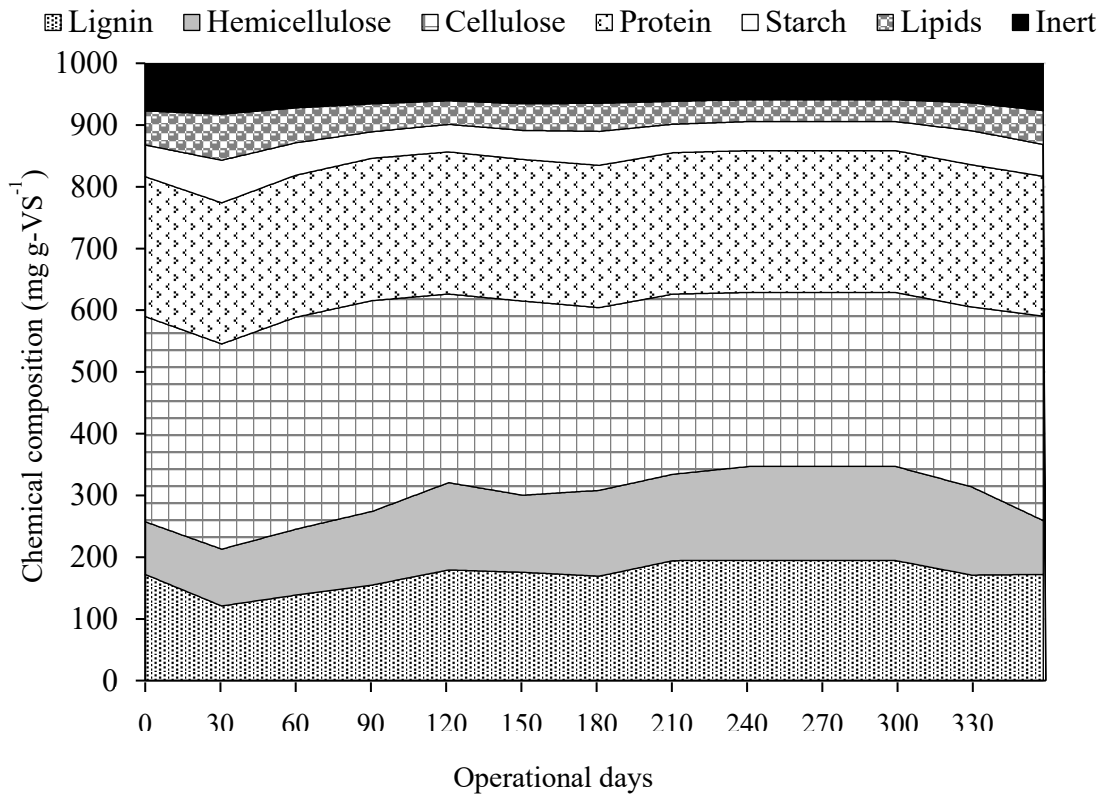
Figure 5-3. Variation of the chemical compositions of harvested aquatic weeds from Lake Biwa. The value was calculated by species composition of harvested aquatic weeds (Ohmi Environment Conservation Foundation, 2015) and the chemical compositions of each aquatic weed species analyzed in this study.
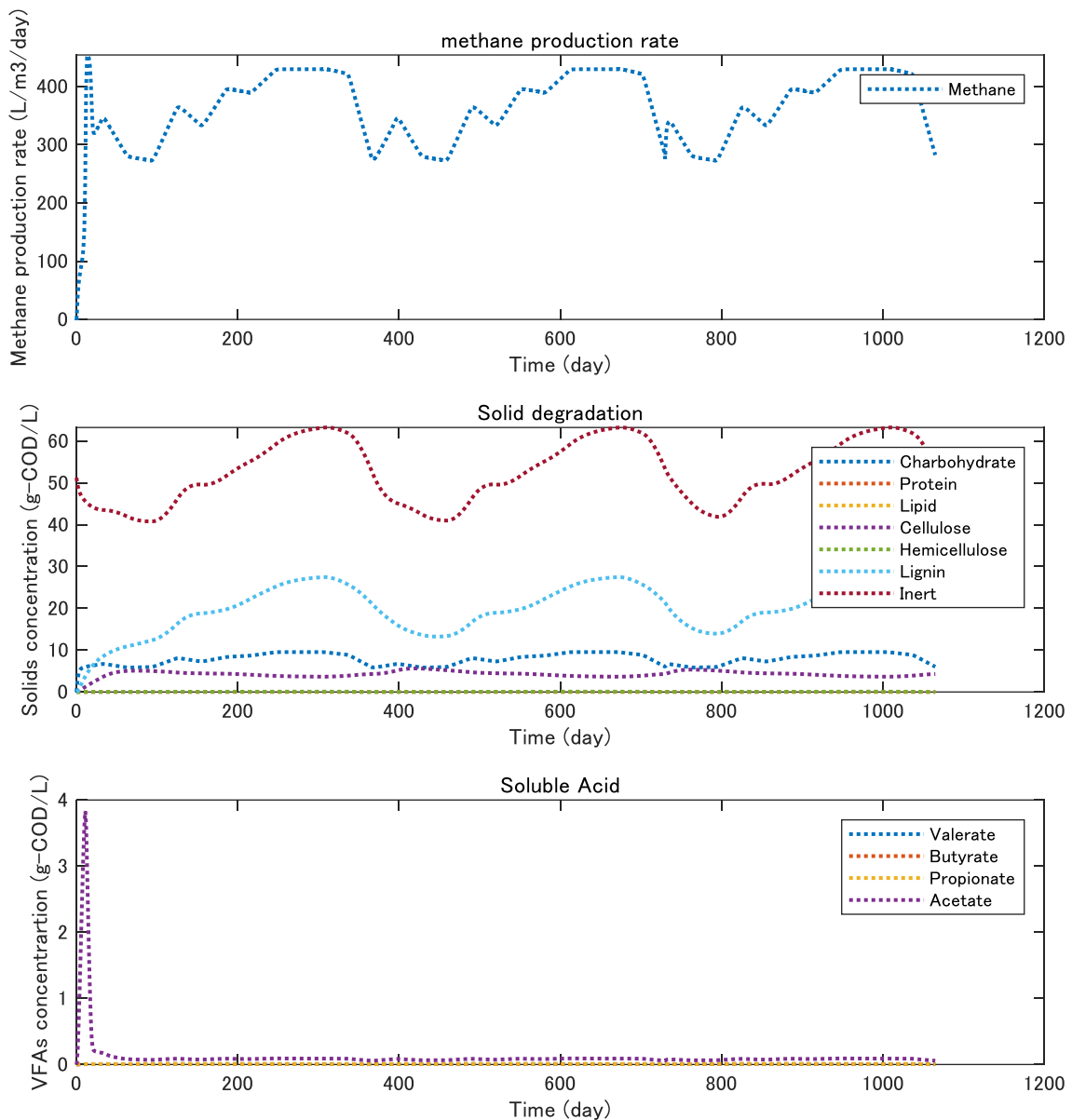
Figure 5-4. Simulation results of three-years semicontinuous anaerobic digestion of harvested aquatic weeds from Lake Biwa. Operational conditions were assumed that 10 m$^3$ day$^{-1}$ of harvested aquatic weeds were treated by 300 m$^3$ digester with HRT 30 days. Chemical compositions were calculated by species compositions of harvested aquatic weeds from Lake Biwa (Ohmi Environment Conservation Foundation, 2015) and the chemical compositions of each aquatic weed species analyzed in this study. Used ADM1 was developed in the present study.
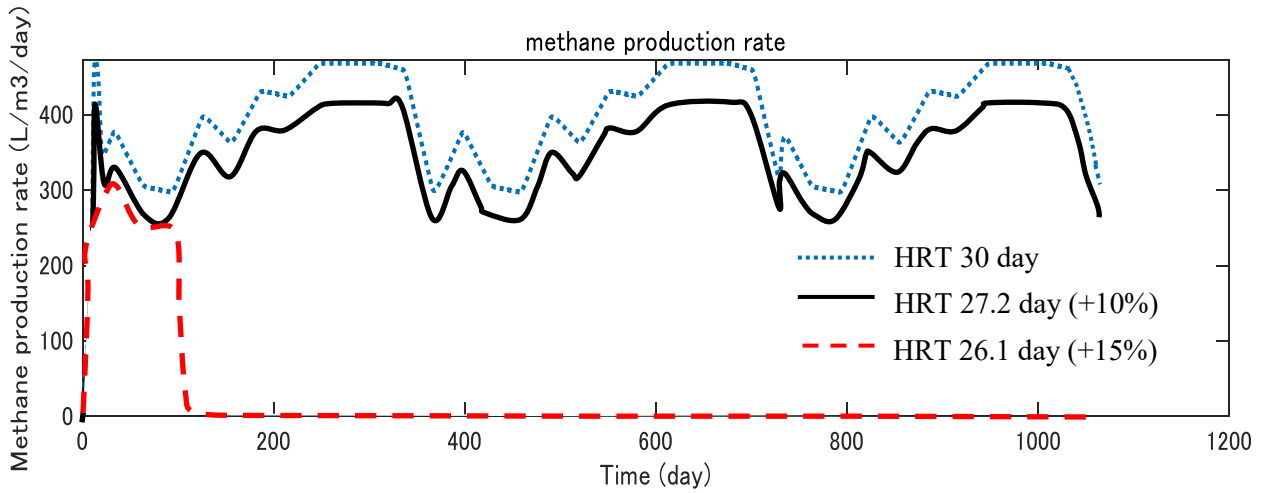
Figure 5-5. Simulation results of three-years semicontinuous anaerobic digestion of harvested aquatic weeds from Lake Biwa with different HRT conditions. Operational conditions were assumed that 10 m$^3$ day$^{-1}$ of harvested aquatic weeds were treated by 300 m$^3$ digester with HRT 30 days. Chemical compositions were calculated by species compositions of harvested aquatic weeds from Lake Biwa (Ohmi Environment Conservation Foundation, 2015) and the chemical compositions of each aquatic weed species analyzed in this study. Used ADM1 was developed in the present study.

# Reference

Abbasi, S.A., Nipaney, P.C., Schaumberg, G.D., 1990. Bioenergy potential of eight common aquatic weeds. Biol. Wastes 34, 359–366. https://doi.org/10.1016/0269-7483(90)90036-R

Alibardi, L., & Cossu, R., 2015. Composition variability of the organic fraction of municipal solid waste and effects on hydrogen and methane production potentials. Waste Management, 36, 147-155.

Aloo, P., Ojwang, W., Omondi, R., Njiru, J.M., Oyugi, D., 2013. A review of the impacts of invasive aquatic weeds on the bio- diversity of some tropical water bodies with special reference to Lake Victoria (Kenya). Biodivers. J. 4, 471–482.

American Public Health Association,2005. Standard Methods for the Examination of Water and Wastewater. 21th edit. (Washington DC, USA).

Asaeda, T., Fujino, T., Manatunge, J., 2005. Morphological adaptations of emergent plants to water flow: a case study with *Typha angustifolia*, Zizania latifolia and Phragmites australis. Freshw. Biol. 50, 1991–2001. https://doi.org/10.1111/j.1365-2427.2005.01445.x

Ban, S., Toda, T., Koyama, M., Ishikawa, K., Kohzu, A., Imai, A., 2018. Modern lake ecosystem management by sustainable harvesting and effective utilization of aquatic macrophytes. Limnology. https://doi.org/10.1007/s10201-018-0557-z

Best, E.P.H., Dassen, J.H.A., 1987. A seasonal study of growth characteristics and the levels of carbohydrates and proteins. Aquat. Bot. 28, 353–372.

Buitrón, G., Hernández-juárez, A., Hernández-ramírez, M.D., Sánchez, A., 2019. Biochemical methane potential from lignocellulosic wastes hydrothermally pretreated. Ind. Crop. Prod. 139, 111555. https://doi.org/10.1016/j.indcrop.2019.111555

Carrillo, Y., Guarín, A., Guillot, G., 2006. Biomass distribution, growth and decay of Egeria densa in a tropical high-mountain reservoir (NEUSA, Colombia). Aquat. Bot. 85, 7–15. https://doi.org/10.1016/j.aquabot.2006.01.006

Chappuis, E., Gacia, E., Ballesteros, E., 2014. Environmental factors explaining the distribution and

diversity of vascular aquatic macrophytes in a highly heterogeneous Mediterranean region. Aquat. Bot. 113, 72–82. https://doi.org/10.1016/j.aquabot.2013.11.007

Chen, X., Chen, Z., Wang, X., Huo, C., Hu, Z., Xiao, B., Hu, M., 2016. Application of ADM1 for modeling of biogas production from anaerobic digestion of Hydrilla verticillata. Bioresour. Technol. 211, 101–107. https://doi.org/10.1016/j.biortech.2016.03.002

Copeland, R.S., Nkubaye, E., Nzigidahera, B., Epler, J.H., Cuda, J.P., Overholt, W.A., 2012. The Diversity of Chironomidae (Diptera) Associated With Hydrilla verticillata (Alismatales: Hydrocharitaceae) and Other Aquatic Macrophytes in Lake Tanganyika, Burundi. Ann. Entomol. Soc. Am. 105, 206–224. https://doi.org/10.1603/an11076https://doi.org/10.1016/j.biortech.2014.10.115

Crocamo, A., Di Bernardino, S., Di Giovanni, R., Fabbricino, M., Martins-Dias, S., 2015. An integrated approach to energy production and nutrient recovery through anaerobic digestion of Vetiveria zizanoides. Biomass and Bioenergy 81, 288–293. https://doi.org/10.1016/j.biombioe.2015.07.023

Dahunsi, S.O., 2019. Mechanical pre-treatment of lignocelluloses for enhanced biogas production : Methane yield prediction from biomass structural components. Bioresour. Technol. 280, 18–26. https://doi.org/10.1016/j.biortech.2019.02.006

Dasgupta, A., & Chandel, M. K., 2019. Enhancement of biogas production from organic fraction of municipal solid waste using hydrothermal pre-treatment. Bioresour. Technol.Reports, 7, 100281.

Dragoni, F., Giannini, V., Ragaglini, G., Bonari, E., Silvestri, N., 2017. Effect of harvest time and frequency on biomass quality and biomethane potential of common reed (Phragmites australis) under paludiculture conditions. Bioenergy Res. 10, 1066–1078. https://doi.org/10.1007/s12155-017-9866-z

Dragoni, F., o Di Nasso, N.N., Tozzini, C., Bonari, E., Ragaglini, G., 2015. Aboveground Yield and Biomass Quality of Giant Reed (Arundo donax L.) as Affected by Harvest Time and Frequency. Bioenergy Res. 8, 1321–1331. https://doi.org/10.1007/s12155-015-9598-x

Frydendal-Nielsen, S., Hjorth, M., Baby, S., Felby, C., Jørgensen, U., Gislum, R., 2016. The effect of harvest time, dry matter content and mechanical pre-treatments on anaerobic digestion and enzymatic hydrolysis of miscanthus. Bioresour. Technol. 218, 1008–1015. https://doi.org/10.1016/j.biortech.2016.07.046

Fujiwara, M., Koyama, M., Akizuki, S., Watanabe, K., Ishikawa, K., 2019. Seasonal changes in the chemical composition and anaerobic digestibility of harvested submerged Macrophytes. BioEnergy Res. 1–10. https://doi.org/https://doi.org/10.1007/s12155-019-10082-x

Ghosh, S., Henry, M.P., Christopher, R.W., 1985. Hemicellulose conversion by anaerobic digestion. Biomass 6, 257–269. https://doi.org/10.1016/0144-4565(85)90052-6

Godin, B., Mayer, F., Agneessens, R., Gerin, P., Dardenne, P., Delfosse, P., Delcarte, J., 2015. Bioresource Technology Biochemical methane potential prediction of plant biomasses : Comparing chemical composition versus near infrared methods and linear versus non-linear models. Bioresour. Technol. 175, 382–390.

Gómez, L.D., Amalfitano, C., Andolfi, A., Simister, R., Somma, S., Ercolano, M.R., Borrelli, C., McQueen-Mason, S.J., Frusciante, L., Cuciniello, A., Caruso, G., 2017. Valorising faba bean residual biomass: Effect of farming system and planting time on the potential for biofuel production. Biomass and Bioenergy 107, 227–232. https://doi.org/10.1016/j.biombioe.2017.10.019

Gonzales, R.R., Sivagurunathan, P., Kim, S.H., 2016. Effect of severity on dilute acid pre-treatment of lignocellulosic biomass and the following hydrogen fermentation. Int. J. Hydrogen Energy 41, 21678–21684. https://doi.org/10.1016/j.ijhydene.2016.06.198

González-Fernández, C., Méndez, L., Tomas-Pejó, E., Ballesteros, M., 2018. Biogas and volatile fatty acids production: Temperature as a determining factor in the anaerobic digestion of Spirulina platensis. Waste and Biomass Valorization 0, 1–9. https://doi.org/10.1007/s12649-018-0275-0

Grabber, J.H., Ralph, J., Hatfield, R.D., 1998. Ferulate cross-links limit the enzymatic degradation of synthetically lignified primary walls of maize. J. Agric. Food Chem. 46, 2609–2614.

https://doi.org/10.1021/jf9800099

Güngören Madenoğlu, T., Jalilnejad Falizi, N., Kabay, N., Güneş, A., Kumar, R., Pek, T., Yüksel, M., 2019. Kinetic Analysis of Methane Production from Anaerobic Digestion of Water Lettuce (Pistia stratiotes L.) with Waste Sludge. J. Chem. Technol. Biotechnol. https://doi.org/10.1002/jctb.5968

Gunnarsson, C.C., Petersen, C.M., 2007. Water hyacinths as a resource in agriculture and energy production: A literature review. Waste Manag. 27, 117–129. https://doi.org/10.1016/j.wasman.2005.12.011

Haga, H., Ashiya, M., Ohtsuka, T., Matsuda, M., Tuji, A., Baba, K., Numahata, S., Yamane, T., 2006. Relationship between dissolved oxygen concentration of bottom water and macrophyte biomass in the southern basin of Lake Biwa, Japan. Japanese J. Limnol. 67, 23–27. https://doi.org/10.3739/rikusui.67.23

Haga, H., Ishikawa, K., 2016. Spatial distribution of submerged macrophytes in the southern Lake Biwa basin in the summer of 2014, in comparison with those in 2002, 2007 and 2012. Japanese J. Limnol. (Rikusuigaku Zasshi) 77, 55–64.

Hamabata, E., 1997. Distribution, fluctuation stand structure of Elodea nuttallii, and yearly biomass an alien species in lake Biwa studies. Japanese J. Limnol. (Rikusuigaku Zasshi) 173–190. https://doi.org/10.3739/rikusui.58.173

Haramoto, T., Ikusima, I., 1988. Life cycle of Egeria densa planch., an aquatic weed naturalized in Japan. Aquat. Bot. 30, 389–403. https://doi.org/10.1016/0304-3770(88)90070-8

Hassan, S.S., Williams, G.A., Jaiswal, A.K., 2018. Emerging technologies for the pre-treatment of lignocellulosic biomass. Bioresour. Technol. 262, 310–318. https://doi.org/10.1016/j.biortech.2018.04.099

Hoffmann, L., Rooney, W.L., 2014. Accumulation of Biomass and Compositional Change Over the Growth Season for Six Photoperiod Sorghum Lines. Bioenergy Res. 7, 811–815. https://doi.org/10.1007/s12155-013-9405-5

Hübner, M., Oechsner, H., Koch, S., Seggl, A., Hrenn, H., Schmiedchen, B., Wilde, P., Miedaner, T., 2011. Impact of genotype, harvest time and chemical composition on the methane yield of winter rye for biogas production. Biomass and Bioenergy 35, 4316–4323. https://doi.org/10.1016/j.biombioe.2011.07.021

Imamoto, H., Matsumoto, J., Furusato, E., Washitani, I., 2008. Light and water temperature parameters of 6 species of submerged macrophytes in Lake Biwa (in Japanese). Ecol. Civ. Eng. 11, 1–12. https://doi.org/10.3825/ece.11.1

Jain, M.S., Kalamdhad, A.S., 2018. A review on management of Hydrilla verticillata and its utilization as potential nitrogen-rich biomass for compost or biogas production. Bioresour. Technol. Reports 1, 69–78. https://doi.org/10.1016/j.biteb.2018.03.001

Kadono, Y., 1984. Comparative ecology of Japanese Potamogeton: An extensive survey with special reference to growth form and life cycle. Japanese J. Ecol. 34, 161–172.

Kafle, G.K., Kim, S.H., 2013. Anaerobic treatment of apple waste with swine manure for biogas production: Batch and continuous operation. Appl. Energy 103, 61–72. https://doi.org/10.1016/j.apenergy.2012.10.018

Kandel, T.P., Sutaryo, S., Møller, H.B., Jørgensen, U., Lærke, P.E., 2013. Chemical composition and methane yield of reed canary grass as influenced by harvesting time and harvest frequency. Bioresour. Technol. 130, 659–666. https://doi.org/10.1016/j.biortech.2012.11.138

Kaur, M., Kumar, M., Singh, D., Sachdeva, S., Puri, S.K., 2019. A sustainable biorefinery approach for efficient conversion of aquatic weeds into bioethanol and biomethane. Energy Convers. Manag. 187, 133–147. https://doi.org/10.1016/j.enconman.2019.03.018

Kist, D.L., Cano, R., Sapkaite, I., Pérez-Elvira, S.I., Monteggia, L.O., 2018. Macrophytes as a digestion substrate. Assessment of a sonication pre-treatment. Waste and Biomass Valorization 0, 0. https://doi.org/10.1007/s12649-018-0502-8

Kobayashi, N., Noel, E.A., Barnes, A., Watson, A., Rosenberg, J.N., Erickson, G., Oyler, G.A., 2013. Characterization of three Chlorella sorokiniana strains in anaerobic digested effluent from cattle

manure. Bioresour. Technol. 150, 377–386. https://doi.org/10.1016/j.biortech.2013.10.032

Kobayashi, T., Wu, Y.-P., Lu, Z.-J., Xu, K.-Q., 2014. Characterization of anaerobic degradability and kinetics of harvested submerged aquatic weeds used for nutrient phytoremediation. Energies 8, 304–318. https://doi.org/10.3390/en8010304

Koyama, M., Yamamoto, S., Ishikawa, K., Ban, S., Toda, T., 2014. Anaerobic digestion of submerged macrophytes: Chemical composition and anaerobic digestibility. Ecol. Eng. 69, 304–309. https://doi.org/10.1016/j.ecoleng.2014.05.013

Koyama, M., Yamamoto, S., Ishikawa, K., Ban, S., Toda, T., 2015. Enhancing anaerobic digestibility of lignin-rich submerged macrophyte using thermochemical pre-treatment. Biochem. Eng. J. 99, 124–130. https://doi.org/10.1016/j.bej.2015.03.013

Koyama, M., Yamamoto, S., Ishikawa, K., Ban, S., Toda, T., 2016. Inhibition of anaerobic digestion by dissolved lignin derived from alkaline pre-treatment of an aquatic macrophyte. Chem. Eng. J. 311, 55–62. https://doi.org/10.1016/j.cej.2016.11.076

Kumagai, A., Endo, T., 2018. Comparison of the surface constitutions of hemicelluloses on lignocellulosic nanofibers prepared from softwood and hardwood. Cellulose 25, 3885–3897. https://doi.org/10.1007/s10570-018-1861-9

Kumar, S., 2011. Aquatic weeds problems and management in India. Indian J. Weed Sci. 43, 118–138.

Kunii, H., 1984. Seasonal growth and profile structure development of Elodea nuttallii (Planch.) St. John in pond Ojaga-Ike, Japan. Aquat. Bot. 18, 239–247. https://doi.org/10.1016/0304-3770(84)90065-2

Lambert, E., Dutartre, A., Coudreuse, J., Haury, J., 2010. Relationships between the biomass production of invasive Ludwigia species and physical properties of habitats in France. Hydrobiologia 656, 173–186. https://doi.org/10.1007/s10750-010-0440-3

Langone, M., Soldano, M., Fabbri, C., Pirozzi, F., Andreottola, G., 2018. Anaerobic digestion of cattle manure influenced by swirling jet induced hydrodynamic cavitation. Applied biochem. and

biotechnol., 184(4), 1200-1218.

Li, H., Chen, Z., Fu, D., Wang, Y., Zheng, Y., Li, Q., 2020. Improved ADM1 for modelling C , N , P fates in anaerobic digestion process of pig manure and optimization approaches to biogas production. Renew. Energy 146, 2330–2336. https://doi.org/10.1016/j.renene.2019.08.086

Li, H., Song, W., Cheng, J., Ding, L., Zhou, J., 2019. Effects of harvest month on biochemical composition of alligator weed for biohydrogen and biomethane cogeneration : Identifying critical variations in microbial communities. Int. J. Hydrogen Energy 45, 4161–4173. https://doi.org/10.1016/j.ijhydene.2019.11.208

Li, W., Khalid, H., Zhu, Z., Zhang, R., Liu, G., Chen, C., Thorin, E., 2018. Methane production through anaerobic digestion: Participation and digestion characteristics of cellulose, hemicellulose and lignin. Applied Energy, 226, 1219-1228.

Liu, X., Bayard, R., Benbelkacem, H., Buffière, P., Gourdon, R., 2015. Evaluation of the correlations between biodegradability of lignocellulosic feedstocks in anaerobic digestion process and their biochemical characteristics. Biomass and Bioenergy 81, 534–543. https://doi.org/10.1016/j.biombioe.2015.06.021

Lo, F., Lin, K., Pai, T.-Y., Yang, W.-G., Tzeng, Y.-M., Chiu, H.-Y., Lo, S.-W., Hsiao, K.-C., Banks, C.J., Lo, H.-M., 2019. Biogas production from most agricultural organic wastes by anaerobic digestion in Taiwan. Environ. Prog. Sustain. Energy 38, 1–9. https://doi.org/10.1002/ep.13242

Mailu, A.M., 2001. Preliminary assessment of the social, economic and environmental impacts of water hyacinth in the Lake Victoria basin and the status of control, in: ACIAR Proceedings; 1998. pp. 130–139.

Maruno, S., Hamabata, E., 2016. Effects of macrophyte reaping on macrophyte community at southern part of Lake Biwa. Izunuma-Uchinuma Wetl. Res. 10, 9–19.

McEniry, J., O'Kiely, P., 2013. Anaerobic methane production from five common grassland species at sequential stages of maturity. Bioresour. Technol. 127, 143–50. https://doi.org/10.1016/j.biortech.2012.09.084

Melts, I., Normak, A., Nurk, L., Heinsoo, K., 2014. Chemical characteristics of biomass from nature conservation management for methane production. Bioresour. Technol. 167, 226–231. https://doi.org/10.1016/j.biortech.2014.06.009

Ministry of Economy Trade and Industry (METI) (2020) Feed-in tariff for electricity from renewable energy sources.

(consulted http://www.enecho.meti.go.jp/category/saving_and_new/saiene/kaitori/kakaku.html)

Mussatto, S.I., Fernandes, M., Milagres, A.M.F., Roberto, I.C., 2008. Effect of hemicellulose and lignin on enzymatic hydrolysis of cellulose from brewer's spent grain. Enzyme Microb. Technol. 43, 124–129. https://doi.org/10.1016/j.enzmictec.2007.11.006

Ohmi Environment Conservation Foundation, 2015. State of aquatic weeds growth in Lake Biwa and effective utilization. Tommorows Ohmi 12.

Peng, F., Peng, P., Xu, F., Sun, R., 2012. Fractional purification and bioconversion of hemicelluloses. Biotechnol. Adv. J. 30, 879–903. https://doi.org/10.1016/j.biotechadv.2012.01.018

Pérez, J., Muñoz-Dorado, J., De La Rubia, T., Martínez, J., 2002. Biodegradation and biological treatments of cellulose, hemicellulose and lignin: An overview. Int. Microbiol. 5, 53–63. https://doi.org/10.1007/s10123-002-0062-3

Rabemanolontsoa, H., Saka, S., 2012. Characterization of Lake Biwa macrophytes in their chemical composition. J. Japan Inst. Energy 91, 621–628.

Rabemanolontsoa, H., Saka, S., 2013. Comparative study on chemical composition of various biomass species. RSC Adv. 3, 3946–3956. https://doi.org/10.1039/c3ra22958k

Rennie, E.A., Scheller, H.V., 2014. Xylan biosynthesis. Curr. Opin. Biotechnol. 26, 100–107. https://doi.org/10.1016/j.copbio.2013.11.013

Rueda, J.A., Ortega-Jiménez, E., Hernández-Garay, A., Enríquez-Quiroz, J.F., Guerrero-Rodríguez, J.D., Quero-Carrillo, A.R., 2016. Growth, yield, fiber content and lodging resistance in eight varieties of Cenchrus purpureus (Schumach.) Morrone intended as energy crop. Biomass and Bioenergy 88, 59–65. https://doi.org/10.1016/j.biombioe.2016.03.007

Santamaría, L., Hootsmans, M.J.M., 1998. The effect of temperature on the photosynthesis , growth and reproduction of a Mediterranean submerged macrophyte, Ruppia drepanensis. Aquat. Bot. 60, 188. https://doi.org/10.1016/S0304-3770(97)00050-8

Sawatdeenarunat, C., Surendra, K.C., Takara, D., Oechsner, H., Kumar Khanal, S., 2014. Anaerobic digestion of lignocellulosic biomass: Challenges and opportunities. Bioresour. Technol. 178, 178–186. https://doi.org/10.1016/j.biortech.2014.09.103

Schittenhelm, S., 2008. Chemical composition and methane yield of maize hybrids with contrasting maturity. Eur. J. Agron. 29, 72–79. https://doi.org/10.1016/j.eja.2008.04.001

Schroyen, M., Vervaeren, H., Vandepitte, H., Van Hulle, S.W.H., Raes, K., 2015. Effect of enzymatic pre-treatment of various lignocellulosic substrates on production of phenolic compounds and biomethane potential. Bioresour. Technol. 192, 696–702. https://doi.org/10.1016/j.biortech.2015.06.051

Sharip, Z., Schooler, S.S., Hipsey, M.R., Hobbs, R.J., 2012. Eutrophication, agriculture and water level control shift aquatic weed communities from floating-leaved to submerged macrophytes in Lake Chini, Malaysia. Biol. Invasions 14, 1029–1044. https://doi.org/10.1007/s10530-011-0137-1

Shiga prefecture

Taheruzzaman, Q., Kushari, D.P., 1989. Evaluation of some common aquatic macrophytes cultivated in enriched water as possible source of protein and biogas. Hydrobiol. Bull. 23, 207–212. https://doi.org/10.1007/BF02256739

Terrett, O.M., Dupree, P., 2018. Covalent interactions between lignin and hemicelluloses in plant secondary cell walls. Curr. Opin. Biotechnol. 56, 97–104. https://doi.org/10.1016/j.copbio.2018.10.010

Theuretzbacher, F., Lizasoain, J., Lefever, C., Saylor, M.K., Enguidanos, R., Weran, N., Gronauer, A., Bauer, A., 2015. Steam explosion pre-treatment of wheat straw to improve methane yields: Investigation of the degradation kinetics of structural compounds during anaerobic digestion.

Bioresour. Technol. 179, 299–305. https://doi.org/10.1016/j.biortech.2014.12.008

Tonon, G., Magnus, B.S., Mohedano, R.A., Leite, W.R.M., da Costa, R.H.R., Filho, P.B., 2017. Pre treatment of Duckweed Biomass, Obtained from Wastewater Treatment Ponds, for Biogas Production. Waste and Biomass Valorization 8, 2363–2369. https://doi.org/10.1007/s12649-016-9800-1

Triolo, J.M., Sommer, S.G., Møller, H.B., Weisbjerg, M.R., Jiang, X.Y., 2011. A new algorithm to characterize biodegradability of biomass during anaerobic digestion: Influence of lignin concentration on methane production potential. Bioresour. Technol. 102, 9395–9402. https://doi.org/10.1016/j.biortech.2011.07.026

Van Soest, P.J., Robertson, J.B., Lewis, B.A., 1991. Methods for dietary fiber, neutral detergent fiber, and nonstarch polysaccharides in relation to animal nutrition. J. Dairy Sci. 74, 3583–97. https://doi.org/10.3168/jds.S0022-0302(91)78551-2

Van Wijk, R.J., 1988. Ecological studies on Potamogeton pectinatus L. I. General characteristics, biomass production and life cycles under field conditions. Aquat. Bot. 31, 211–258. https://doi.org/10.1016/0304-3770(88)90015-0

Wang, Y., Byrd, C.S., Barlaz, M.A., 1994. Anaerobic biodegradability of cellulose and hemicellulose in excavated refuse samples using a biochemical methane potential assay. J. Ind. Microbiol. 13, 147–153.

Yarrow, M., Marín, V.H., Finlayson, M., Tironi, A., Delgado, L.E., Fischer, F., 2009. The ecology of egeria densa planchon (liliopsida: Alismatales): A wetland ecosystem engineer. Rev. Chil. Hist. Nat. 82, 299–313. https://doi.org/10.4067/S0716-078X2009000200010

Zehnsdorf, A., Hussner, A., Eismann, F., Rönicke, H., Melzer, A., 2015. Management options of invasive Elodea nuttallii and Elodea canadensis. Limnologica 51, 110–117. https://doi.org/10.1016/j.limno.2014.12.010

Zhang, H., Fangel, J.U., Willats, W.G.T., Selig, M.J., Lindedam, J., Jørgensen, H., Felby, C., 2014. Assessment of leaf/stem ratio in wheat straw feedstock and impact on enzymatic conversion.